A RAPID TESTING INSTRUMENT TO ESTIMATE THERMAL PROPERTIES OF FOOD MATERIALS AT ELEVATED TEMPERATURES DURING NONISOTHERMAL HEATING

By

Dharmendra Kumar Mishra

A DISSERTATION

Submitted to
Michigan State University
In partial fulfillment of the requirements
for the degree of

Biosystems Engineering - Doctor of Philosophy

2013

ABSTRACT

A RAPID TESTING INSTRUMENT TO ESTIMATE THERMAL PROPERTIES OF FOOD MATERIALS AT ELEVATED TEMPERATURES DURING NONISOTHERMAL HEATING

By

Dharmendra Kumar Mishra

Modeling kinetics of thermal degradation of nutrients for food quality or kinetics of microbial reduction for food safety requires reliable estimates of the thermal properties. Thermophysical properties, especially thermal conductivity and specific heat, are important in establishing thermal processes for food manufacturing, especially at higher processing temperatures. Hence, in this study, a novel instrument (TPCell) was designed and developed using principles of intrinsic verification and inverse heat conduction. An intrinsic verification method was developed to ascertain the parameter identifiability in the model and to check the accuracy of the numerical codes used to solve the partial differential equation for heat conduction. The concept of intrinsic sum was introduced, which is sum of all the scaled sensitivity coefficients in the model. The intrinsic sum was derived using dimensionless derivation of scaled sensitivity coefficients. The design of the instrument was based on the insight gained from the dimensionless scaled sensitivity coefficients and the intrinsic sum. With the instrument, thermal conductivity can be measured from room temperature to higher processing temperature of 140^{o}C. Several food materials were tested using the instrument.

Sweet potato puree thermal conductivity was measured to be 0.539 W/m^{o}C at 20^{o}C and 0.574 W/m^{o}C at 140^{o}C. The experimental time with TPCell is less than a minute, as compared to 5-6 hours with quasi-isothermal method employed by currently available instruments. TPCell has advantages over traditional methods, as it avoids the decomposition of materials that result when achieving the quasi-isothermal state at higher temperatures. Temperature-dependent thermal properties were used to estimate the kinetic parameters of nutrient degradation during aseptic and conventional retort processing. Vitamin C and thiamin were selected as model nutrients for degradation study. Sweet potato puree was used as a food matrix. Aseptic processing had 50% higher retention of Vitamin C as compared to retort processing. Thiamin retention could not be quantified, as it survived well in aseptic as well as retort processing. The rate of reaction for ascorbic acid in aseptic processing and retort processing was 0.0073 min^{-1} and 0.0114 min^{-1} at a reference temperature of 127^{o}C, respectively. The activation energy for ascorbic acid in aseptic processing and retort processing was 26.62 KJ/g-mol and 3.43 KJ/g-mol, respectively. The kinetic parameter of thiamin could not be estimated due to insufficient degradation in aseptic as well as in retort processing.

DEDICATION

To my father, Sri Ras Bihari Mishra and my mother, Smt Sabita Mishra, for their selfless sacrifice and for believing in me and providing all the assistance I needed at all times. To my sister Usha Pandey and to my brothers Binod K Mishra, Ashok K Mishra and Ravindra K Mishra for their love and affection and to the younger generation. To Patnarin Benyathiar for her affection and support and to Sri Balram Singh who taught me the concept of belief.

ACKNOWLEDGEMENTS

I would like to express my utmost gratitude to my advisor, Dr. Kirk Dolan, for his consistent support and guidance throughout my M.S. and Ph.D. research period. His mentorship has helped me become a better person. Dr. Dolan's high motivation and expectations inspired me to achieve beyond my capabilities. Under his mentorship I gained exposure to numerous problem-solving techniques not only in academics but also in personal and professional life as well. I would like to thank Dr. Ferhan Ozadali for his relentless support. He jump started my professional career and provided much needed guidance. Because of him and with generous help from Gene Ford, my Ph.D. project was funded by Nestle. I extend my thanks to Gene Ford for his continued support for my research and also to Dr. Curt Emenhiser. I would also like to thank Dr. James Beck for his mentorship and selfless help throughout my research. He taught me the invaluable lessons, which I am going to need all my life. I would like to thank my committee members Dr. Bradley Marks and Dr. Lijian Yang for their valuable time and effort in the completion of this research work and were the source of invaluable advice through our engaging discussions. I would like to express my gratitude to Dr. Mark Uebersax, Dr. Neil Wright and Dr. Robert J. Tempelman for providing opportunities that have helped me immensely. One more wonderful person whom I could not forget is Dr. R. Paul Singh for paving my way to higher studies.

My sincere thanks goes to Jonathan R. Althouse and Mark Ven Ee for his dedicated help in designing the data logging system for the instrument and to Phil Hill for his help with the instrument design. My heartfelt thanks extend to my colleagues at Nestle Nutrition, PTC Fremont for their encouragement and help.

My deepest thanks to lovely Patnarin Benyathiar (Oh) for her selfless help all the time. I would not be able to complete my research without her being there for me. My appreciation also goes to Dr. Winnie Chiang-Dolan for her guidance, support and valuable advices. My very warm thanks to Dr. Rabiha Sulaiman for her passionate help with my project and to Hayati Samsudin who was always there for me when I needed help.

I am also grateful to the faculty and staff of Biosystems Engineering as well as Food Science, MSU. I am also thankful to all my friends and fellow graduate students who have provided me the wonderful friendly atmosphere throughout my research. Special thanks to my lab mates at room 129 in Food Science Trout Building for their love and encouragement all the time.

Finally, I would like to thank my parents and all family members, as they are the inspiration for what I am today.

TABLE OF CONTENTS

LIST OF TABLES

LIST OF FIGURES

KEY TO SYMBOLS AND ABBREVIATIONS

δ constant for calculation of sensitivity coefficient

$\tilde{x}$ dimensionless axial distance

$\tilde{r}$ dimensionless radial distance

$\tilde{X}_k$ dimensionless scaled sensitivity coefficient of thermal conductivity

$\tilde{T}$ dimensionless temperature

$\tilde{t}$ dimensionless time

$\overline{C}$ mass-average concentration mg/100g

β parameter

$\hat{X}_k$ scaled sensitivity coefficient of thermal conductivity, ^{o}C

$\left(\overline{C}/C_0\right)$ vitamin retention, where $0 \le \left(\overline{C}/C_0\right) \le 1$)

$\tilde{X}_C$ dimensionless scaled sensitivity coefficient of volumetric heat capacity

$\hat{X}_C$ scaled sensitivity coefficient of volumetric heat capacity, ^{o}C

$SumSSC$ absolute sum of scaled sensitivity coefficients, ^{o}C

$\tilde{x}$ dimensionless axial distance

$\tilde{h}$ dimensionless heat transfer coefficient

β parameter

$\tilde{X}_h$ dimensionless scaled sensitivity coefficient of heat transfer coefficient

$\tilde{X}_C$ dimensionless scaled sensitivity coefficient of volumetric heat capacity

A constant

C volumetric heat capacity, J/Kg-^{o}C

C_1 volumetric heat capacity, J/Kg-^{o}C at temperature T_1

C_2 volumetric heat capacity, J/Kg-^{o}C at temperature T_2

C_o initial mass-average concentration, mg/100g

D diameter of pipe, in

E_a activation energy, J/g-mol

F_o Sterilization value, min

g power, W/m^3

h heat transfer coefficient, W/m^2-^{o}C

I_S intrinsic sum, ^{o}C

K Consistency coefficient, Pa.s^n

k thermal conductivity, W/m-^{o}C

k_1 thermal conductivity of sample, W/m-^{o}C at temperature T_1

k_2 thermal conductivity of sample, W/m-^{o}C at temperature T_2

k_h thermal conductivity of heater, W/m-^{o}C

k_r rate constant at reference temperature T_r, min^{-1}

L thickness of slab, m

n flow behavior index

$N_{Re,PL}$ Reynolds number

q heat flux, W/m^2

Q power generated by heater, W/m

r radial position, m

R resistance of the heater, ohm

R_g gas constant (J/g-mole K)

R_0 Inner radius of the heater, m

R_1 Interface of heater and sample, m

R_2 Outer radius of the cup, m

T temperature (K)

t time, sec

T temperature, ^oC

T_∞ steam temperature, K

T_0 initial temperature, ^oC

t_0 time correction factor, sec

t_1 start of heating time, sec

T_1 initial temperature for thermal properties, ^oC

t_2 end of heating time, sec

T_2 final temperature for thermal properties, ^{o}C

T_{r} reference temperature, K

$\bar{u}$ velocity of product in pipe

X sensitivity matrix

x axial position, m

z temperature required to reduce microorganism by one log

z' axial position

β parameter

ρ product density, Kg/m^3

Chapter 1

Introduction

1.1 Introduction

Thermal processing of food products relies on time-temperature data obtained from either actual measurements or from mathematical models. A sufficient lethality, calculated based on time-temperature data, needs to be accumulated to make sure that the food is safe for distribution and consumption. In the case where no direct measurement can be made, the time-temperature data can be obtained from simulation with the mathematical model. This procedure requires two things to be reasonably accurate: 1) the numerical code that is used to solve the problem, and 2) thermal properties of the product. Numerical code, either developed individually or commercial code, must be checked so that it can provide accurate results. Sometimes, not using the correct settings in the commercially available software can also lead to significant deviation in results. Hence, verification of numerical code is an important step in the modeling.

Thermal properties are often temperature-dependent, as they can change as the temperature is changed. It is relatively easy to measure thermal parameters at room temperature. However, if one requires the thermal parameters at elevated temperatures, there is no instrument currently available that can be used. The quasi-isotherm way of measuring thermal properties is good if the data are needed only a one particular temperature, as the instrument needs to be in equilibrium with

the sample that is being tested. This requirement becomes even more difficult if temperature is > 100^{o}C, as the whole system needs to be pressurized. Achieving equilibrium conditions at such a high temperature is also difficult, and by the time it achieves equilibrium, the sample would be sufficiently degraded to provide little useful information. Hence, an instrument is needed that can measure thermal properties over a wide range of temperatures in a short time.

Food quality is also affected by the thermal processing. Most often there is a negative effect of higher temperatures on nutrients of the food materials. Hence, temperature-dependent thermal properties are needed to design the thermal processes accurately. Nutritional degradation kinetics can be reliable if the mathematical models include the temperature dependence of the thermal properties.

1.2 Objectives of the study

There were three objectives of the study:

1. Develop a method for intrinsic verification in parameter estimation problems and check for accuracy in numerical codes.
2. Design and develop an instrument that can measure thermal properties at elevated temperatures.
3. Compare nutrient degradation in an aseptic processing system and conventional retort processing.

1.3 Overview of the dissertation

The dissertation is divided in four different chapters, excluding the current chapter. Each chapter covers topics related to the objective mentioned above.

1. Chapter 2 – This chapter deals with the topic of intrinsic verification. The dimensionless derivation of sensitivity coefficients is presented with several case studies. The dimensionless derivation is a simple and straightforward approach for deriving the intrinsic sum, which is the sum of all scaled sensitivity coefficients in the model. The intrinsic sum has two significant advantages:
    a. It can help to identify if all parameters can be estimated in a specific mathematical model.
    b. It can be used to verify the large numerical codes.
2. Chapter 3 – The principles presented in this chapter are based on chapter 2, but has been extended to thermal parameters that are temperature-dependent. The derivation is presented with several case studies for heat transfer problems in Cartesian and cylindrical coordinate system.
3. Chapter 4 – A thermal properties measurement instrument (TPCell) is presented with the design and mathematical model. The advantages of the instrument are discussed as to how it compares with currently available instruments. Several food materials were tested and the results are presented in this chapter.

4. Chapter 5 – This chapter is focused around the nutritional studies in an aseptic processing system compared to those in conventional retort processing. Kinetic degradation parameters were analyzed for vitamin degradation and the results are presented.

1.4 Literature Review

Thermal properties of a food material are important for several reasons, such as designing the thermal process and processing equipment. Thermal conductivity measurement poses a challenge as it depends on the structural arrangements as well as chemical composition of the food material (Sweat 1995). Thermal properties also depend on the temperature history of the product. Previous studies have shown that thermal properties can be either predicted using a predictive model or measured by using equipment.

1.4.1 Predictive model

There are several predictive equations proposed for the prediction of thermal conductivity based on the composition of the food material. Choi and Okos proposed the predictive equation for thermal conductivity based on the composition of food materials as given in Eq. (1.1)-(1.7) (Choi and Okos 1986). However, this is valid only in the temperature range of 0 – 90^{o}C.

$$k_{water} = 0.57109 + 1.7625 \times 10^{-3}T - 6.7036 \times 10^{-6}T^2 \quad (1.1)$$

$$k_{CHO} = 0.20141 + 1.3874 \times 10^{-3}T - 4.3312 \times 10^{-6}T^2 \quad (1.2)$$

$$k_{protein} = 0.17881 + 1.1958 \times 10^{-3}T - 2.7178 \times 10^{-6}T^2 \quad (1.3)$$

$$k_{fat} = 0.18071 - 2.7604 \times 10^{-3}T - 1.7749 \times 10^{-7}T^2 \quad (1.4)$$

$$k_{ash} = 0.32961 + 1.4011 \times 10^{-3}T - 2.9069 \times 10^{-6}T^2 \quad (1.5)$$

$$k_{ice} = 2.2196 - 6.2489 \times 10^{-3}T + 1.0154 \times 10^{-6}T^2 \quad (1.6)$$

$$k_{fiber} = 0.18331 + 1.2497 \times 10^{-3}T - 3.1683 \times 10^{-6}T^2 \quad (1.7)$$

1.4.2 Thermal conductivity devices

1.4.2.1 Line heat source method

Devices used for thermal conductivity measurement of food materials are mainly based on the line heat source method. Other methods such as guarded hot plate is not suitable for food materials due to long temperature equilibration time, moisture migration in sample and the need for large sample size (Sweat 1995). The line heat source method requires small sample size and is recommended for food applications (Sweat 1995; Monsenin 1980). Improvement on the construction of the probe and linearity of the temperature versus logarithm of time was done to improve the accuracy of thermal conductivity measurements (Baghe-Khandan and others 1981). A thermal conductivity probe is shown in Figure 1.1.

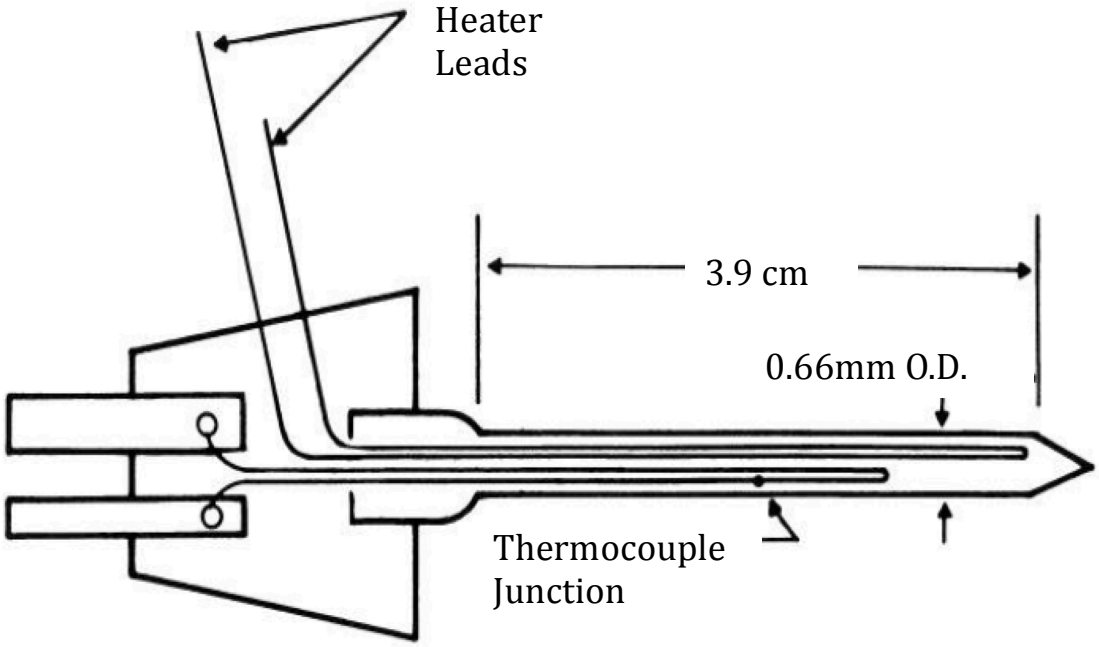

Figure 1.1 A thermal conductivity probe (Sweat 1995)

The theory behind the line heat source method is that the probe heats a sample, initially at uniform temperature. The temperature at the surface of the probe is monitored. After a brief transient phase, the plot of temperature versus the logarithm of time is linear. The slope of this line is given by $Q/4\pi k$. Thermal conductivity can be calculated by Eq. (1.8).

$$k = Q\frac{\ln[(t_2 - t_0)/(t_1 - t_0)]}{4\pi(T_2 - T_1)} \tag{1.8}$$

Several researchers have reported that the position of thermocouple inside the probe does not influence the thermal conductivity measurement (Lentz 1952; Hooper and Lepper 1950; Sweat 1995). Also, for a probe diameter of less than 0.66 mm, it was concluded that the time correction factor was negligible (Sweat 1995).

This type of probe was calibrated with water with 0.5% agar solution and with glycerol.

1.4.2.2 Modified Fitch method

The Fitch device is based on the principles of heat transfer from a sample, kept at uniform temperature at one side and standard copper on the other. Copper is insulated on the other sides. The lumped heat transfer in copper is monitored. The solution to the heat transfer problem is simplified by assuming quasi-steady-state heat transfer through the sample. The thermal conductivity is determined by analyzing the liner portion of the temperature rise (U.S. Department of Agriculture 2013).

1.4.3 Thermal properties at elevated temperatures

Compilations of thermal conductivity of food products are presented in several publications (Qashou and others 1972; Choi and Okos 1983). Most of these values are based on either using the predictive model using compositions of food materials or by using the line heat source method. However, measurements of thermal properties of food materials at elevated temperatures, especially >90°C are scarce (Nesvadba 2005). The problem at elevated temperatures is the moisture migration in and moisture loss from the sample. However, the moisture migration and loss can be minimized by using a pressurized system. The work that has been done at elevated temperatures requires a pressurized sample holder in which the line heat source can be inserted (Shrivastava and Datta 1999). One important criterion of the line heat source method is that the sample and heater must be in equilibrium before starting the test (Sweat 1995). The drift in initial temperature

will produce erroneous thermal conductivity values (Sweat 1995). The line heat source method has advantages in terms of mathematical processing of the results and the control of experimental conditions (Sahin and Sumnu 2006). The disadvantages of this method include a long time to achieve a condition of equilibrium and moisture migration during long tests (Sahin and Sumnu 2006). Using an oil bath to control the temperature inside the pressurized sample cup can take an hour to achieve equilibrium. The equilibrium condition time increases as the temperature of the bath is increased to elevated temperatures, such as 140°C. For example, a test that include measurement at 25°C and one measurement at 140°C, can take at least 2 hours. If several other temperatures are added to the experiment then the time could be >6 hours. One severe disadvantage of this method is that because thermal properties also depend on temperature history, the state of the sample may have been changed dramatically by holding the product at such high temperatures for significantly long time (hours). Therefore, there is a need for a reliable instrument that can measure thermal conductivity of food materials in less time and at elevated temperature that can cover the entire processing range for commercial processes (25^{o}C - 140^{o}C).

1.5 Conclusions

Whenever a mathematical model is used to establish a thermal process for food processing, accurate and reliable thermal properties are needed to ensure good quality and safety of food. Traditional methods of measuring thermal properties at elevated temperatures may not be accurate as the sample degrades significantly

before the measurement can be made. However, there is no instrument currently available that can be used to measure thermal conductivity at elevated temperatures in a short time as compared to six hours using traditional methods.

REFERENCES

REFERENCES

Baghe-Khandan MS, Choi Y, Okos MR. 1981. Improved Line Heat Source Thermal Conductivity Probe. Journal of Food Science 46(5):1430-2.

Choi Y, Okos M. 1983. Thermal properties of liquid foods: review. American Society of Agricultural Engineers, Chicago, Paper No. 83-6516.

Choi Y, Okos M. 1986. Effects of temperature and composition on the thermal properties of foods. Food engineering and process applications 1:93-101.

Hooper F, Lepper F. 1950. Transient heat flow apparatus for the determination of thermal conductivities: National Emergency Training Center.

Lentz C. 1952. A Transient Heat Flow Method of Determining Thermal Conductivity: Application to Insulating Materials. Canadian Journal of Technology 30(6):153-66.

Monsenin N. 1980. Thermal properties of foods and other agricultural materials: CRC Press.

Nesvadba P. 2005. Thermal Properties of Unfrozen Foods. In: Rao MA, Rizvi SS, Datta AK, editors. Engineering properties of foods. Boca Raton, FL: CRC Press.

Qashou M, Vachon R, Touloukian Y. 1972. Thermal conductivity of foods. ASHRAE Trans 78(1):165-83.

Sahin S, Sumnu Slm. 2006. Thermal Properties of Foods. Physical Properties of Foods: Springer New York. p. 107-55.

Shrivastava M, Datta AK. 1999. Determination of specific heat and thermal conductivity of mushrooms (Pleurotus florida). Journal of Food Engineering 39(3):255-60.

Sweat VE. 1995. Thermal properties of foods. In: Rao MA, Rizvi SSH, editors. Food Science and Technology. New York: Marcel Dekker, Inc. p. 99-135.

Chapter 2

Use of Scaled Sensitivity Coefficient Relations for Intrinsic Verification of Numerical Codes and Parameter Estimation

Abstract

Numerical codes are important in providing solutions to partial differential equations in many areas, such as the heat transfer problem. However, verification of these codes is very critical. A methodology is presented in this paper as an intrinsic verification method to the solution to the partial differential equation. Derivation of dimensionless form of scaled sensitivity coefficient has been presented, and the sum of scaled sensitivity coefficients has been used in the dimensionless form to provide a method for verification. Intrinsic verification methodology is demonstrated using examples of heat transfer problems in Cartesian and cylindrical coordinate. The intrinsic verification method presented here is applicable to analytical as well as numerical solutions to partial differential equations.

Keywords: Parameter estimation, Intrinsic verification, Sensitivity coefficients, Inverse problems, Heat transfer, Intrinsic sum

2.1 Introduction

Verification of large numerical codes, such as finite element and finite control volume method, is an important issue. The accuracy of such programs needs to be assured (Beck and others 2006). For example, engineers often rely on simulation for various engineering problems and hence the numerical code that

they use has to be reliable. Accuracy of numerical code is also important in parameter estimation problem.

2.1.1 Numerical code verification

Coding mistakes can lead to serious flaws in the result (Salari and Knupp 2000). There are two aspects of verification; 1) code verification, and 2) code validation. The method presented in this paper deals with the code verification. However, it has potential for the code validation as well.

Some of the methods that have been used in code verification are:

1. Trend – This method is applied to see any trend in the numerical solution of a problem. The solution accuracy is not checked in this method. This method provides only a means to say that the change in solution is in the right direction when a specific parameter in the model is changed (Salari and Knupp 2000).

2. Symmetry – The symmetry method is a check for symmetry in the solution. A problem can be set up so that it provides a symmetric solution. For example, an axi-symmetric problem for cylindrical heating can be employed in the numerical code. If the solution does not produce a symmetrical result, then there is some error in the code (Salari and Knupp 2000).

3. Comparison – In this method, the existing code is compared with another well-established code. A problem is solved using both codes and results are compared to check for accuracy (Salari and Knupp 2000).

4. Exact Solution (MES) – This is a widely used method for code verification. If an exact solution to the partial differential equation can be obtained, it is compared with the numerical result from the code. A criterion is set for the code to achieve to pass the verification process (Roy 2005; Salari and Knupp 2000).

5. Manufactured solution (MMS) – Also widely accepted and used for code verification. In this method, a manufactured solution to a problem is defined and the code is used to solve this manufactured solution. Acceptance criteria should be defined before starting the test (Roy 2005; Salari and Knupp 2000).

Only MES and MMS are appropriate for code verification (Salari and Knupp 2000). The disadvantage of MES is that one must know the exact solution to compare it with the numerical solution. However, in many situations finding an exact solution, such as problems involving nonlinear problems, can be very difficult or not possible at all. There are some disadvantages of MMS for code verification as well. MMS requires arbitrary source terms that have to be incorporated into the code (Roy 2005). Hence, MMS is code-intrusive and cannot be performed on large software where code is not accessible.

In such cases, there is a need for a method that can be relied on to assure the accuracy of the code. That is where the concept of intrinsic verification method (IVM) provides a tool to check the accuracy of the numerical code. Intrinsic verification methods (IVM) provide a convenient way to check accuracy of solutions for such numerical codes (Beck and others 2006). In this paper, IVM for several cases for checking the accuracy of numerical codes has been presented. The idea of IVM presented in this article is based on the scaled sensitivity coefficients. A model-specific identity for a partial differential equation can be derived based on dimensionless analysis of scaled sensitivity coefficients. A good feature of the dimensionless analysis of scaled sensitivity coefficient is that it is simple and can be replicated for various models with less work than other methods. Also, a major advantage of the presented method is that the exact solution of the partial differential equation is not needed. Mistakes in discretization can be detected with the IVM presented in this article. Some examples cases are shown to prove the effectiveness of this method. This method also demonstrates that any minor coding error, such as typographical mistakes, can be detected.

2.1.2 Parameter estimation and sensitivity coefficient

The IVM presented in this paper is a combination of sensitivity coefficients used in verification of numerical codes and parameter estimation. The sensitivity coefficient of a parameter is the first partial derivative of the function involving the parameter, with respect to the parameter (Beck 1970). Consider a simple function:

$$T = f(k, C, x, t) \tag{2.1}$$

where k and C are parameters of the function T.

The sensitivity coefficients of k and C are $\frac{\partial T}{\partial k}$ and $\frac{\partial T}{\partial C}$, respectively. After multiplying sensitivity with its parameter, the scaled sensitivity coefficients are represented by

$$\hat{X}_k = k\frac{\partial T}{\partial k},\ \hat{X}_C = C\frac{\partial T}{\partial C} \tag{2.2}$$

for k and C respectively.

The importance and use of sensitivity coefficients has been discussed and presented by Beck and others (Beck and Arnold 1977a; Blackwell and others 1999; Sun and others 2001; Chen and Tong 2004). Sensitivity coefficients provide considerable insight into the parameter estimation problem (Beck 1967; Dowding and others 1999b). Some of the applications of sensitivity coefficients are in optimal experimental design (Beck 1969; Beck and Woodbury 1998) and parameter estimation (Beck and Arnold 1977a; Dolan and others 2012; Koda and others 1979). Some other insight can be gained. An example is, if the sensitivity coefficient is a function of the parameter, then the estimation problem is nonlinear and should be solved using nonlinear regression techniques (Beck and Arnold 1977a). In that regard, it is also noted that a linear partial differential equation can produce a nonlinear estimation problems.

It can be shown, using the solution of the heat transfer problem, whether the parameters can be estimated individually or as a group. One of the conditions that is necessary in parameter estimation is that the sum of the scaled sensitivity coefficients is not equal to zero. Scaled sensitivity coefficients must not have linear dependence among them. Specifically, if the measured quantity is temperature T, the linear dependence relation

$$A_1\beta_1\frac{\partial T}{\partial \beta_1}+A_2\beta_2\frac{\partial T}{\partial \beta_2}+\cdots+A_p\beta_p\frac{\partial T}{\partial \beta_p}=0 \tag{2.3}$$

where at least one of the coefficients A_i is not zero. The i^{th} scaled sensitivity coefficient is defined to be

$$\beta_i=\beta_i\frac{\partial T}{\partial \beta_i} \tag{2.4}$$

The units must be consistent; one way to have this consistency is to have each A_i coefficient be equal to unity. The Eq. (2.3) shows that such a linear relationship can occur; when it does occur, all the parameters cannot be simultaneously and independently estimated. Hence, relationships between the sensitivity coefficients are important. They are discussed in detail in following sections. The relationship can also be used to provide intrinsic verification as well.

There are three novel concepts presented in this paper:

1. Dimensionless derivation of sums of scaled sensitivity coefficients.

2. Intrinsic verification of numerical codes using sum of scaled sensitivity coefficients.
3. Number of parameters that can be estimated in a model.

Several case studies are presented based on transient heat conduction problems in Cartesian and cylindrical coordinate system with various boundary conditions. Scaled sensitivity summation relations are derived using dimensionless analysis, and its effectiveness is shown for verifying numerical codes.

2.2 Derivation of sensitivity coefficients in one-dimensional heat conduction problem

In the following section, two derivations of scaled sensitivity coefficients are given. The first derivation is the regular way of deriving sensitivity coefficient and the second one is a derivation using dimensionless analysis. The numbering system for heat conduction problems (Beck and Litkouhi 1988) has been used for each of the case studies.

2.2.1 Case 1: One-dimensional transient heat conduction in a flat plate with heat flux on one side and insulated on another (X22B-0T1)

The mathematical model for one-dimensional transient heat conduction in a plate can be given by,

$$k\frac{\partial^2 T}{\partial x^2} = C\frac{\partial T}{\partial t} \qquad 0 < x < L, \;\; t > 0 \tag{2.5}$$

where boundary and initial conditions are

$$-k\frac{\partial T}{\partial x}(0,t)=q_0 f(t) \quad \frac{\partial T}{\partial x}(L,t)=0 \quad T(x,0)=T_0 \tag{2.6}$$

Note that T is a function of (x,L,t,C,T_0,q_0).

The scaled sensitivity coefficients are derived based on the derivatives of Eq. (2.5) (Beck and Arnold 1977a). The dimensionless derivation is discussed later in this section. The sensitivity coefficient for k can be computed by taking the derivative of Eq. (2.5) with respect to k as follows,

$$X_k=\frac{\partial^2 T}{\partial x^2}+k\frac{\partial^2}{\partial x^2}\left(\frac{\partial T}{\partial k}\right)=C\frac{\partial}{\partial t}\left(\frac{\partial T}{\partial k}\right) \tag{2.7}$$

and the initial and boundary conditions can be found by taking the derivatives with respect to k ,of the original boundary conditions given in Eq. (2.6).

$$-\frac{\partial T}{\partial x}(0,t)-k\frac{\partial}{\partial x}\left(\frac{\partial T}{\partial k}\right)(0,t)=0 \qquad \frac{\partial}{\partial x}\left(\frac{\partial T}{\partial k}\right)(L,t)=0 \qquad \frac{\partial T}{\partial k}(x,0)=0 \tag{2.8}$$

Repeating the calculation steps as above for the sensitivity coefficient for parameter C gives;

$$X_C=k\frac{\partial^2}{\partial x^2}\left(\frac{\partial T}{\partial C}\right)=\frac{\partial T}{\partial t}+C\frac{\partial}{\partial t}\left(\frac{\partial T}{\partial C}\right) \tag{2.9}$$

$$-k\frac{\partial}{\partial x}\left(\frac{\partial T}{\partial C}\right)(0,t)=0 \qquad \frac{\partial}{\partial x}\left(\frac{\partial T}{\partial C}\right)(L,t)=0 \qquad \frac{\partial T}{\partial C}(x,0)=0 \tag{2.10}$$

by multiplying and adding kX_k+CX_C , the result is;

$$\Rightarrow \quad k\frac{\partial^2 T}{\partial x^2}+k\frac{\partial^2}{\partial x^2}\left(k\frac{\partial T}{\partial k}+C\frac{\partial T}{\partial C}\right)=C\frac{\partial T}{\partial t}+C\frac{\partial}{\partial t}\left(k\frac{\partial T}{\partial k}+C\frac{\partial T}{\partial C}\right)$$

Since

$$k\frac{\partial^2 T}{\partial x^2}=C\frac{\partial T}{\partial t}$$

these two terms can be eliminated on the left and right sides, respectively:

$$\Rightarrow \quad k\frac{\partial^2}{\partial x^2}\left(k\frac{\partial T}{\partial k}+C\frac{\partial T}{\partial C}\right)=C\frac{\partial}{\partial t}\left(k\frac{\partial T}{\partial k}+C\frac{\partial T}{\partial C}\right) \tag{2.11}$$

the boundary and initial conditions are re-stated from Eq. (2.8) and (2.10):

$$-\frac{\partial T}{\partial x}(0,t)-k\frac{\partial}{\partial x}\left(\frac{\partial T}{\partial k}\right)(0,t)=0 \qquad \frac{\partial}{\partial x}\left(\frac{\partial T}{\partial k}\right)(L,t)=0 \qquad \frac{\partial T}{\partial k}(x,0)=0 \tag{2.12}$$

$$-k\frac{\partial}{\partial x}\left(\frac{\partial T}{\partial C}\right)(0,t)=0 \qquad \frac{\partial}{\partial x}\left(\frac{\partial T}{\partial C}\right)(L,t)=0 \qquad \frac{\partial T}{\partial C}(x,0)=0 \tag{2.13}$$

For $x = 0$, again multiply and add kX_k+CX_C:

$$-k\frac{\partial T}{\partial x}(0,t)-k\frac{\partial}{\partial x}\left(k\frac{\partial T}{\partial k}+C\frac{\partial T}{\partial C}\right)(0,t)=0 \tag{2.14}$$

Setting the first term equal to the flux from Eq. (2.6) yields:

$$\Rightarrow \quad -k\frac{\partial}{\partial x}\left(k\frac{\partial T}{\partial k}+C\frac{\partial T}{\partial C}\right)(0,t)=-q_o \tag{2.15}$$

at $x = L$

$$\frac{\partial}{\partial x}\left(k\frac{\partial T}{\partial k}+C\frac{\partial T}{\partial C}\right)(L,t)=0 \tag{2.16}$$

and at $t = 0$

$$\left(k\frac{\partial T}{\partial k}+C\frac{\partial T}{\partial C}\right)(x,0)=0 \tag{2.17}$$

Using the initial condition, Eq. (2.17) can be written as follows,

$$k\frac{\partial T}{\partial k}+C\frac{\partial T}{\partial C}=-(T-T_0) \tag{2.18}$$

Equation (2.18) provides an important relationship of scaled sensitivity coefficients of the parameters in the model given by Eq. (2.5). The larger the difference in $T(x,t)-T_o$, the greater will be the magnitude of the scaled sensitivity coefficients. Larger scaled sensitivity coefficients are desired to have a good estimate of the parameters with lower standard error. Because the right side of Eq. (2.18) is non-zero, it also suggests that the sensitivity coefficients might be uncorrelated and hence could be identified uniquely. When right side of Eq. (2.18) is equal to zero, it is not possible to independently estimate k and C from data obtained from the related experiment.

2.2.1.1 Dimensionless analysis of sensitivity coefficient

In this section, dimensionless derivation of sensitivity coefficient is presented. The heat transfer model is made dimensionless by using dimensionless groups and the sensitivity coefficients are derived. For the same model and boundary conditions given by Eq. (2.5), the model in a dimensionless form and then derive the sensitivity relation. Let

$$\tilde{x} \equiv \frac{x}{L},\ \tilde{t} \equiv \frac{kt}{CL^2},\ \tilde{T} \equiv \frac{T - T_0}{\frac{q_0 L}{k}} \tag{2.19}$$

The dimensionless scaled sensitivity coefficient is represented by Eq. (2.20).

$$\tilde{X} = \frac{\beta_i}{\left(q_0 L / k\right)} \frac{\partial T}{\partial \beta_i} \tag{2.20}$$

With model and with a known and fixed boundary heat flux, the dimensionless temperature is given symbolically by

$$\tilde{T} = \tilde{T}(\tilde{x}, \tilde{t}) \tag{2.21}$$

Now the partial derivatives of temperature T are found. Notice that

$$T - T_0 = \frac{q_0 L}{k} \tilde{T}\left(\tilde{x}, \tilde{t}(k, C)\right) \tag{2.22}$$

Using the chain rule of differentiation, the derivative with respect to k is

$$\left.\frac{\partial T}{\partial k}\right|_C = -\frac{q_0 L}{k^2}\tilde{T} + \frac{q_0 L}{k}\left[\left.\frac{\partial \tilde{T}}{\partial \tilde{t}}\right|_C \frac{\partial \tilde{t}}{\partial k}\right]$$

$$k\left.\frac{\partial T}{\partial k}\right|_C = -\frac{q_0 L}{k}\tilde{T} + \frac{q_0 L}{k}\left[\tilde{t}\left.\frac{\partial \tilde{T}}{\partial \tilde{t}}\right|_C\right] \tag{2.23}$$

Similarly, the scaled sensitivity coefficients for C is

$$C\left.\frac{\partial T}{\partial C}\right|_k = \frac{q_0 L}{k}\left[-\tilde{t}\left.\frac{\partial \tilde{T}}{\partial \tilde{t}}\right|_k\right] \tag{2.24}$$

Adding Eqs. (2.23) and (2.24) gives

$$k\left.\frac{\partial T}{\partial k}\right|_C + C\left.\frac{\partial T}{\partial C}\right|_k = -\frac{q_0 L}{k}\tilde{T} + \frac{q_0 L}{k}\left[\tilde{t}\left.\frac{\partial \tilde{T}}{\partial \tilde{t}}\right|_C\right] + \frac{q_0 L}{k}\left[-\tilde{t}\left.\frac{\partial \tilde{T}}{\partial \tilde{t}}\right|_k\right] = -\frac{q_0 L}{k}\tilde{T} \tag{2.25}$$

which can be expressed as,

$$k\left.\frac{\partial T}{\partial k}\right|_C + C\left.\frac{\partial T}{\partial C}\right|_k = -(T - T_0) \tag{2.26}$$

Equation (2.18) is same as the Eq. (2.26), which was derived using dimensionless analysis. Dimensionless analysis is very powerful, as one does not need to find exact derivatives for complex problems. It simplifies the problem of obtaining the relationship of sum of scaled sensitivity coefficients as shown in Eq. (2.26). A number of applications of Eq. (2.26) can be cited. It can be used in

parameter estimation. It indicates that it might be possible to simultaneously estimate all of the thermal properties, k and C in a related experiment.

Also, Eq. (2.18) can be written as,

$$k\frac{\partial T}{\partial k}+C\frac{\partial T}{\partial C}+(T-T_0)=0 \tag{2.27}$$

In this form, Eq. (2.27) is termed as Intrinsic Sum (IS). It is a relation that can be used to provide intrinsic verification of finite element and finite control volume computer codes for heat conduction. Note that Eq. (2.3) (sum of scaled sensitivity coefficients = 0) is not satisfied by Eq. (2.26), since the sum of the scaled sensitivity coefficients of k and C is not zero.

An important application is to verify large numerical codes. The verification can be obtained by using the code to generate the sensitivity coefficients by using finite differences, such as

$$\begin{aligned} k\left.\frac{\partial T}{\partial k}\right|_C &\approx k\frac{T(x,t,(1+\delta)k,C)-T(x,t,k,C)}{(1+\delta)k-k} \\ &\approx \frac{T(x,t,(1+\delta)k,C)-T(x,t,k,C)}{\delta} \end{aligned} \tag{2.28}$$

where δ is a small value such as 0.0001. This is a forward difference first order approximation. A more accurate central difference could be used. The second order approximation for the scaled sensitivity coefficient (Dunker 1984) can be expressed as,

$$k\left.\frac{\partial T}{\partial k}\right|_C \approx \frac{T(x,t,(1+\delta)k,C)-T(x,t,(1-\delta)k,C)}{2\delta} \tag{2.29}$$

For simplicity in notation, let

$$T_{\delta k} = T(x,t,(1+\delta)k,C) \tag{2.30}$$

Then using the forward difference approximation as given by Eq. (2.28) in Eq. (2.26) gives

$$\frac{T_{\delta k}-T}{\delta}+\frac{T_{\delta C}-T}{\delta}+(T-T_0)\approx 0 \tag{2.31}$$

or

$$\frac{T_{\delta k}}{\delta}+\frac{T_{\delta C}}{\delta}-\frac{2T}{\delta}+(T-T_0)\approx 0 \tag{2.32}$$

Finally after re-arranging,

$$T_{\delta k}+T_{\delta C}-2T+\delta(T-T_0)\approx 0 \tag{2.33}$$

Recall that Eq. (2.33) is for the case when the heat flux is known and the thermal properties are constant. Equation (2.33) is the important equation to use for intrinsic verification for this problem. It requires only three complete computations, one for *T*, one for $T_{\delta k}$, and finally for $T_{\delta C}$. The summation can be evaluated over the complete domain of the problem to see if it indeed is nearly equal to zero for all locations and times of the numerical solution.

For the situations where the step size δ can be very small, a more accurate sensitivity coefficient can be obtained using method of complex variables (Martins and others 2000).

$$k\frac{\partial T}{\partial k}\bigg|_C \approx \frac{\mathrm{Im}(T(x,t,(1+i\delta)k,C))}{\delta} \tag{2.34}$$

One of the major advantages of using complex variable for calculating sensitivity coefficients is that the truncations error is minimized, as there is no difference involved in numerator of Eq. (2.34) as compared to finite difference method (Martins and others 2000). However, in this article finite difference methods have been used to calculate sensitivity coefficients.

The following values, which are typical for foods, are considered as an example for each of the cases. Dimensionless scaled sensitivity coefficients are calculated for k = 0.5 W/mK, C = 3.5x10^6 J/m^{3}K, T_0 = 20^{o}C, δ = 0.0001, x/L =0, L = 20 mm, $\Delta x / L = 0.02$, $\alpha \Delta t / L = 3.5714 \times 10^{-05}$. The maximum temperature rise = 100°C. A finite element code (COMSOL®) is used to demonstrate the concepts. An analytical solution is not needed for this intrinsic verification case. Problem explained in case 1 is solved numerically and the relationship given by eq. (2.33) is calculated.

Dimensionless scaled sensitivity coefficients for k and C are shown in Fig. 2.1 at the heated surface. Note that the shapes of two curves are equal for a

dimensionless time of 0.2. This suggests that they are linearly dependent or correlated. Hence, an experiment performed for dimensionless time <0.2, it will not be possible to estimate both parameters. For dimensionless time >0.2, the value of $\tilde{X}_k$ goes to a constant value and $\tilde{X}_C$ keeps increasing. Hence, to estimate both parameters, the experiment has to be performed at least for $\tilde{t}$ of 0.6. However, since $\tilde{X}_C$ is larger the standard error will be lower than that for $\tilde{X}_k$.

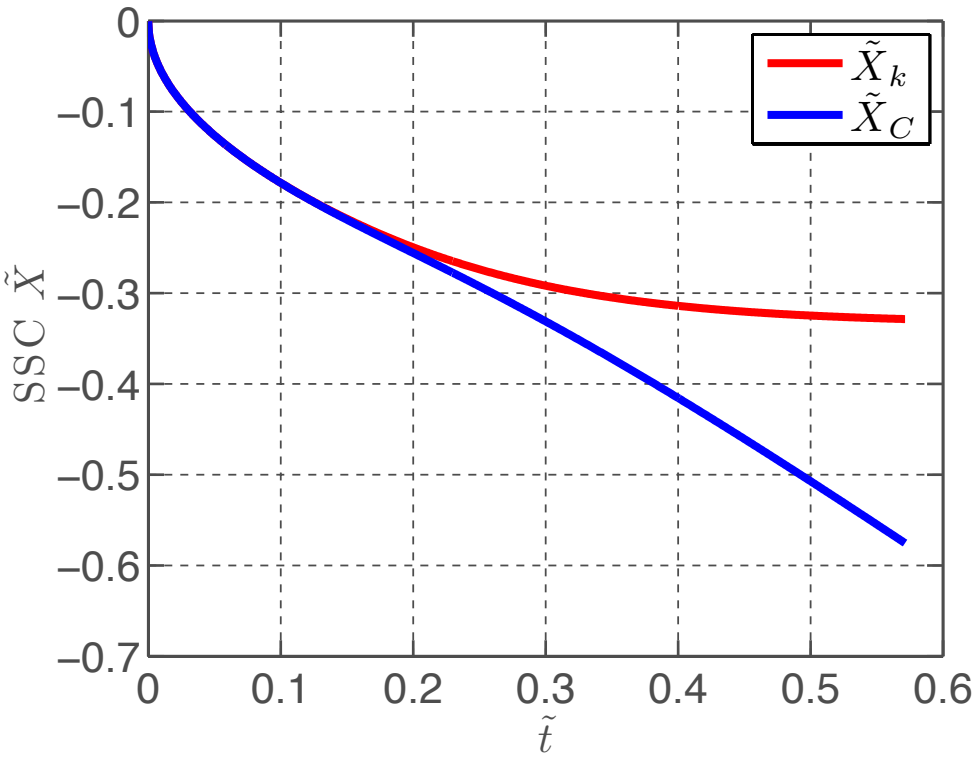

Figure 2.1 Dimensionless scaled sensitivity coefficient for *k* and *C* in case 1: X22B10T0, for *k* = 0.5 W/mK, *C* = 3.5x10^6 J/m^{3}K, delta = 0.0001, x/L =0, $\Delta x / L = 0.02$ (For interpretation of the references to color in this and all other figure, the reader is referred to the electronic version of this dissertation.)

Table 2.1 Solutions to the heat transfer problems in case 1: X22B10T1 with first order approximation

t	x	δ	$\tilde{T}$	$\tilde{X}_k$	$\tilde{X}_C$	I_S
0.1	0	0.0001	0.36386368	-0.18189423	-0.18194214	-0.0032773
0.21	0	0.0001	0.51386064	-0.25315515	-0.26066516	-0.00483891
0.31	0	0.0001	0.63351296	-0.29462794	-0.33883058	-0.00653256
0.41	0	0.0001	0.74245078	-0.31578265	-0.42659962	-0.00822166
0.52	0	0.0001	0.84751112	-0.32568253	-0.52174708	-0.00978089

Table 2.1 shows the scaled sensitivity calculation using the first order derivative mentioned in Eq. (2.28). Scaled sensitivity coefficients values are presented along with the time, position, delta and temperature rise. In the last column the absolute sum of scaled sensitivity coefficient is presented after subtracting with the temperature rise (Eq. (2.26)). The values are very close to zero as expected, which suggests that the finite element program has passed the intrinsic verification test.

Table 2.2 Solutions to the heat transfer problems in case 1: X22B10T1 with second order approximation

t	x	δ	$\tilde{T}$	$\tilde{X}_k$	$\tilde{X}_C$	I_S
0.1	0	0.0001	0.36386368	-0.18190788	-0.1819558	0.00000029
0.21	0	0.0001	0.51386064	-0.25317494	-0.2606857	0.00000046
0.31	0	0.0001	0.63351296	-0.29465296	-0.33886001	0.00000067
0.41	0	0.0001	0.74245078	-0.31581137	-0.42663942	0.0000009
0.52	0	0.0001	0.84751112	-0.32571349	-0.52179764	0.00000113

However, the values of I_S can be improved by using a more accurate second order approximation as mentioned in Eq. (2.29). The values for the second order

approximation are presented in Table 2.2. The I_S is plotted in Figure 2.2 and note that the values are increasing over time. Comparing the values of I_S in Table 2.1 for first order and Table 2.2 for second order approximation, the difference is quite large. Second order approximation provides better accuracy than the first order approximation. Again, the finite element code has passed the intrinsic verification process.

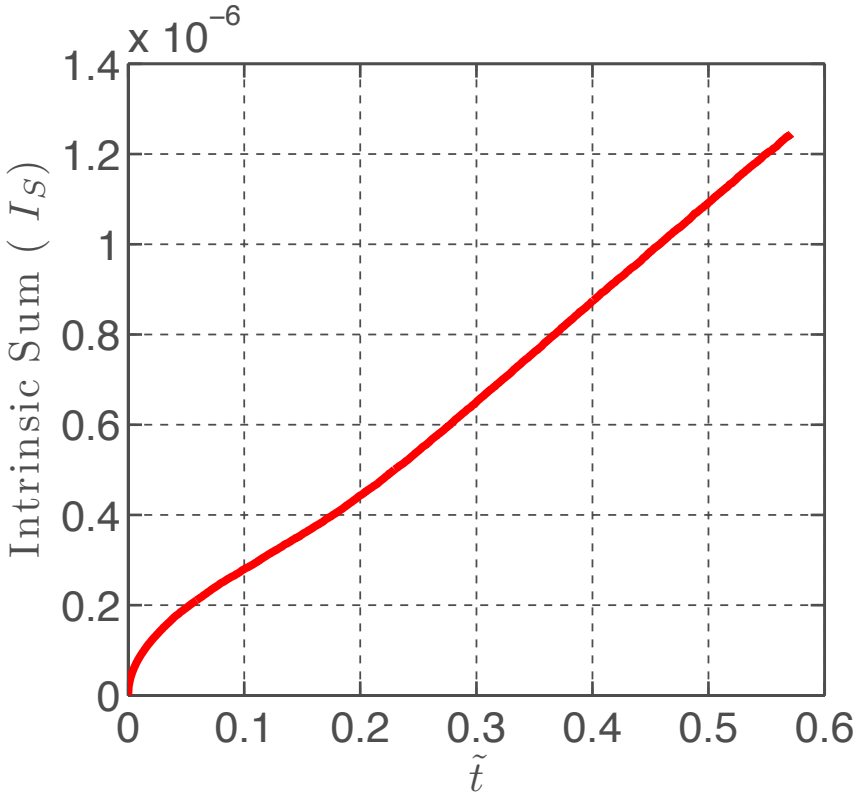

Figure 2.2 Plot of I_S in case 1: X22B10T0, using 2nd-order finite difference

So far IVM has worked well and showed that the finite element model was adequate. To show the strength of the IVM, consider a small imperfection in the finite element method. To demonstrate this, an unrefined model is considered with

the refined model in case 1. The initial finer time step from the finite element program was eliminated to create the unrefined model. In the refined model, this initial fine time step size was 0.0001 sec. However, make this as 0.1 sec, which is same as the time step of solution method. The result from this imperfection is presented in Figure 2.3. There is substantial error in the unrefined model as compared to the refined model. This error would not have been obvious without the use of IVM. Also, during the parameter estimation problem the unrefined model would not provide good estimates of the parameters and would have a signature in residuals, large root mean squared error and large standard error of the parameters.

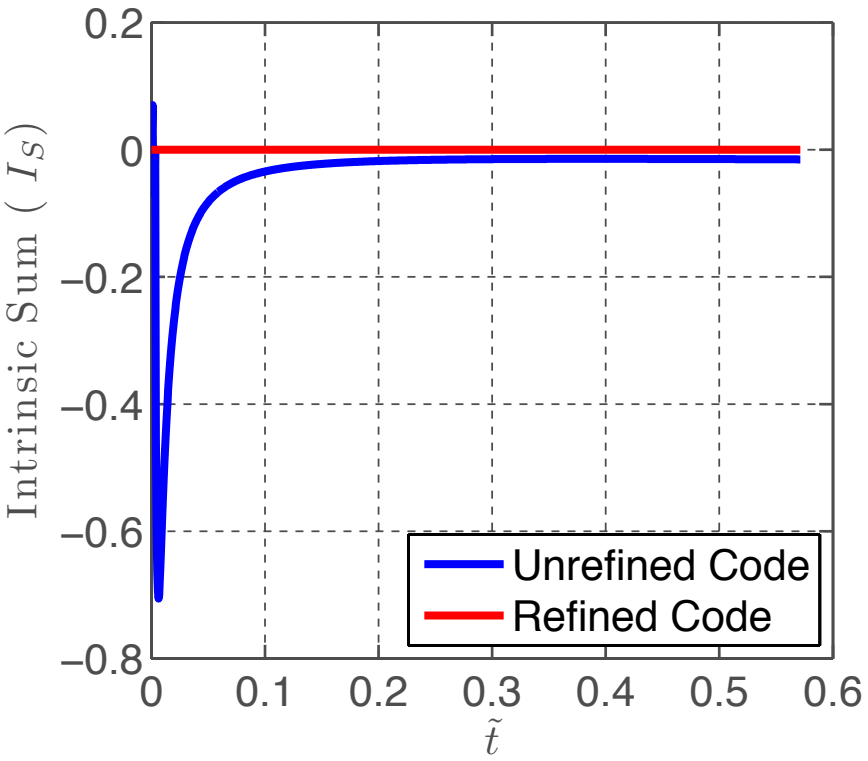

Figure 2.3 Plot of I_S in case 1: X22B10T0 with refined and unrefined finite element code

2.2.2 Case 2: One-dimensional transient heat conduction in a flat plate with time varying temperature on one side and insulated on another (X12B-0T1)

In this case, I_S is derived with a different boundary condition. If the non-homogeneous boundary condition of a given heat flux in Eq. (2.6) were replaced by

$$T(0,t) = T_1 + (T_0 - T_1) f(t) \tag{2.35}$$

A significantly different relation than Eq. (2.26) is obtained. In this case the $\tilde{T}$ function is defined by

$$\tilde{T} = \frac{T - T_1}{T_0 - T_1} \tag{2.36}$$

Notice that now Eq. (2.22) becomes

$$T - T_1 = (T_0 - T_1)\tilde{T}\left(\tilde{x}, \tilde{t}(k, C)\right) \tag{2.37}$$

The scaled sensitivity coefficient for k is

$$\left.\frac{\partial T}{\partial k}\right|_C = (T_0 - T_1)\left[\left.\frac{\partial \tilde{T}}{\partial \tilde{t}}\right|_C \frac{\partial \tilde{t}}{\partial k}\right]$$

$$\left. k\frac{\partial T}{\partial k}\right|_C = (T_0 - T_1)\left[\tilde{t}\left.\frac{\partial \tilde{T}}{\partial \tilde{t}}\right|_C\right] \tag{2.38}$$

The sensitivity coefficient for C is

$$\left. C\frac{\partial T}{\partial C}\right|_k = (T_0 - T_1)\left[-\tilde{t}\left.\frac{\partial \tilde{T}}{\partial \tilde{t}}\right|_k\right] \tag{2.39}$$

and Eq. (2.26) becomes

$$\left. k\frac{\partial T}{\partial k}\right|_C + \left. C\frac{\partial T}{\partial C}\right|_k = 0 \tag{2.40}$$

Comparing Eq. (2.40) with (2.26), the only difference is that the right-hand side of Eq. (2.40) is zero. Equation (2.40) demonstrates linear dependence as given by Eq. (2.3). Hence, in this case the parameters k and C cannot be estimated uniquely and simultaneously (Figure 2.4). Only a combination of parameters, such as thermal diffusivity, can be estimated. The numerical values are represented in Table 2.3.

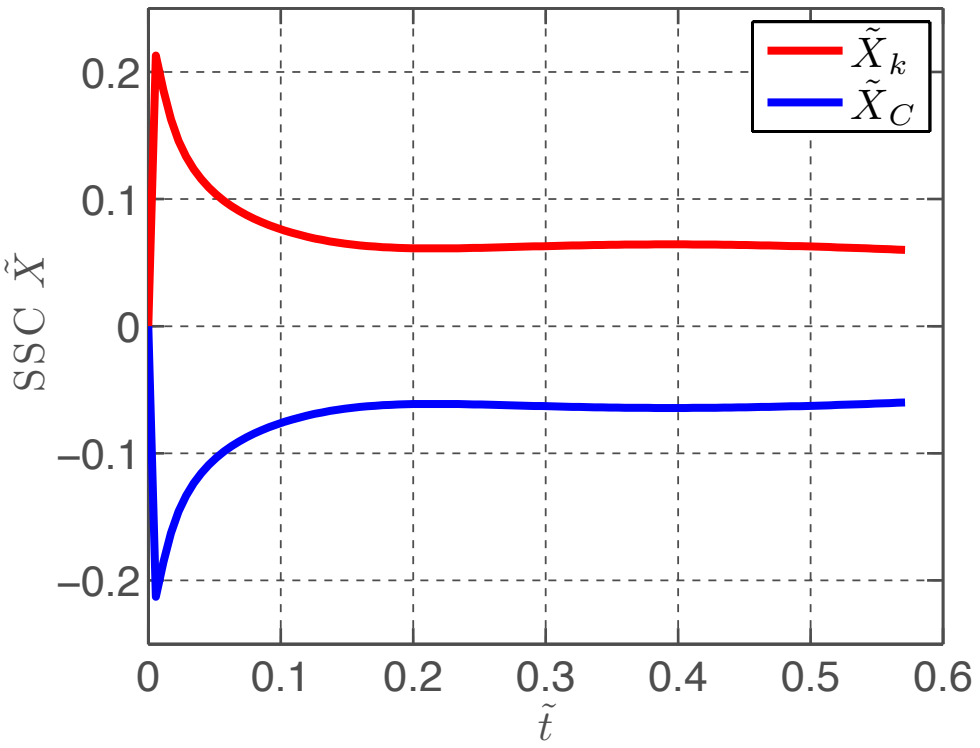

Figure 2.4 Scaled sensitivity coefficients for *k* and *C* in case 2: X12B10T0

Table 2.3 Solutions to the heat transfer problems in Case 2: X12B10T1

t	x	δ	$\tilde{T}$	$\tilde{X}_k$	$\tilde{X}_C$	I_S
0.1	0.5	0.0001	0.72316561	0.07492805	-0.07492805	0.00000003
0.21	0.5	0.0001	0.76868147	0.06123446	-0.06123446	0.00000013
0.31	0.5	0.0001	0.79366186	0.06322003	-0.06322003	0.00000019
0.41	0.5	0.0001	0.81201048	0.06426641	-0.06426641	0.00000023
0.52	0.5	0.0001	0.8261412	0.0621557	-0.0621557	0.00000026

2.2.3 Case 3: Scaled sensitivity relation for one-dimensional transient heat conduction in a cylindrical coordinate system for boundary condition of second kind (R22B10T1)

So far, case studies with the dimensionless analysis and scaled sensitivity coefficient relationships in the Cartesian coordinate system are presented. Given the boundary conditions are same, the relation still holds true for cylindrical coordinate system. This will be demonstrated by showing different cases. Let us consider a hollow cylinder with inner radius R_1 and outer radius R_2.

For the model;

$$\frac{k}{r}\frac{\partial}{\partial r}\left(r\frac{\partial T}{\partial r}\right)=C\frac{\partial T}{\partial t} \qquad R_1<r<R_2,\ \ t>0 \tag{2.41}$$

Where boundary and initial conditions are

$$-k\frac{\partial T}{\partial r}(R_1,t)=q_o \quad \frac{\partial T}{\partial r}(R_2,t)=0 \quad T(r,0)=T_1 \tag{2.42}$$

Note that T is a function of (r,R,t,C,T_0,q_0).

$$\tilde{r}\equiv\frac{r}{R_1},\tilde{R}_2\equiv\frac{R_2}{R_1},\ \tilde{t}\equiv\frac{kt}{CR_1{}^2},\ \tilde{T}\equiv\frac{T-T_1}{\frac{q_0R_1}{k}} \tag{2.43}$$

With this model and with a known and fixed boundary heat flux, the dimensionless temperature is given symbolically by

$$\tilde{T} = \tilde{T}(\tilde{r}, \tilde{R}_2, \tilde{t}) \tag{2.44}$$

Now the partial derivatives of temperature T are found. Notice that

$$T - T_1 = \frac{q_0 R_1}{k} \tilde{T}\left(\tilde{r}, \tilde{R}_2, \tilde{t}(k, C)\right) \tag{2.45}$$

The derivative with respect to k is

$$\begin{aligned} \left.\frac{\partial T}{\partial k}\right|_C &= -\frac{q_0 R_1}{k^2} \tilde{T} + \frac{q_0 R_1}{k}\left[\left.\frac{\partial \tilde{T}}{\partial \tilde{t}}\right|_C \frac{\partial \tilde{t}}{\partial k}\right] \\ k\left.\frac{\partial T}{\partial k}\right|_C &= -\frac{q_0 R_1}{k} \tilde{T} + \frac{q_0 R_1}{k}\left[\tilde{t}\left.\frac{\partial \tilde{T}}{\partial \tilde{t}}\right|_C\right] \end{aligned} \tag{2.46}$$

The sensitivity coefficients for C is

$$C\left.\frac{\partial T}{\partial C}\right|_k = \frac{q_0 R_1}{k}\left[-\tilde{t}\left.\frac{\partial \tilde{T}}{\partial \tilde{t}}\right|_k\right] \tag{2.47}$$

Adding Eqs. (2.46) and (2.47) gives

$$k\left.\frac{\partial T}{\partial k}\right|_C + C\left.\frac{\partial T}{\partial C}\right|_k = -\frac{q_0 R_1}{k} \tilde{T} + \frac{q_0 R_1}{k}\left[\tilde{t}\left.\frac{\partial \tilde{T}}{\partial \tilde{t}}\right|_C\right] + \frac{q_0 R_1}{k}\left[-\tilde{t}\left.\frac{\partial \tilde{T}}{\partial \tilde{t}}\right|_k\right] = -\frac{q_0 R_1}{k} \tilde{T} \tag{2.48}$$

which can be expressed as,

$$k\left.\frac{\partial T}{\partial k}\right|_C + C\left.\frac{\partial T}{\partial C}\right|_k = -(T - T_1) \tag{2.49}$$

Even in the case of a cylindrical coordinate system for same boundary conditions, the relationship of scaled sensitivity (Eq. (2.49)) coefficients is the same as in the Cartesian coordinate system (Eq. (2.26)). In this case as well, since the sum of scaled sensitivity coefficients is not zero, the parameters can be estimated uniquely and simultaneously. It can be seen from Fig. 2-5 that the shapes of $\tilde{X}_k$ are very different form that of $\tilde{X}_C$. Also, the magnitude of $\tilde{X}_k$ keeps increasing with time more than $\tilde{X}_C$, suggesting that in this case thermal conductivity can be estimated with good accuracy. Also, as compared to the X22B10T1 problem, R22B10T1 provides a solution where the estimation of *k* and *C* might be possible for even smaller times. This is possible because of the shape of $\tilde{X}_k$ and $\tilde{X}_C$. For the dimensionless time of <0.2, $\tilde{X}_k$ and $\tilde{X}_C$ are correlated in X22B10T1 and uncorrelated in R22B10T1.

The intrinsic verification identity given by Eq. (2.49) is shown in Table 2.4 as I_S. The finite element code again has done well in this case. The values of the identity are very small and can be safely assumed to be approximately zero. For checking the effectiveness of this identity, an unrefined model was created by not refining the initial time steps. The resulting values are plotted in Fig. 2.6. The unrefined model will not produce good results and also will not do very well when one tries to estimate parameters based on this model. These kinds of imperfections in large numerical code can be easily detected by the use of IVM.

Table 2.4 Solutions to the heat transfer problems in Case 3: R22B10T1

t	x	δ	$\tilde{T}$	$\tilde{X}_k$	$\tilde{X}_C$	I_S
0.1	0	0.0001	0.38364793	-0.24094645	-0.14270148	0.00000025
0.21	0	0.0001	0.50257048	-0.28473387	-0.21783661	0.00000043
0.31	0	0.0001	0.60869499	-0.29227133	-0.31642366	0.00000053
0.41	0	0.0001	0.71356111	-0.29333138	-0.42022974	0.00000059
0.52	0	0.0001	0.81830343	-0.293467	-0.52483643	0.00000063

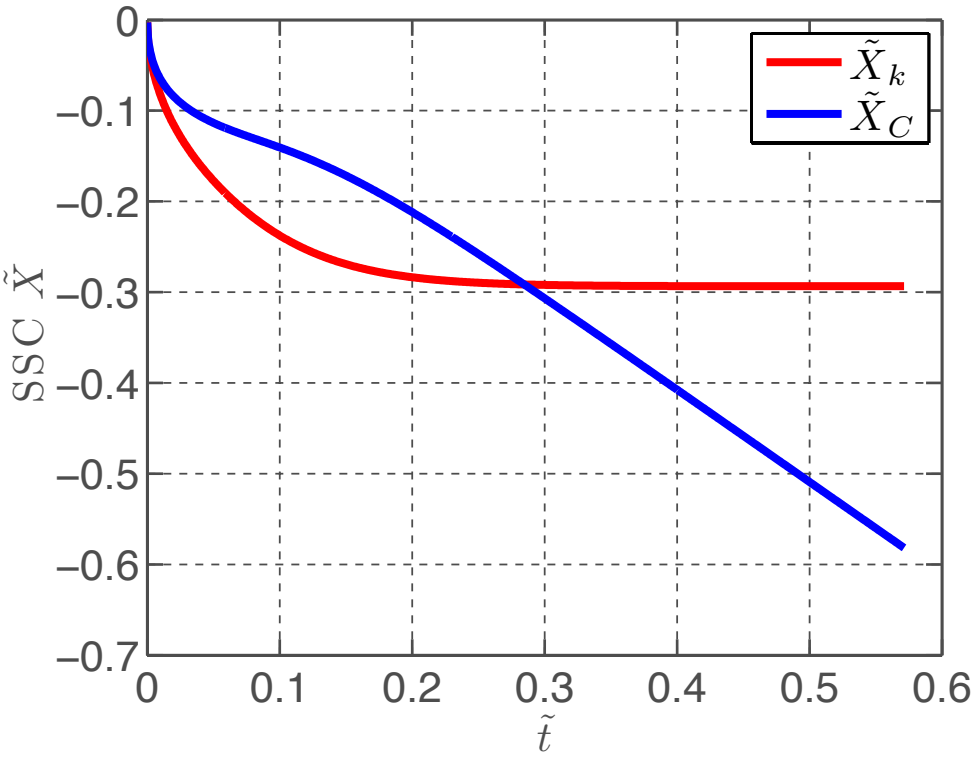

Figure 2.5 Scaled sensitivity coefficients for *k* and *C* in case 3: R22B10T0

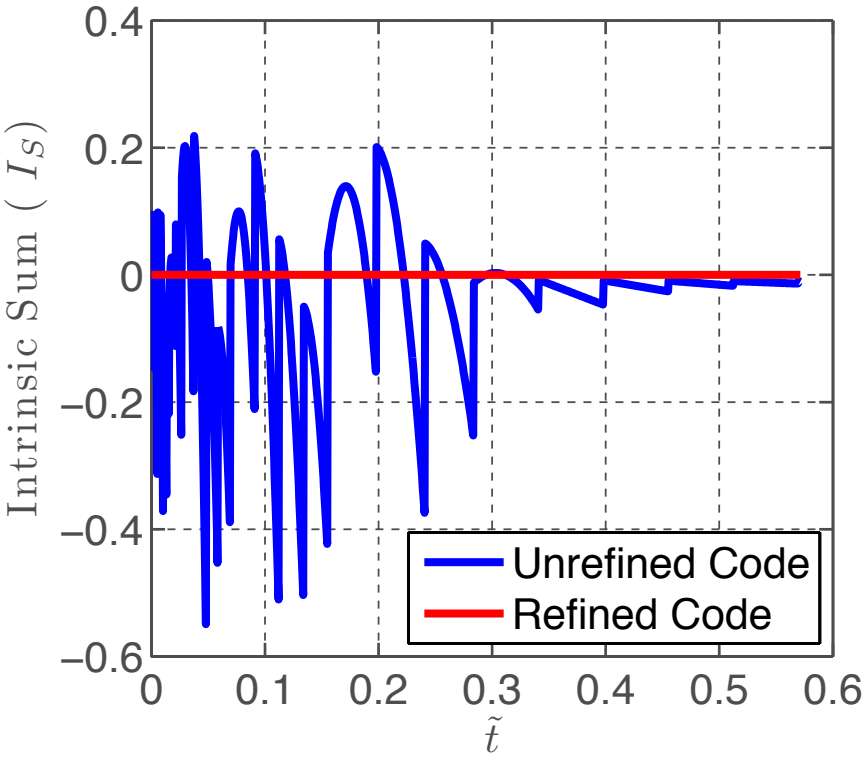

Figure 2.6 Plot of I_S in case 3: R22B10T0 with refined and unrefined finite element code.

2.2.4 Case 4: Scaled sensitivity relation for one-dimensional transient heat conduction in a cylindrical coordinate system for boundary condition of first kind (R12B10T1)

In this case, scaled sensitivity relation with a different boundary condition is investigated. If the non-homogeneous boundary condition of a given heat flux in Eq. (2.42) were replaced by

$$T(R,t) = T_1 + (T_0 - T_1) f(t) \tag{2.50}$$

In this case the $\tilde{T}$ function is defined by

$$\tilde{T} = \frac{T - T_1}{T_0 - T_1} \tag{2.51}$$

Notice that now Eq. (2.22) becomes

$$T - T_1 = (T_0 - T_1)\tilde{T}\left(\tilde{r}, \tilde{R}_2, \tilde{t}(k, C)\right) \tag{2.52}$$

The scaled sensitivity coefficients for k is

$$\begin{aligned} \left.\frac{\partial T}{\partial k}\right|_C &= (T_0 - T_1)\left[\left.\frac{\partial \tilde{T}}{\partial \tilde{t}}\right|_C \frac{\partial \tilde{t}}{\partial k}\right] \\ k\left.\frac{\partial T}{\partial k}\right|_C &= (T_0 - T_1)\left[\tilde{t}\left.\frac{\partial \tilde{T}}{\partial \tilde{t}}\right|_C\right] \end{aligned} \tag{2.53}$$

The sensitivity coefficients for C is

$$C\left.\frac{\partial T}{\partial C}\right|_k = (T_0 - T_1)\left[-\tilde{t}\left.\frac{\partial \tilde{T}}{\partial \tilde{t}}\right|_k\right] \tag{2.54}$$

Adding Eqss. (2.53) and (2.54) gives

$$k\left.\frac{\partial T}{\partial k}\right|_C + C\left.\frac{\partial T}{\partial C}\right|_k = 0 \tag{2.55}$$

Comparing Eq. (2.55) with (2.40), the sum of scaled sensitivity coefficients are equal to zero. The cylindrical coordinate system and the Cartesian coordinate system have same result. Both of these equations show linear dependence as given by Eq. (2.3). Hence, in this case also the parameters k and C cannot be estimated simultaneously (Fig. 2.7). Only a combination of parameters, such as thermal diffusivity, can be estimated. Sum of scaled sensitivity coefficients as given by Eq. (2.55) is zero and it is shown in Table 2.5.

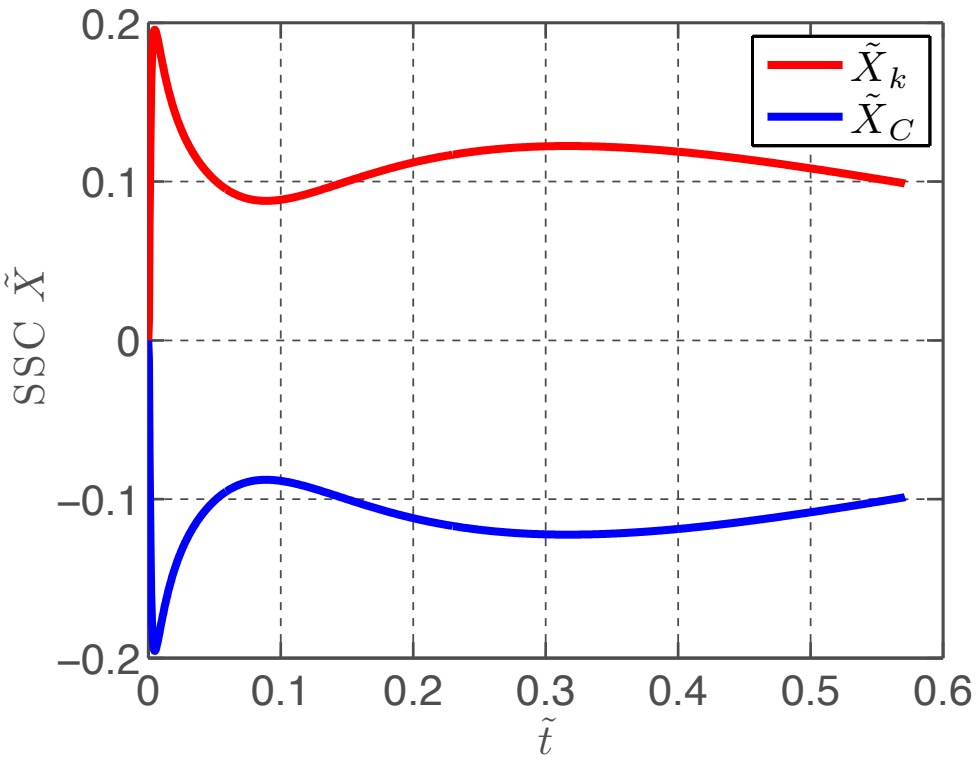

Figure 2.7 Scaled sensitivity coefficient for k and C in case 4: R12B10T0

2.2.5 Case 5: Scaled sensitivity relation for one-dimensional transient heat conduction in a cylindrical coordinate system for boundary condition of third kind (R32B10T1)

In this case, the I_S is derived with a convective boundary condition. If the non-homogeneous boundary condition of a given heat flux in Eq. (2.42) were replaced by

In this case, the I_S is derived with a convective boundary condition. If the non-homogeneous boundary condition of a given heat flux in Eq. (2.42) were replaced by

$$-k\frac{\partial T}{\partial r}(R_1,t)=h\left(T(R_1,t)-T_\infty\right) \tag{2.56}$$

In this case the $\tilde{T}$ function is defined by

$$\tilde{T}=\frac{T}{T_\infty} \tag{2.57}$$

Notice that by using the dimensionless form of equations, Eq. (2.56) becomes

$$\frac{\partial \tilde{T}}{\partial \tilde{r}}(1,\tilde{t})=\tilde{h} \tag{2.58}$$

Where, $\tilde{h}=\frac{hR_1}{k}$

Which leads to the following temperature relation:

$$T = \left(T_\infty\right)\tilde{T}\left(\tilde{r}, \tilde{R}_2, \tilde{t}(k,C), \tilde{h}\right) \tag{2.59}$$

The derivative with respect to *k* is

$$\left.\frac{\partial T}{\partial k}\right|_{C,h} = T_\infty\left[\left.\frac{\partial \tilde{T}}{\partial \tilde{t}}\right|_{C,h}\frac{\partial \tilde{t}}{\partial k} + \left.\frac{\partial \tilde{T}}{\partial \tilde{h}}\right|_{C,h}\frac{\partial \tilde{h}}{\partial k}\right]$$

$$k\left.\frac{\partial T}{\partial k}\right|_{C,h} = T_\infty\left[\tilde{t}\left.\frac{\partial \tilde{T}}{\partial \tilde{t}}\right|_{C,h} - \tilde{h}\left.\frac{\partial \tilde{T}}{\partial \tilde{h}}\right|_{C,h}\right] \tag{2.60}$$

The scaled sensitivity coefficients for *C* is

$$C\left.\frac{\partial T}{\partial C}\right|_{k,h} = T_\infty\left[-\tilde{t}\left.\frac{\partial \tilde{T}}{\partial \tilde{t}}\right|_{k,h}\right] \tag{2.61}$$

The scaled sensitivity coefficients for *h* is

$$h\left.\frac{\partial T}{\partial h}\right|_{k,C} = T_\infty\left[\tilde{h}\left.\frac{\partial \tilde{T}}{\partial \tilde{h}}\right|_{k,C}\right] \tag{2.62}$$

Adding Eqss. (2.60), (2.61) and (2.62) provides,

$$k\left.\frac{\partial T}{\partial k}\right|_{C,h} + C\left.\frac{\partial T}{\partial C}\right|_{k,h} + h\left.\frac{\partial T}{\partial h}\right|_{C,h} = 0 \tag{2.63}$$

With the convective boundary condition, the sum of scaled sensitivity coefficients is equal to zero (Eq. (2.63)). Hence, in this case the parameters *k*, *C* and *h* cannot be estimated uniquely and simultaneously. For a value of *h* = 1000 W/m^2-K, the $\tilde{X}_k, \tilde{X}_C$ and $\tilde{X}_h$ are shown in Fig. 2.8. For very large values of *h*, the boundary condition tends to be same as a temperature boundary condition and in that case the $\tilde{X}_h$ is very small and $\tilde{X}_k$ and $\tilde{X}_C$ are highly correlated. The sum of scaled sensitivity coefficients is presented in Fig. 2.9.

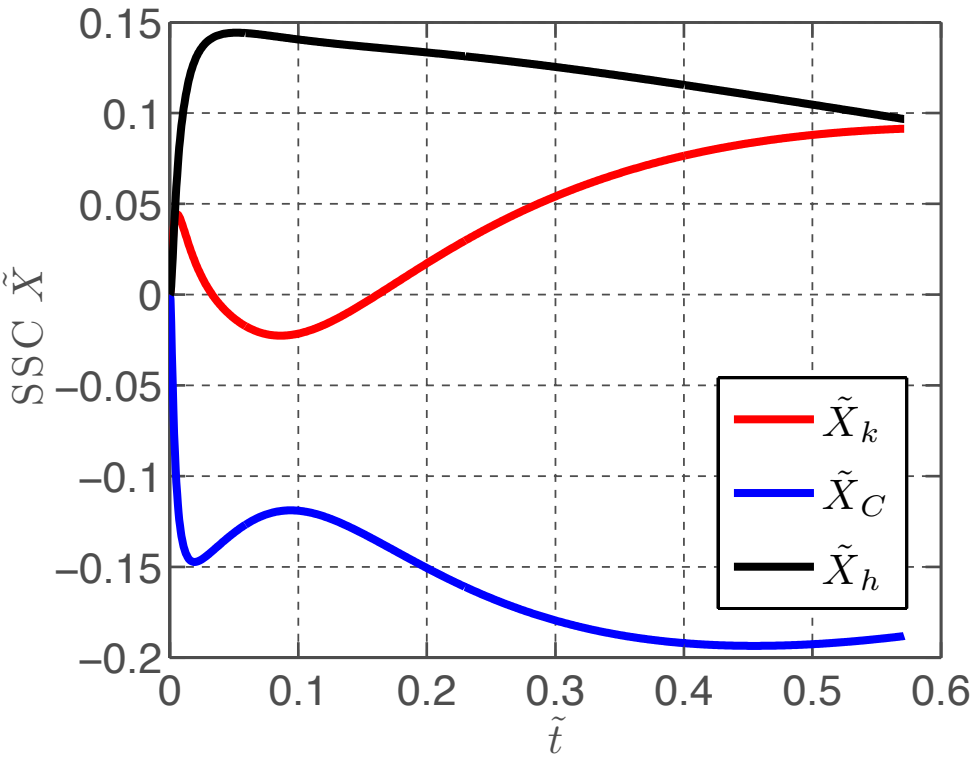

Figure 2.8 Scaled sensitivity coefficients for *k, C* and *h* in case 5: R32B10T0 with *h* = 1000 W/m^2-K

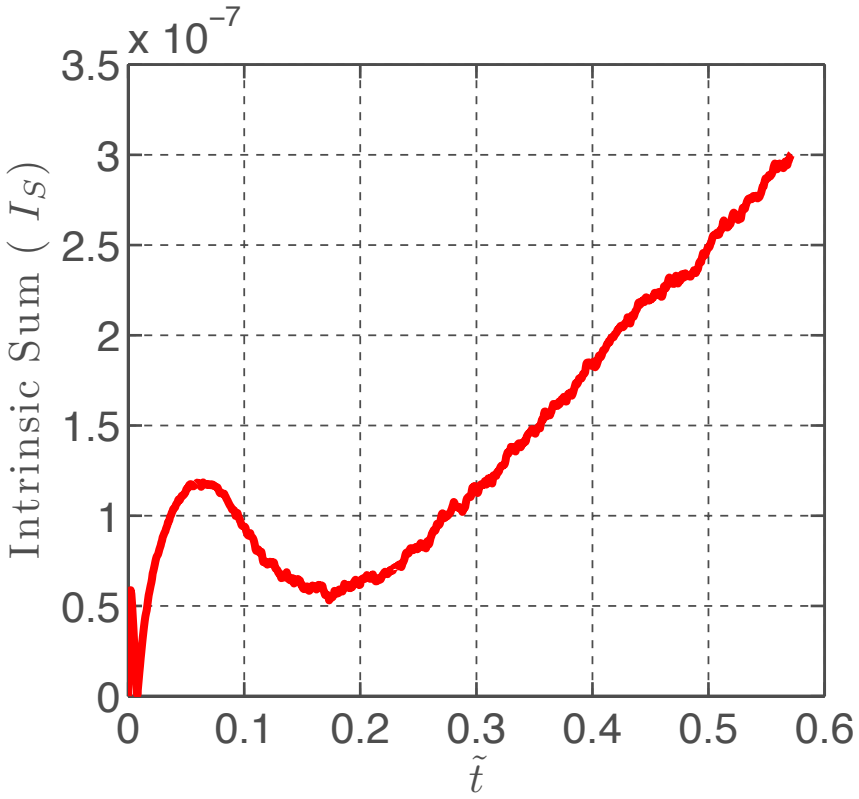

Figure 2.9 Plot of I_S in case 5: R32B10T0

Table 2.5 Solutions to the heat transfer problems in Case 4: R12B10T1

t	x	δ	$\tilde{T}$	$\tilde{X}_k$	$\tilde{X}_C$	I_S
0.1	0.5	0.0001	0.67490936	0.08902885	-0.08902885	0.00000001
0.21	0.5	0.0001	0.7435452	0.11325045	-0.11325045	0
0.31	0.5	0.0001	0.79155742	0.1223164	-0.1223164	0.00000005
0.41	0.5	0.0001	0.82624201	0.11776184	-0.11776184	0.00000012
0.52	0.5	0.0001	0.8513107	0.1063334	-0.1063334	0.00000017

2.3 Conclusions

The dimensionless derivation of scaled sensitivity coefficients was presented. Two important applications were discussed. The first application is related to the idea of intrinsic verification of large numerical codes. The identity given by scaled sensitivity relations for heat transfer problems provides a method for checking the accuracy of a computer code at interior and boundary points and at any time. Several equations are presented in each case that gives a suggested way to implement the concept. The concept is quite general and is not restricted to heat conduction or linear problems. The concept may be very important for intrinsic verification of computer codes for various engineering problems. The second application is related to the problems in parameter estimation. The scaled sensitivity coefficient can provide useful insight in to the parameter estimation problem. It can show if all the parameters in the model can be estimated and with what accuracy. With the scaled sensitivity relation, it has been shown that in certain boundary conditions, not all the parameters in the model can be estimated. As a general rule, if the sum of scaled sensitivity coefficients is equal to zero then not all the parameters in the model can be estimated uniquely and simultaneously. Instead, only a combination of the parameters, such as a ratio, can be estimated.

REFERENCES

REFERENCES

Beck JV. 1967. Transient sensitivity coefficients for the thermal contact conductance. International Journal of Heat and Mass Transfer 10(11):1615-7.

Beck JV. 1969. Determination of optimum, transient experiments for thermal contact conductance. International Journal of Heat and Mass Transfer 12(5):621-33.

Beck JV. 1970. Nonlinear estimation applied to the nonlinear inverse heat conduction problem. International Journal of Heat and Mass Transfer 13(4):703-16.

Beck JV, Arnold KJ. 1977. Parameter Estimation. New York: Wiley.

Beck JV, Litkouhi B. 1988. Heat conduction numbering system for basic geometries. International Journal of Heat and Mass Transfer 31(3):505-15.

Beck JV, McMasters R, Dowding KJ, Amos DE. 2006. Intrinsic verification methods in linear heat conduction. International Journal of Heat and Mass Transfer 49(17,Äì18):2984-94.

Beck JV, Woodbury KA. 1998. Inverse problems and parameter estimation: integration of measurements and analysis. Measurement Science and Technology 9(6):839.

Blackwell BF, Dowding KJ, Cochran RJ. 1999. Development and implementation of sensitivity coefficient equation for heat conduction problems. Numerical Heat Transfer, Part B: Fundamentals 36(1):15-32.

Chen B, Tong L. 2004. Sensitivity analysis of heat conduction for functionally graded materials. Materials & Design 25(8):663-72.

Dolan K, Valdramidis V, Mishra D. 2012. Parameter estimation for dynamic microbial inactivation; which model, which precision? Food Control.

Dowding KJ, Blackwell BF, Cochran RJ. 1999. Application of sensitivity coefficients for heat conduction problems. Numerical Heat Transfer, Part B: Fundamentals 36(1):33-55.

Dunker AM. 1984. The decoupled direct method for calculating sensitivity coefficients in chemical kinetics. The Journal of Chemical Physics 81(5):2385-93.

Koda M, Dogru AH, Seinfeld JH. 1979. Sensitivity analysis of partial differential equations with application to reaction and diffusion processes. Journal of Computational Physics 30(2):259-82.

Martins J, Kroo IM, Alonso JJ. 2000. An automated method for sensitivity analysis using complex variables. AIAA paper 689:2000.

Roy CJ. 2005. Review of code and solution verification procedures for computational simulation. Journal of Computational Physics 205(1):131-56.

Salari K, Knupp P. 2000. Code Verification by the Method of Manufactured Solutions. Other Information: PBD: 1 Jun 2000. p. Medium: P; Size: 124 pages.

Sun N, Sun NZ, Elimelech M, Ryan JN. 2001. Sensitivity analysis and parameter identifiability for colloid transport in geochemically heterogeneous porous media. Water Resources Research 37(2):209-22.

Chapter 3

Intrinsic Verification in Parameter Estimation Problems for Temperature-Dependent Thermal Properties

Abstract

Verification of numerical codes is important, because the accuracy of the code not only affects the estimation of parameters in the inverse problem, but also the model prediction while solving the forward problem. The current study is focused on the numerical verification of numerical codes in the context of parameter estimation. The inverse heat conduction problem is solved in the Cartesian as well as the cylindrical coordinate system with the temperature-dependent thermal properties. Dimensionless derivation of sensitivity coefficient is presented and the Intrinsic Sum is derived for each case. The intrinsic Sum for the cases presented in this article shows that it is possible to estimate thermal conductivity and specific heat simultaneously. It also shows that verification of the numerical code is possible with this identity.

Keywords: Numerical code verification, sensitivity analysis, inverse problems, heat transfer, intrinsic sum

3.1 Introduction

Thermal properties are important for conduction heat transfer problems for the prediction of temperature. However, knowledge of these properties is often limited for new materials. Whether temperature-dependent thermal conductivity and specific heat can be estimated simultaneously depends on the defined boundary conditions and initial condition (Beck and Arnold 1977c). Temperature-dependent thermal properties are especially important to predict the true temperature field at specific processing temperatures. Estimation of these properties involves inverse heat conduction problems (IHCP). Temperature dependence of thermal properties makes the heat conduction problem nonlinear. Since the IHCP are often ill-posed, estimation of temperature-dependent properties is difficult. Estimated parameter accuracy depends on the measurement accuracy and the inverse approach (Cui and others 2012). If a numerical solution is used for the inverse problem, then its accuracy also affects the accuracy of the estimated parameters. Hence, the numerical solution must be verified before using it for the inverse problems.

Estimation of temperature-dependent thermal properties has received considerable attention and many methods have been proposed for the inverse problem (Chang and Payne 1990; Cui and others 2012; Hays and Curd 1968; Imani and others 2006; Kevin J. Dowding 1999; Kim 2001; Kim and others 2003a; Kim and others 2003b; Mierzwiczak and Kołodziej 2011; Yang 1998; Yang 1999; Yang 2000b; Huang and Ozisik 1991; Huang and Jan-Yuan 1995; Chen and others 1996; Dowding and others 1999; Beck and Osman 1990; Dowding and Blackwell 1999;

Dowding and others 1998; Emery and Fadale 1997). Huang and Ozisik (Huang and Ozisik 1991) proposed a direct integration method for simultaneously estimating temperature-dependent thermal conductivity and specific heat. They also used this method to accurately provide the initial guesses of the parameters. Due to the nonlinearity of the problem with temperature-dependent thermal properties estimation, an exact solution is not possible. Hence, there are several numerical techniques that have been used as a solution to this problem (Huang and Ozisik 1991). However, an exact solution have been proposed for the case where thermal diffusivity is constant (Lesnic and others 1995). Simultaneous estimation of temperature-dependent thermal properties using a one-dimensional heat conduction problem was solved using nonlinear estimation for the Carbon/Epoxy material during curing (Scott and Beck 1992). Temperature-dependent thermal conductivity was estimated using the one-dimensional heat conduction problem by a linear inverse model (Yang 1998). Temperature-dependent thermal conductivity was estimated using nonlinear estimation (Yang 1999). Simultaneous estimation of temperature-dependent thermal conductivity and specific heat was performed using a nonlinear method and nonisothermal experiments (Yang 2000b). Dowding and Blackwell considered the linear variation in thermal conductivity and specific heat and proposed an optimal experimental design for simultaneous estimation of temperature-dependent parameters (Dowding and Blackwell 1999).

Verification of numerical codes has been an issue where no exact solution to the heat transfer problem exists (Salari and Knupp 2000). In this paper, a

verification method is proposed with a potential to verify the accuracy of the numerical code used for estimating temperature-dependent thermal properties. The intrinsic verification method (IVM) presented in this paper is based on dimensionless derivation of sensitivity coefficients. The sensitivity coefficient of a parameter is the first partial derivative of the function involving the parameter, with respect to the parameter (Beck and Arnold 1977c; Bennie F. Blackwell 1999). Sum of the scaled sensitivity coefficients should not be equal to zero in the parameter estimation problem. That means there should not be any linear dependence among the sensitivity coefficients. If the measured quantity is temperature *T*, the linear dependence relation can be given by,

$$A_1\beta_1\frac{\partial T}{\partial \beta_1} + A_2\beta_2\frac{\partial T}{\partial \beta_2} + \cdots + A_p\beta_p\frac{\partial T}{\partial \beta_p} = 0 \tag{3.1}$$

where at least one of the coefficients A_i is not zero. The i[th] scaled sensitivity coefficient is defined to be

$$\hat{\beta}_i = \beta_i\frac{\partial T}{\partial \beta_i} \tag{3.2}$$

The units of each term in Eq. (2.3) must be consistent. One way to have this consistency is to let each A_i coefficient be equal to unity. This result for Eq. (2.3) shows that when such a linear relationship occurs, not all the parameters can be simultaneously and independently estimated. Hence, relationships among the sensitivity coefficients are important for parameter identifiability.

The objective of this paper is to demonstrate a verification method for numerical codes using examples of temperature-dependent thermal properties. The heat conduction problem in Cartesian and cylindrical coordinate systems with initial and boundary conditions are chosen. The intrinsic sum is derived using the dimensionless derivation of sensitivity coefficients.

3.2 Case 1: One-dimensional transient heat conduction in a flat plate with heat flux on one side and insulated on another (X22B10T1)

The one-dimensional transient heat conduction equation for temperature-variable thermal conductivity and volumetric heat capacity (caused by changes in the specific heat) can be given as

$$\frac{\partial}{\partial x}\left[k_1 f_k \frac{\partial T}{\partial x} \right] = C_1 f_C \frac{\partial T}{\partial t},\ 0 < x < L,\ t > 0 \tag{3.3}$$

where

$$\tilde{k} = \frac{k_2}{k_1},\ \tilde{C} = \frac{C_2}{C_1} \tag{3.4}$$

Linear functions of temperature for the thermal conductivity and volumetric heat capacity are considered (Beck 1964); they are

$$f_k(T - T_0, \tilde{k}) = 1 + \frac{\left(T - T_0\right) - \left(T_1 - T_0\right)}{\left(T_2 - T_0\right) - \left(T_1 - T_0\right)}(\tilde{k} - 1) \tag{3.5}$$

$$f_C(T - T_0, \tilde{C}) = 1 + \frac{\left(T - T_0\right) - \left(T_1 - T_0\right)}{\left(T_2 - T_0\right) - \left(T_1 - T_0\right)}(\tilde{C} - 1) \tag{3.6}$$

which gives the thermal conductivity value of k_1 at T_1 and k_2 at T_2.

The temperature dependence causes Eq. (3.3) to be nonlinear in T. The boundary conditions are

$$-k_1 f_k \frac{\partial T}{\partial x}(0,t) = q_0 f(t) \tag{3.7}$$

$$\frac{\partial T}{\partial x}(L,t) = 0 \tag{3.8}$$

where the function on the right of Eq. (3.7) is known; also the q_0 value is known. The initial condition is

$$T(x,0) = T_0 \tag{3.9}$$

The above problem is now put in a dimensionless form. Let

$$\tilde{x} \equiv \frac{x}{L},\ \tilde{t} \equiv \frac{k_1 t}{C_1 L^2},\ \tilde{T} \equiv \frac{T - T_0}{\frac{q_0 L}{k_1}},\ \tilde{k} \equiv \frac{k_2}{k_1},\ \tilde{C} \equiv \frac{C_2}{C_1},\ \tilde{T}_1 \equiv \frac{T_1 - T_0}{\frac{q_0 L}{k_1}},\ \tilde{T}_2 \equiv \frac{T_2 - T_0}{\frac{q_0 L}{k_1}} \tag{3.10}$$

Then the describing differential equation becomes

$$\frac{\partial}{\partial \tilde{x}}\left[\left(1 + \frac{\tilde{T} - \tilde{T}_1}{\tilde{T}_2 - \tilde{T}_1}(\tilde{k} - 1)\right)\frac{\partial \tilde{T}}{\partial \tilde{x}}\right] = \left(1 + \frac{\tilde{T} - \tilde{T}_1}{\tilde{T}_2 - \tilde{T}_1}(\tilde{C} - 1)\right)\frac{\partial \tilde{T}}{\partial \tilde{t}},\ 0 < \tilde{x} < 1,\ \tilde{t} > 0 \tag{3.11}$$

The boundary conditions become

$$-\left(1 + \frac{\tilde{T} - \tilde{T}_1}{\tilde{T}_2 - \tilde{T}_1}(\tilde{k} - 1)\right)\frac{\partial \tilde{T}}{\partial \tilde{x}}(0,\tilde{t}) = f(\tilde{t}) \tag{3.12}$$

$$\frac{\partial \tilde{T}}{\partial \tilde{x}}(1,\tilde{t}) = 0 \tag{3.13}$$

The initial temperature distribution is

$$\tilde{T}(\tilde{x},0) = 0 \tag{3.14}$$

With this model and with a known and fixed boundary heat flux in Eq. (3.12) the dimensionless temperature is given symbolically by

$$\tilde{T} = \tilde{T}(\tilde{x},\tilde{t},\tilde{k},\tilde{C},\tilde{T}_1,\tilde{T}_2) \tag{3.15}$$

Now the partial derivatives of temperature T are found. Notice that

$$T - T_0 = \frac{q_0 L}{k_1}\tilde{T}\left(\tilde{x},\tilde{t}(k_1,C_1),\tilde{k}(k_1,k_2),\tilde{C}(C_1,C_2),T_1(k_1,T_1-T_0),T_2(k_1,T_2-T_0)\right) \tag{3.16}$$

The derivative with respect to k_1 is

$$\begin{aligned}
\frac{\partial T}{\partial k_1} &= -\frac{q_0 L}{k_1^2}\tilde{T} + \frac{q_0 L}{k_1}\left[\frac{\partial \tilde{T}}{\partial \tilde{t}}\frac{\partial \tilde{t}}{\partial k_1} + \frac{\partial \tilde{T}}{\partial \tilde{k}}\frac{\partial \tilde{k}}{\partial k_1} + \frac{\partial \tilde{T}}{\partial T_1}\frac{\partial T_1}{\partial k_1} + \frac{\partial \tilde{T}}{\partial T_2}\frac{\partial T_2}{\partial k_1}\right] \\
\hat{X}_{k_1} &= k_1\frac{\partial T}{\partial k_1} = -\frac{q_0 L}{k_1}\tilde{T} + \frac{q_0 L}{k_1}\left[\tilde{t}\frac{\partial \tilde{T}}{\partial \tilde{t}} - \tilde{k}\frac{\partial \tilde{T}}{\partial \tilde{k}} + T_1\frac{\partial \tilde{T}}{\partial T_1} + T_2\frac{\partial \tilde{T}}{\partial T_2}\right]
\end{aligned} \tag{3.17}$$

Repeat for the derivative with respect to k_2 to get scaled sensitivity coefficient

$$\hat{X}_{k_2} = k_2\frac{\partial T}{\partial k_2} = \frac{q_0 L}{k_1}\left[\tilde{k}\frac{\partial \tilde{T}}{\partial \tilde{k}}\right] \tag{3.18}$$

The scaled sensitivity coefficients for C_1 and C_2 are

$$\hat{X}_{C_1} = C_1 \frac{\partial T}{\partial C_1} = + \frac{q_0 L}{k_1} \left[-\tilde{t} \frac{\partial \tilde{T}}{\partial \tilde{t}} - C \frac{\partial \tilde{T}}{\partial C} \right] \tag{3.19}$$

$$\hat{X}_{C_2} = C_2 \frac{\partial T}{\partial C_2} = \frac{q_0 L}{k_1} \left[C \frac{\partial \tilde{T}}{\partial C} \right] \tag{3.20}$$

Notice that sum of Eqs. (2.24) and (3.20) is negative if the temperature is increasing with time. Hence the effect of increasing the volumetric heat capacity is to decrease the computed temperature. Next the derivative with respect to T_1-T_0 and T_2-T_0 is found; it is

$$\hat{X}_{(T_1 - T_0)} = (T_1 - T_0) \frac{\partial T}{\partial (T_1 - T_0)} = \frac{q_0 L}{k_1} \tilde{T}_1 \frac{\partial \tilde{T}}{\partial \tilde{T}_1} \tag{3.21}$$

$$\hat{X}_{(T_2 - T_0)} = (T_2 - T_0) \frac{\partial T}{\partial (T_2 - T_0)} = \frac{q_0 L}{k_1} \tilde{T}_2 \frac{\partial \tilde{T}}{\partial \tilde{T}_2} \tag{3.22}$$

Adding Eqs. (2.23), (3.18), (2.24) and (3.20) while subtracting Eq. (3.21) and (3.22) gives

$$\hat{X}_{k_1} + \hat{X}_{k_2} + \hat{X}_{C_1} + \hat{X}_{C_2} - \hat{X}_{(T_1 - T_0)} - \hat{X}_{(T_2 - T_0)} + \left(T - T_0 \right) = 0 \tag{3.23}$$

If the perfect insulation boundary condition at $\tilde{x} = 1$ given by Eq. (3.13) were replaced by the isothermal condition of

$$\tilde{T}(1, \tilde{t}) = 0 \tag{3.24}$$

the relation given by Eq. (3.23) is still valid.

Intrinsic Sum (IS) for this case is given by Eq. (3.23). The four sensitivity coefficients are also for fixed *x* and *t* values. The final two derivatives are the rate of change in the computed temperature when the specified temperature T_1 and T_2 is changed. Equation (3.23) indicates that the four parameters k_1, k_2, C_1 and C_2 may be simultaneously estimated when temperatures are measured in the plate and the heat flux is prescribed. The IS relation can be used to provide intrinsic verification of finite element and finite control volume computer codes for heat conduction. Note that Eq. (2.3) (sum of scaled sensitivity coefficients = 0) is not satisfied by Eq. (3.23), since the sum of the scaled sensitivity coefficients of k_1, k_2, C_1 and C_2 is not zero. Scaled sensitivity coefficients of ($T_1 - T_0$) and ($T_2 - T_0$) are extra terms that appear because of the temperature dependence of the thermal conductivity and specific heat.

To implement the I_S, the scaled sensitivity coefficients can be evaluated numerically. Scaled sensitivity can be computed as a forward difference first order approximation. However, a more accurate central difference could be used. The second order approximation for the scaled sensitivity coefficient can be expressed as,

$$\beta_i \frac{\partial T}{\partial \beta_i} \approx \frac{T((1+\delta)\beta_i) - T((1-\delta)\beta_i)}{2\delta} \tag{3.25}$$

where δ is a small value such as 0.0001.

The following values are considered as an example for this case. Dimensionless scaled sensitivity coefficients are calculated for k_1 = 0.5 W/mK, k_2 = 0.55 W/mK, C_1 = 3.5x10^6 J/m^3K, C_2 = 3.9x10^6 J/m^3K, T_0 = 20°C, x/L =0, L = 5 mm, $\Delta x / L = 0.02$. The maximum temperature rise is ~100°C at the heated surface. A finite element code (COMSOL®, (COMSOL 2012)) is used to demonstrate the concepts. An analytical solution is not needed for this intrinsic verification case. The problem explained in case 1 is solved numerically and the relationship given by Eq. (3.23) is calculated. Dimensionless scaled sensitivity coefficients are calculated as

$$\hat{X}_{\beta_i} = \frac{\beta_i}{\frac{q_0 L}{k_1}} \frac{\partial T}{\partial \beta_i} \tag{3.26}$$

Dimensionless scaled sensitivity coefficients for all the parameters are plotted in Figure 3.1. The dimensionless scaled sensitivities of k_1 and C_1 are larger than those for k_2 and C_2. It is also important to notice that the dimensionless scaled sensitivities of k_1 and C_1 are almost same for dimensionless time less than 0.05. Hence, it would not be possible to estimate them uniquely if an experiment is performed only for dimensionless time up to 0.05. This information is important for device design related to estimating temperature-dependent thermal properties. The accuracy of the estimated parameters depends on the absolute magnitude of scaled sensitivity coefficients as compared to the temperature rise. In this case, the order of

accuracy for estimated parameters would be C_1, k_1, k_2, and C_2. The parameters (T_1 – T_0) and (T_2 – T_0) are nuisance parameters; the lower the values of these, the better the accuracy of thermal parameters.

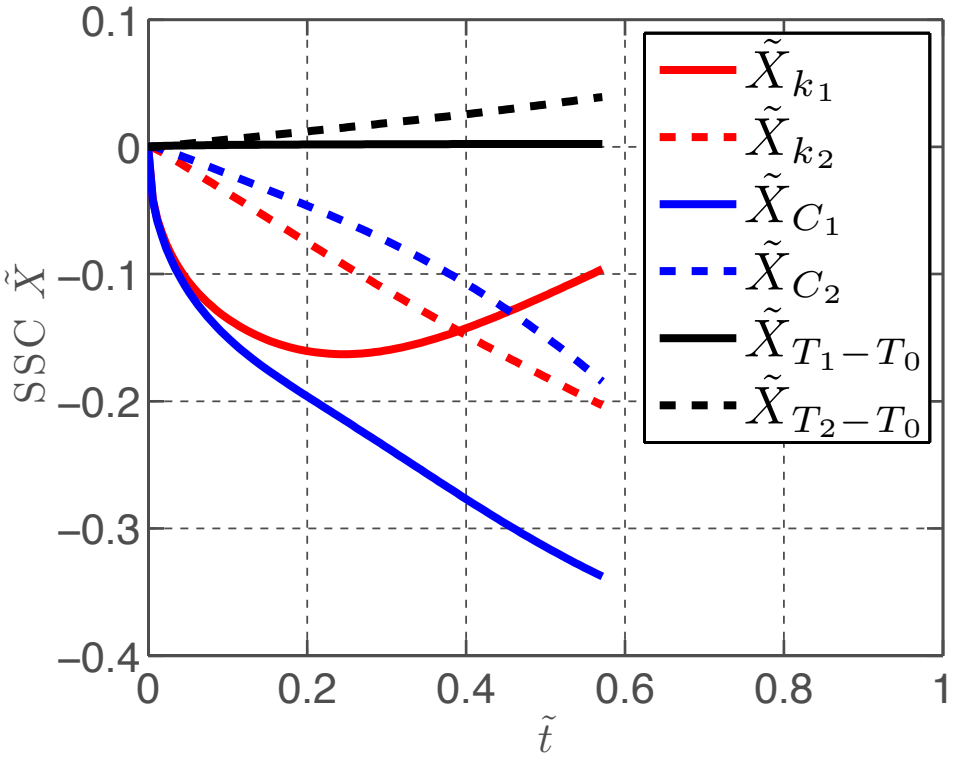

Figure 3.1 Dimensionless scaled sensitivity coefficient for the temperature-dependent parameters of heat transfer problems in case 1 (X22B10T0). T_1 = 25°C and T_2 = 130°C.

Intrinsic Sum (Eq. (3.23)) is plotted in Figure 3.2. The values of I_S are on the order of 10^{-7}, a small number that can be considered approaching zero. This result confirms the identity relationship of the IVM, and show that the numerical code is

accurate. Any imperfection in the model or numerical code will result in larger I_S than the value shown in Figure 3.2. The results are shown in Table 3.1. This is a good test to perform before doing any inverse problems or even forward problem where accuracy in prediction is very important. Even while developing models in the commercial numerical codes, it is important to do this verification to avoid coding errors in the software.

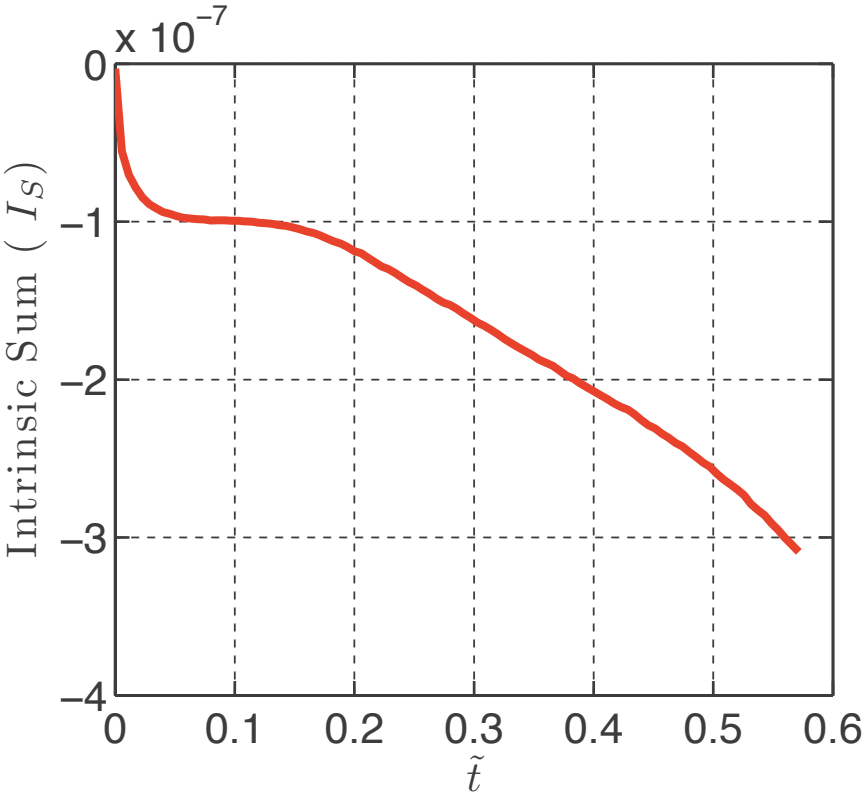

Figure 3.2 Intrinsic sum for the heat transfer problems in case 1 (X22B10T0).

Table 3.1 Intrinsic Sum and dimensionless scaled sensitivity coefficients for case 1: X22B10T1

$\tilde{t}$	$\tilde{X}_{k_1}$	$\tilde{X}_{k_2}$	$\tilde{X}_{C_2}$	$\tilde{X}_{C_2}$	$\tilde{X}_{(T_1-T_0)}$	$\tilde{X}_{(T_2-T_0)}$	$I_S \times 10^{-7}$
0.01	-0.0565	-0.0023	-0.0582	-0.0006	0.0006	0.0003	-0.7
0.11	-0.1408	-0.0418	-0.1580	-0.0248	0.0015	0.0066	-1.0
0.22	-0.1620	-0.0817	-0.2031	-0.0507	0.0019	0.0132	-1.3
0.32	-0.1576	-0.1199	-0.2444	-0.0800	0.0021	0.0200	-1.7
0.42	-0.1372	-0.1558	-0.2859	-0.1164	0.0022	0.0273	-2.2
0.53	-0.1095	-0.1891	-0.3233	-0.1615	0.0023	0.0354	-2.7

The choices of T_1 and T_2 also affect the sensitivity coefficients of parameters and eventually the parameter estimates. In Figure 3.1, the temperatures for evaluation were, T_1 = 25^{o}C and T_2 = 130^{o}C. The values for T_1 and T_2 are in the range of the experimental temperatures; T_1 is close to the initial temperature and T_2 is close to the final temperature of the product. For example, Figure 3.3 shows the effect on dimensionless scaled sensitivity coefficients if the value of T_2 is changed to 300^{o}C, which is much higher than the maximum temperature attained by the product. Results of this case are presented in Table 3.2. The dimensionless scaled sensitivity coefficients of k_2 and C_2 are very small, so these parameters might not be estimated with good accuracy. Also, k_1 and C_1 are correlated for dimensionless time of 0.1, which means that the experiment must be performed >0.1 sec to estimated both k_1 and C_1.

Table 3.2 Intrinsic Sum and dimensionless scaled sensitivity coefficients for case 1: X22B10T1 with T_2 = 300 ^{o}C

$\tilde{t}$	$\tilde{X}_{k_1}$	$\tilde{X}_{k_2}$	$\tilde{X}_{C_2}$	$\tilde{X}_{C_2}$	$\tilde{X}_{(T_1-T_0)}$	$\tilde{X}_{(T_2-T_0)}$	$I_S \times 10^{-7}$
0.01	-0.0583	-0.0009	-0.0590	-0.0002	0.0002	0.0001	-0.8
0.11	-0.1703	-0.0168	-0.1774	-0.0099	0.0007	0.0026	-1.9
0.22	-0.2186	-0.0334	-0.2418	-0.0207	0.0009	0.0052	-2.5
0.32	-0.2392	-0.0498	-0.3051	-0.0331	0.0011	0.0081	-3.2
0.42	-0.2413	-0.0657	-0.3735	-0.0487	0.0012	0.0112	-3.8
0.53	-0.2338	-0.0809	-0.4438	-0.0684	0.0013	0.0146	-4.0

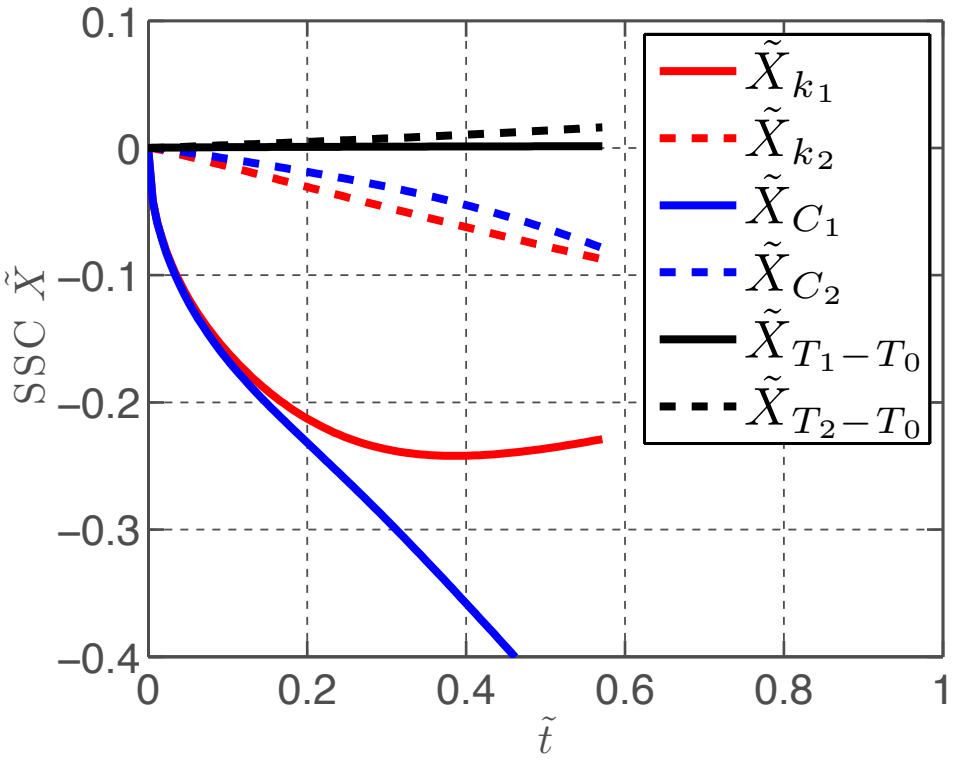

Figure 3.3 Dimensionless scaled sensitivity coefficient for the temperature-dependent parameters of heat transfer problems in case 1 (X22B10T0). T_1 = 25^{o}C and T_2 = 300^{o}C.

3.3 Case 2: Transient heat conduction in a hollow cylinder with heat flux on inside and insulated on the outside (R22B10T1)

One important point about the Eq. (3.23) is that it holds true also for the cylindrical heat transfer problems in r and z. In this section we are going to demonstrate that Eq. (3.23) is applicable to cylindrical heat transfer problems. The one-dimensional transient heat conduction equation for temperature-variable thermal conductivity and volumetric heat capacity (caused by changes in the specific heat) can be given as

$$\frac{1}{r}\frac{\partial}{\partial r}\left[k_1 f_k r\frac{\partial T}{\partial r}\right]+\frac{\partial}{\partial z}\left[k_1 f_k\left(T,K\right)\frac{\partial T}{\partial z}\right]=C_1 f_C\frac{\partial T}{\partial t} \qquad (3.27)$$
$$R_1<r<R_2, 0<z<Z,\ t>0$$

where

$$\tilde{k}=\frac{k_2}{k_1},\ \tilde{C}=\frac{C_2}{C_1} \qquad (3.28)$$

Linear functions of temperature for the thermal conductivity and volumetric heat capacity are considered; they are

$$f_k(T-T_0,\tilde{k})=1+\frac{\left(T-T_0\right)-\left(T_1-T_0\right)}{\left(T_2-T_0\right)-\left(T_1-T_0\right)}(\tilde{k}-1) \qquad (3.29)$$

$$f_C(T-T_0,\tilde{C})=1+\frac{\left(T-T_0\right)-\left(T_1-T_0\right)}{\left(T_2-T_0\right)-\left(T_1-T_0\right)}(\tilde{C}-1) \qquad (3.30)$$

which gives the thermal conductivity value of k_1 at T_1 and k_2 at T_2.

The temperature dependence causes Eq. (3.27) to be nonlinear in T. The boundary conditions are

$$-k_1 f_k \frac{\partial T}{\partial r}(R_1, z, t) = q_0 f(t) \tag{3.31}$$

$$\frac{\partial T}{\partial r}(R_2, z, t) = 0 \quad \frac{\partial T}{\partial z}(r, 0, t) = 0 \quad \frac{\partial T}{\partial z}(r, Z, t) = 0 \tag{3.32}$$

where the function on the right of Eq. (3.31) is known; also the q_0 value is known. The initial condition is

$$T(r, z, 0) = T_0 \tag{3.33}$$

The above problem is now put in a dimensionless form. Let

$$\tilde{r} \equiv \frac{r}{R_1}, \tilde{R}_2 \equiv \frac{R_2}{R_1}, \tilde{z} \equiv \frac{z}{R_1}, \tilde{t} \equiv \frac{k_1 t}{C_1 {R_1}^2}, \ \tilde{T} \equiv \frac{T - T_0}{\frac{q_0 R_1}{k_1}}, \ \tilde{k} \equiv \frac{k_2}{k_1}, \tilde{C} \equiv \frac{C_2}{C_1} \tag{3.34}$$

and

$$\tilde{T}_1 \equiv \frac{T_1 - T_0}{\frac{q_0 R_1}{k_1}}, \ \tilde{T}_2 \equiv \frac{T_2 - T_0}{\frac{q_0 R_1}{k_1}} \tag{3.35}$$

With this model and with a known and fixed boundary heat flux in Eq. (3.31) the dimensionless temperature is given symbolically by

$$\tilde{T} = \tilde{T}(\tilde{r}, \tilde{R}_2, \tilde{z}, \tilde{t}, \tilde{k}, \tilde{C}, \tilde{T}_1, \tilde{T}_2) \tag{3.36}$$

Now the partial derivatives of temperature T are found. Notice that

$$T - T_0 = \frac{q_0 L}{k_1} \tilde{T}\left(\tilde{r}, \tilde{R}_2, \tilde{z}, \tilde{t}(k_1, C_1), \tilde{k}(k_1, k_2), \tilde{C}(C_1, C_2), T_1(k_1, T_1 - T_0), T_2(k_1, T_2 - T_0)\right) \quad (3.37)$$

The important point to note in Eq. (3.37) is that it is similar to Eq. (2.22) with the extra terms of $\tilde{R}_2$ and $\tilde{z}$. However, when we take the derivative of Eq. (3.37) with respect to k_1, k_2, C_1, C_2, T_1-T_0 and T_2-T_0, we will get the same result as given by Eq. (3.23). Hence, this derivation shows that the Eq. (3.23) does not depend on the co-ordinate system. This result is demonstrated below.

The derivative with respect to k_1 is

$$\hat{X}_{k_1} = -\frac{q_0 R_1}{k_1} \tilde{T} + \frac{q_0 R_1}{k_1} \left[\tilde{t} \frac{\partial \tilde{T}}{\partial \tilde{t}} - \tilde{k} \frac{\partial \tilde{T}}{\partial \tilde{k}} + T_1 \frac{\partial \tilde{T}}{\partial T_1} + T_2 \frac{\partial \tilde{T}}{\partial T_2} \right] \quad (3.38)$$

Repeat for the derivative with respect to k_2 to get

$$\hat{X}_{k_2} = \frac{q_0 R_1}{k_1} \left[\tilde{k} \frac{\partial \tilde{T}}{\partial \tilde{k}} \right] \quad (3.39)$$

The sensitivity coefficients for C_1 and C_2 are

$$\hat{X}_{C_1} = \frac{q_0 R_1}{k_1} \left[-\tilde{t} \frac{\partial \tilde{T}}{\partial \tilde{t}} - C \frac{\partial \tilde{T}}{\partial C} \right] \quad (3.40)$$

$$\hat{X}_{C_2} = \frac{q_0 R_1}{k_1} \left[C \frac{\partial \tilde{T}}{\partial C} \right] \quad (3.41)$$

Next the derivative with respect to T_1-T_0 and T_2-T_0 is found; it is

$$\hat{X}_{(T_1-T_0)} = \frac{q_0 R_1}{k_1} \tilde{T}_1 \frac{\partial \tilde{T}}{\partial \tilde{T}_1} \tag{3.42}$$

$$\hat{X}_{(T_2-T_0)} = \frac{q_0 R_1}{k_1} \tilde{T}_2 \frac{\partial \tilde{T}}{\partial \tilde{T}_2} \tag{3.43}$$

Adding Eqs. (3.38), (3.39), (3.40) and (3.41) while subtracting Eq. (3.42) and (3.43) gives

$$\hat{X}_{k_1} + \hat{X}_{k_2} + \hat{X}_{C_1} + \hat{X}_{C_2} - \hat{X}_{(T_1-T_0)} - \hat{X}_{(T_2-T_0)} + \left(T - T_0\right) = 0 \tag{3.44}$$

In the case of cylindrical coordinates and boundary conditions similar to case 1, the I_S is the same as shown by Eqs. (3.23) and (3.44). Even though the I_S is same in both cases, the scaled sensitivity coefficients might not be the same. However, the sum of all the scaled sensitivity coefficients in both the cases would be same as the absolute value of the temperature rise. Eq. (3.44) suggests that the sum of scaled sensitivity coefficients is not equal to zero and does not satisfy Eq. (2.3). Hence, in this case, it might be possible to estimate parameters k_1, k_2, C_1 and C_2 uniquely and simultaneously.

The following values are considered as an example for this case. Dimensionless scaled sensitivity coefficients are calculated for k_1 = 0.5 W/mK, k_2 = 0.55 W/mK, C_1 = 3.5x10^6 J/m^{3}K, C_2 = 3.9x10^6 J/m^{3}K, T_0 = 20^{o}C, R = 5 mm,

$\Delta r / R = 0.02$. The heat flux is 2.4 x10^4 W/m^2. The dimensionless scaled sensitivity coefficients for temperature-dependent properties are plotted in Figure 3.4, for T_1 = 25^{o}C and T_2 = 130^{o}C. The order of the magnitude of sensitivity coefficients is k_1, C_1, k_2 and C_2, hence k_1 will have the lowest relative error of all the estimated parameters.

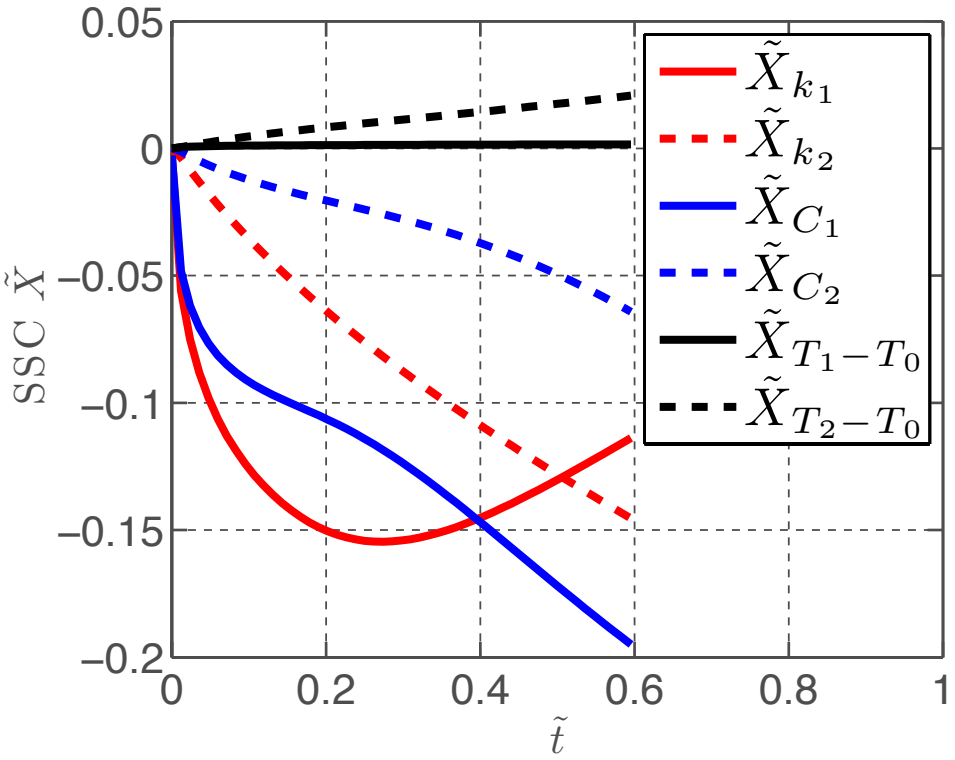

Figure 3.4 Dimensionless scaled sensitivity coefficient for the temperature-dependent parameters of heat transfer problems in case 2 (R22B10T0). T_1 = 25^{o}C and T_2 = 130^{o}C, q = 2.4 x10^4 W/m^2

Table 3.3 Intrinsic Sum and dimensionless scaled sensitivity coefficients for case 2: R22B10T1

$\tilde{t}$	$\tilde{X}_{k_1}$	$\tilde{X}_{k_2}$	$\tilde{X}_{C_2}$	$\tilde{X}_{C_2}$	$\tilde{X}_{(T_1-T_0)}$	$\tilde{X}_{(T_2-T_0)}$	$I_S \times 10^{-7}$
0.02	-0.0752	-0.0085	-0.0619	-0.0031	0.0007	0.0012	-0.9
0.13	-0.1361	-0.0449	-0.0969	-0.0152	0.0012	0.0059	-0.9
0.24	-0.1537	-0.0733	-0.1121	-0.0232	0.0013	0.0095	-1.3
0.35	-0.1511	-0.0975	-0.1337	-0.0317	0.0014	0.0127	-1.9
0.45	-0.1378	-0.1191	-0.1600	-0.0433	0.0015	0.0160	-2.3
0.56	-0.1201	-0.1391	-0.1866	-0.0584	0.0016	0.0195	-2.6

One important difference between case 1 and case 2 is that k_1 has a larger absolute scaled sensitivity coefficient in case 2. Hence, if the experimental objective is to estimate thermal conductivity, then a cylindrical geometry would provide a better estimate than a plate geometry. Intrinsic Sum is plotted in Figure 3.5. The I_S is in the magnitude of 10^{-7}, which is very small. This low value of I_S suggests that the numerical code is sufficiently accurate. If an inverse problem is performed using this code, the results might be better for the cylindrical geometry than for the plate geometry. The results are tabulated in Table 3.3.

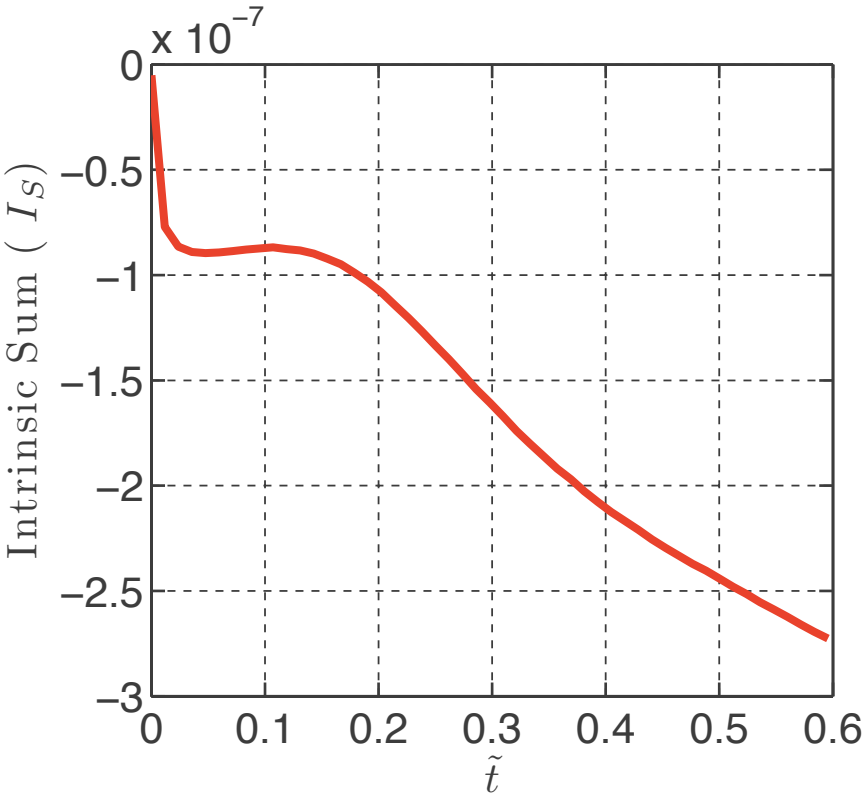

Figure 3.5 Intrinsic sum for the heat transfer problems in case 2 (R22B10T0).

The dimensionless scaled sensitivity coefficients for parameters at higher temperature (k_2 and C_2) are lower in magnitude than the ones at lower temperature (k_1 and C_1), Figure 3.4. In equipment design, this insight will be helpful. For example, if the heat flux in case 2 is increased to 3.8x10^4 W/m^2 as compared to 2.4x10^4 W/m^2, the resulting dimensionless scaled sensitivity coefficients are plotted in Figure 3.6. It should be noted that now $\tilde{X}_{k_2}$ is larger than $\tilde{X}_{k_1}$ for dimensionless time >0.21. So, increasing the heat flux has a positive influence on the

estimation of thermal conductivity at higher temperature. The numerical values are presented in Table 3.4.

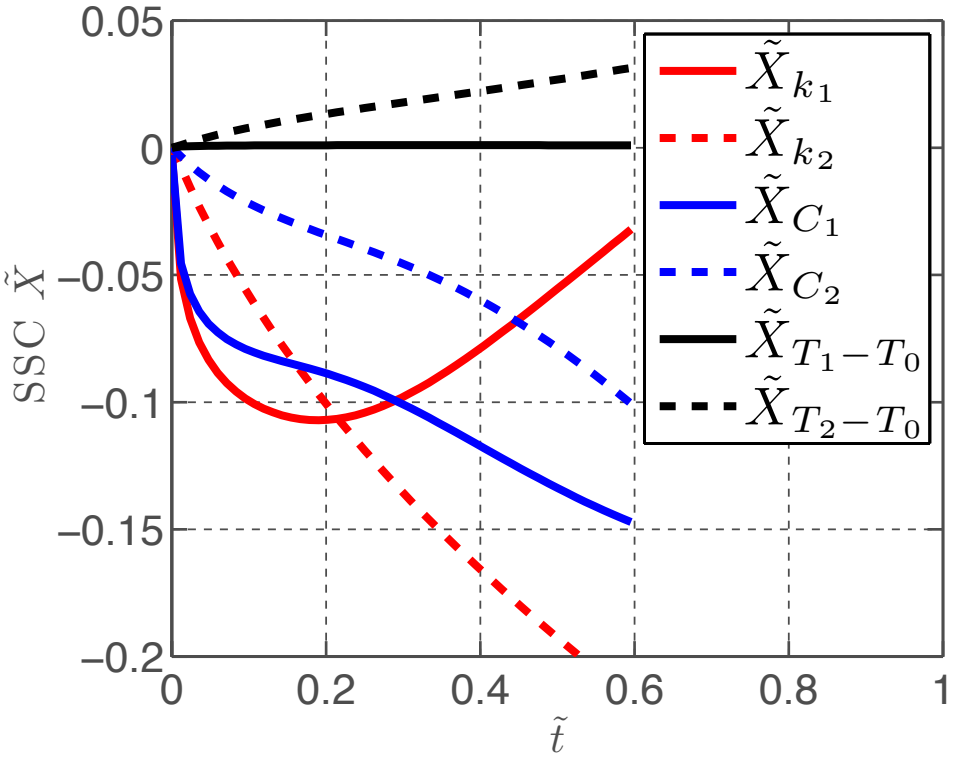

Figure 3.6 Dimensionless scaled sensitivity coefficient for the temperature-dependent parameters of heat transfer problems in case 2 (R22B10T0). T_1 = 25°C and T_2 = 130°C, q = 3.8x10^4 W/m^2

Table 3.4 Intrinsic Sum and dimensionless scaled sensitivity coefficients for case 2: R22B10T1 with increased heat flux

$\tilde{t}$	$\tilde{X}_{k_1}$	$\tilde{X}_{k_2}$	$\tilde{X}_{C_2}$	$\tilde{X}_{C_2}$	$\tilde{X}_{(T_1-T_0)}$	$\tilde{X}_{(T_2-T_0)}$	$I_S \times 10^{-7}$
0.02	-0.0670	-0.0156	-0.0575	-0.0068	0.0006	0.0022	-0.9
0.13	-0.1040	-0.0722	-0.0828	-0.0262	0.0009	0.0097	-1.4
0.24	-0.1051	-0.1147	-0.0926	-0.0384	0.0010	0.0151	-2.9
0.35	-0.0901	-0.1498	-0.1080	-0.0516	0.0010	0.0198	-4.8
0.45	-0.0668	-0.1802	-0.1261	-0.0692	0.0010	0.0246	-6.7
0.56	-0.0409	-0.2075	-0.1425	-0.0919	0.0010	0.0296	-9.0

3.4 Conclusions

Dimensionless derivation of sensitivity coefficients has been presented for temperature-dependent thermal properties. An important aspect of the Intrinsic Sum, numerical code verification, is demonstrated with examples from transient conduction heat transfer. The Intrinsic Sum relation can also be used to identify if all the parameters can be estimated. The relative error of the parameters can also be assessed as it depends on the magnitude of the scaled sensitivity coefficients. The larger the scaled sensitivity coefficient of a parameter as compared to the maximum temperature rise, the lower the standard error will be. Methodologies presented in this article provide great insight into the inverse problems and parameter estimation. Dimensionless derivation of scaled sensitivity coefficients can be conveniently performed for various problems and implemented to check the large numerical codes.

REFERENCES

REFERENCES

Beck JV. 1964. The Optimum Analytical Design of Transient Experiments for Simultaneous Determinations of Thermal Conductivity and Specific Heat. East Lansing, MI: Michigan State University.

Beck JV, Arnold KJ. 1977c. Parameter Estimation in Engineering and Science. New York: Wiley.

Beck JV, Osman AM. 1990. Sequential estimation of temperature-dependent thermal properties. High Temperatures--High Pressures(UK) 23(3):255-66.

Bennie F. Blackwell KJDRJC. 1999. Development and implementation of sensitivity coefficient equations for heat conduction problems. Numerical Heat Transfer, Part B: Fundamentals 36(1):15-32.

Chang KC, Payne UJ. 1990. Analytical and numerical approaches for heat conduction in composite materials. Mathematical and Computer Modelling 14(0):899-904.

Chen H-T, Lin J-Y, Wu C-H, Huang C-H. 1996. Numerical algorithm for estimating temperature-dependent thermal conductivity. Numerical Heat Transfer, Part B: Fundamentals 29(4):509-22.

COMSOL. 2012. COMSOL Multiphysics. 42a ed: COMSOL Inc., Burlington, Massachusetts, United States.

Cui M, Gao X, Zhang J. 2012. A new approach for the estimation of temperature-dependent thermal properties by solving transient inverse heat conduction problems. International Journal of Thermal Sciences 58(0):113-9.

Dowding K, Blackwell B. 1999. Design of experiments to estimate temperature dependent thermal properties. 3rd Int. Conf. on Inverse Problems in Engineering: Theory and Practice. p. 509-18.

Dowding KJ, Beck JV, Blackwell BF. 1998. Estimating temperature-dependent thermal properties of carbon-carbon composite. 7th AIAAJASME Joint Thermophysics and Heat Transfer Conference, AIAA paper. p. 98-2933.

Dowding KJ, Beck JV, Blackwell BF. 1999. Estimating Temperature-Dependent Thermal Properties. Journal of Thermophysics and Heat Transfer 13(3):328-36.

Emery AF, Fadale TD. 1997. Handling temperature dependent properties and boundary conditions in stochastic finite element analysis. Numerical Heat Transfer, Part A: Applications 31(1):37-51.

Hays DF, Curd HN. 1968. Heat conduction in solids: Temperature-dependent thermal conductivity. International Journal of Heat and Mass Transfer 11(2):285-95.

Huang C-H, Jan-Yuan Y. 1995. An inverse problem in simultaneously measuring temperature-dependent thermal conductivity and heat capacity. International Journal of Heat and Mass Transfer 38(18):3433-41.

Huang CH, Ozisik MN. 1991. Direct integration approach for simultaneously estimating temperature dependent thermal conductivity and heat capacity. Numerical Heat Transfer, Part A: Applications 20(1):95-110.

Imani A, Ranjbar AA, Esmkhani M. 2006. Simultaneous estimation of temperature-dependent thermal conductivity and heat capacity based on modified genetic algorithm. Inverse Problems in Science and Engineering 14(7):767-83.

Kevin J. Dowding BFBRJC. 1999. Application of sensitivity coefficients for heat conduction problems. Numerical Heat Transfer, Part B: Fundamentals 36(1):33-55.

Kim S. 2001. A simple direct estimation of temperature-dependent thermal conductivity with kirchhoff transformation. International Communications in Heat and Mass Transfer 28(4):537-44.

Kim S, Chung B-J, Kim MC, Kim KY. 2003a. Inverse estimation of temperature-dependent thermal conductivity and heat capacity per unit volume with the direct integration approach. Numerical Heat Transfer, Part A: Applications 44(5):521-35.

Kim S, Kim MC, Kim KY. 2003b. Non-iterative estimation of temperature-dependent thermal conductivity without internal measurements. International Journal of Heat and Mass Transfer 46(10):1801-10.

Lesnic D, Elliott L, Ingham DB. 1995. A note on the determination of the thermal properties of a material in a transient nonlinear heat conduction problem. International Communications in Heat and Mass Transfer 22(4):475-82.

Mierzwiczak M, Kołodziej JA. 2011. The determination temperature-dependent thermal conductivity as inverse steady heat conduction problem. International Journal of Heat and Mass Transfer 54(4):790-6.

Salari K, Knupp P. 2000. Code Verification by the Method of Manufactured Solutions. Other Information: PBD: 1 Jun 2000. p. Medium: P; Size: 124 pages.

Scott EP, Beck JV. 1992. Estimation of Thermal Properties in Carbon/Epoxy Composite Materials during Curing. p. 20-36.

Yang C-y. 1998. A linear inverse model for the temperature-dependent thermal conductivity determination in one-dimensional problems. Applied Mathematical Modelling 22(1,Äì2):1-9.

Yang C-y. 1999. Estimation of the temperature-dependent thermal conductivity in inverse heat conduction problems. Applied Mathematical Modelling 23(6):469-78.

Yang C-y. 2000b. Determination of the temperature dependent thermophysical properties from temperature responses measured at medium,Äôs boundaries. International Journal of Heat and Mass Transfer 43(7):1261-70.

Chapter 4

A Novel Instrument for Rapid Estimation of Temperature-Dependent Thermal Properties up to 140^{O}C

Abstract

Estimating thermal properties for thick or solid foods at temperatures greater than 100^{O}C is challenging for two reasons: the long time needed to reach a constant temperature, and the pressure needed to be maintained in the sealed container. An instrument (TPCell) was developed based on a rapid non-isothermal method to estimate the temperature-dependent thermal properties within a range of commercial food processes (20 – 140 ^{O}C). The instrument was developed based on simulation and insight from the scaled sensitivity coefficients. The instrument design consists of a custom sample holder and special fittings to accommodate the heater within a pressurized environment. The instrument is kept under pressure during the test. The total time of the experiment is less than 1min., compared to existing isothermal instruments requiring 5-6 hours to cover a similar temperature range. The sequential estimation procedure is used to estimate the parameters from a dynamic experiment. Glycerin is used to calibrate the sensor. Thermal conductivities of different food materials were estimated for the temperature range of commercial food processes. The novelty of the instrument lies in its ability to analyze transient temperature data using a nonlinear form of the two-dimensional heat conduction equations.

4.1 Introduction

Thermophysical properties, especially thermal conductivity and specific heat, are very important in designing and developing processes such as heat exchangers, aseptic processing systems, etc. Thermal properties are also critical in determining scheduled thermal processes for a specific product. Modeling kinetics of thermal degradation of nutrients and thermal inactivation of microorganisms requires reliable estimates of the thermal properties of foods. Mathematical modeling is used for new and novel processes to design and optimize food quality. However, input of thermophysical properties to these models is often a limiting step. For example, maximizing quality and ensuring safety of solid or thick foods requires tracking the food temperature during the process. Thermal properties are needed to predict the food temperature. The "isothermal" (0.5-2^{o}C temperature rise) line-source method has been commonly used, because it is fast at lower temperatures. Yet determining thermal properties at higher temperatures (> 100^{o}C) is challenging, because by the time the entire food sample in the container reaches a constant temperature, the quality is grossly degraded. It is at higher temperatures where rate of quality degradation and microbial inactivation increases very rapidly. Therefore, accurate thermal properties are critical for process design of foods, as well as for other materials, such as biomass, foams, pastes, and thick slurries.

The most common method to estimate thermal properties is the hot-wire probe. Heat-flux boundary conditions or volumetric generation in the heat-transfer

partial differential equation allows for simultaneous estimation of thermal conductivity and volumetric heat capacity (Beck and Arnold 1977a). A heat pulse method can be used to estimate thermal properties (Bristow and others 1994b; Bristow and others 1994a). Nahor and others (2001) performed temperature-independent simultaneous estimation of thermal conductivity and volumetric heat capacity at room temperature, and an optimal design of a heat-generation profile was presented to estimate the parameters. The optimal design for the placement of the sensor was also studied for the estimation of thermal parameters (Nahor and others 2001). In another study, a hot-wire probe method using nonlinear regression was employed for the simultaneous estimation of thermal conductivity and volumetric specific heat (Scheerlinck and others 2008). Scheerlinck et al. (2008) also studied the optimum heat-generation profiles and applied a global optimization technique for optimization of the heating profile and the position of the sensor. One important issue to consider with the hot-wire probe method is the design of the probe and sources of error. Design of a thermal conductivity probe was considered and the possible sources of error were analyzed for the construction of such a probe (Murakami and others 1996). Carefully designed probes have higher accuracy in thermal parameter estimation.

The thermal conductivity and specific heat of carrots at elevated temperatures were estimated by linear regression using the line heat-source probe by performing several experiments at a predetermined initial temperature of the food material (Gratzek and Toledo 1993). The transient line heat-source technique

was used to estimate thermal conductivity of potato granules and maize grits over a temperature range of 30-120^{o}C (Halliday and others 1995). The line heat-source probe method was also used to estimate thermal conductivity of food in a high-pressure (up to 400 MPa) system (Denys and Hendrickx 1999). Thermal conductivity of food material was estimated under heated and pressurized conditions using the transient hot-wire method (Shariaty-Niassar and others 2000). In their study, thermal conductivity of gelatinized potato starch was determined at 25-80^{o}C, 50%-80% moisture, and 0.2-10 MPa. They also found that the thermal conductivity of starch gel increases with temperature and moisture content up to 1 MPa pressure. A dual-needle probe was used to estimate thermal properties under high-pressure processing conditions, and (Zhu and others 2007) found that thermal conductivity and thermal diffusivity increased with increasing pressure. Temperature-dependent thermal conductivity was estimated using nonlinear estimation (Yang 1999). The temperature used in the experiment was in the range of 0-30^{o}C. Simultaneous estimation of temperature-dependent thermal conductivity and specific heat was performed using a nonlinear method and nonisothermal experiments (Yang 2000a). Estimation of temperature-dependent specific heat capacity of food material by the one-dimensional inverse problem was solved for the thawing of fish (-40 to 5^{o}C) (Zueco and others 2004).

The inverse method is a useful tool for parameter estimation (Beck and Arnold 1977a). The inverse method was used to estimate the thermal conductivity

of carrot puree during freezing (Mariani and others 2009) and thermal diffusivity of various foods (Betta and others 2009; Mohamed 2010; Mishra and others 2008; Mishra and others 2011). A temperature-dependent estimation of thermal conductivity was done using a polynomial model for sandwich bread using the cooling curve (Monteau 2008).

One of the drawbacks of these methods is that one has to wait a long time (45 min minimum) from one temperature level to another temperature level, as the probe and food material must be in equilibrium to start the experiment. The experiment can only be performed once the heat source and the sample are in thermal equilibrium. Hence, performing tests at five or six different temperature levels makes the experimental time unacceptably long (5-6 h), and unwanted changes in material properties occur because of long durations at higher temperature.

In the literature reviewed, there was no standard method to estimate thermal properties of conduction-heated materials rapidly over a large temperature range in one experiment. There is a lack of research on rapid estimation of temperature-dependent thermal properties covering the entire relevant food processing temperature range (25 – 140^{o}C) using a single experiment. Development of a device would be of great use to a variety of industries, such as the food, pharmaceutical, and chemical industries. Therefore, the objective of this study was to devise an inverse method and construct a device to accurately estimate

temperature-dependent thermal properties from 20 to 140^{o}C using non-isothermal heating.

4.2 Methodology

4.2.1 Mathematical model and numerical code verification

The transient heat conduction equation in a hollow cylinder for temperature-variable thermal conductivity and volumetric heat capacity (caused by changes in the specific heat) with the heater at the center can be given as

$$\frac{1}{r}\frac{\partial}{\partial r}\left[k_h r\frac{\partial T}{\partial r}\right]+\frac{\partial}{\partial z}\left[k_h\frac{\partial T}{\partial z}\right]+g_0 f(t)=C_h\frac{\partial T}{\partial t}\ \textbf{for}\ R_0<r<R_1, 0<z<Z,\ t>0$$

$$\frac{1}{r}\frac{\partial}{\partial r}\left[k_1 f_k r\frac{\partial T}{\partial r}\right]+\frac{\partial}{\partial z}\left[k_1 f_k\left(T,K\right)\frac{\partial T}{\partial z}\right]=C_1 f_C\frac{\partial T}{\partial t}\ \textbf{for}\ R_1<r<R_2, 0<z<Z,\ t>0 \quad (4.1)$$

This problem was solved numerically with finite element software (COMSOL®, (COMSOL 2012)). Numerical codes are very important in providing a solution to partial differential equations in many areas of study, such as the heat transfer problem. However, verification of these codes is critical (Salari and Knupp 2000; Roy 2005). In this section, an intrinsic verification method to the numerical solution of the partial differential equation is presented. Derivation of the dimensionless form of scaled sensitivity coefficients is presented. The sum of scaled sensitivity coefficients is used in the dimensionless form to provide a method for verification.

The Intrinsic Verification Method (IVM) is based on the scaled sensitivity coefficients and can be used in verification of numerical codes as well as to perform parameter estimation. The sensitivity coefficient of a parameter is the first partial derivative of the function involving the parameter, with respect to the parameter (Beck 1970). Consider a simple function;

$$T = f(k, C, x, t) \tag{4.2}$$

Where *k* and *C* are parameters of the function *T*. The sensitivity coefficient of *k* and *C* are $\frac{\partial T}{\partial k}$ and $\frac{\partial T}{\partial C}$, respectively. After multiplying the sensitivity coefficient by the parameter, we get the scaled sensitivity coefficient represented by $\hat{X}_k = k\frac{\partial T}{\partial k}$ and $\hat{X}_C = C\frac{\partial T}{\partial C}$ for *k* and *C*, respectively.

For the numerical code verification, the heat conduction problem is made dimensionless. Let,

$$\tilde{k} = \frac{k_2}{k_1},\ \tilde{C} = \frac{C_2}{C_1} \tag{4.3}$$

Linear functions of temperature for the thermal conductivity and volumetric heat capacity are considered; they are

$$f_k(T - T_0, \tilde{k}) = 1 + \frac{(T - T_0) - (T_1 - T_0)}{(T_2 - T_0) - (T_1 - T_0)}(\tilde{k} - 1) \tag{4.4}$$

$$f_C(T - T_0, \tilde{C}) = 1 + \frac{(T - T_0) - (T_1 - T_0)}{(T_2 - T_0) - (T_1 - T_0)}(\tilde{C} - 1) \tag{4.5}$$

which gives the thermal conductivity value of k_1 at T_1 and k_2 at T_2. The temperature dependence causes Eq. (4.1) to be nonlinear in T. The boundary conditions are

$$\frac{\partial T}{\partial r}(R_2,z,t)=0 \quad \frac{\partial T}{\partial z}(r,0,t)=0 \quad \frac{\partial T}{\partial z}(r,Z,t)=0 \tag{4.6}$$

The initial condition is

$$T(r,z,0)=T_0 \tag{4.7}$$

Also,

$$\tilde{k}_h \equiv \frac{k_h}{k_1}, \tilde{C}_h \equiv \frac{C_h}{C_1} \tag{4.8}$$

The above problem is now put in a dimensionless form. Let

$$\tilde{r} \equiv \frac{r}{R_1}, \tilde{R}_2 \equiv \frac{R_2}{R_1}, \tilde{z} \equiv \frac{z}{R_1}, \tilde{t} \equiv \frac{k_1 t}{C_1 {R_1}^2}, \ \tilde{k} \equiv \frac{k_2}{k_1}, \tilde{C} \equiv \frac{C_2}{C_1}, \tilde{k}_h \equiv \frac{k_h}{k_1}, \tilde{C}_h \equiv \frac{C_h}{C_1} \tag{4.9}$$

and

$$\tilde{T} \equiv \frac{T-T_0}{\frac{g_0 R_1^2}{k_1}}, \tilde{T}_1 \equiv \frac{T_1-T_0}{\frac{g_0 R_1^2}{k_1}}, \ \tilde{T}_2 \equiv \frac{T_2-T_0}{\frac{g_0 R_1^2}{k_1}} \tag{4.10}$$

With this model and with a known volumetric heat generation, the dimensionless temperature is given symbolically by

$$\tilde{T}=\tilde{T}(\tilde{r},\tilde{R}_2,\tilde{z},\tilde{t},\tilde{k},\tilde{C},\tilde{k}_h,\tilde{C}_h,\tilde{T}_1,\tilde{T}_2) \tag{4.11}$$

Now the partial derivatives of temperature T are found. Notice that

$$T - T_0 = \frac{gR_1^2}{k_1}\tilde{T}\left(\begin{matrix}\tilde{r},\tilde{R}_2,\tilde{z},\tilde{t}(k_1,C_1),\tilde{k}(k_1,k_2),\tilde{C}(C_1,C_2),\ldots \\ \tilde{k}_h(k_h,k_1),\tilde{C}_h(C_h,C_1),T_1(k_1,T_1-T_0),T_2(k_1,T_2-T_0)\end{matrix}\right) \tag{4.12}$$

The scaled sensitivity coefficient with respect to k_1 is

$$\hat{X}_{k_1} = -\frac{g_0 R_1^2}{k_1}\tilde{T} + \frac{g_0 R_1^2}{k_1}\left[\tilde{t}\frac{\partial\tilde{T}}{\partial\tilde{t}} - \tilde{k}\frac{\partial\tilde{T}}{\partial\tilde{k}} - \tilde{k}_h\frac{\partial\tilde{T}}{\partial\tilde{k}_h} + T_1\frac{\partial\tilde{T}}{\partial T_1} + T_2\frac{\partial\tilde{T}}{\partial T_2}\right] \tag{4.13}$$

Repeat for the derivative with respect to k_2 and k_h to get

$$\hat{X}_{k_2} = \frac{g_0 R_1^2}{k_1}\left[\tilde{k}\frac{\partial\tilde{T}}{\partial\tilde{k}}\right] \tag{4.14}$$

$$\hat{X}_{k_h} = \frac{g_0 R_1^2}{k_1}\left[\tilde{k}_h\frac{\partial\tilde{T}}{\partial\tilde{k}_h}\right] \tag{4.15}$$

The scaled sensitivity coefficients for C_1 and C_2 and C_h are

$$\hat{X}_{C_1} = \frac{g_0 R_1^2}{k_1}\left[-\tilde{t}\frac{\partial\tilde{T}}{\partial\tilde{t}} - \tilde{C}\frac{\partial\tilde{T}}{\partial\tilde{C}} - \tilde{C}_h\frac{\partial\tilde{T}}{\partial\tilde{C}_h}\right] \tag{4.16}$$

$$\hat{X}_{C_2} = \frac{g_0 R_1^2}{k_1}\left[\tilde{C}\frac{\partial\tilde{T}}{\partial\tilde{C}}\right] \tag{4.17}$$

$$\hat{X}_{C_h} = \frac{g_0 R_1^2}{k_1}\left[\tilde{C}_h\frac{\partial\tilde{T}}{\partial\tilde{C}_h}\right] \tag{4.18}$$

Next the derivative with respect to T_1-T_0 and T_2-T_0 is found; it is

$$\hat{X}_{(T_1-T_0)} = \frac{g_0 R_1^2}{k_1} \tilde{T}_1 \frac{\partial \tilde{T}}{\partial \tilde{T}_1} \tag{4.19}$$

$$\hat{X}_{(T_2-T_0)} = \frac{g_0 R_1^2}{k_1} \tilde{T}_2 \frac{\partial \tilde{T}}{\partial \tilde{T}_2} \tag{4.20}$$

Adding Eqs. (4.13)-(4.18), while subtracting Eqs. (4.19) and (4.20) gives the Intrinsic Sum, I_S:

$$\hat{X}_{k_1} + \hat{X}_{k_2} + \hat{X}_{k_h} + \hat{X}_{C_1} + \hat{X}_{C_2} + \hat{X}_{C_h} - \hat{X}_{(T_1-T_0)} - \hat{X}_{(T_2-T_0)} + \left(T - T_0\right) = 0 \tag{4.21}$$

The first six scaled sensitivity coefficients in Eq. (4.21) are for fixed x and t values. The final two derivatives are the rate of change in the computed temperature when the specified temperature T_1 or T_2 is changed. As a general rule, if the sum of scaled sensitivity coefficients is equal to zero then all the parameters in the model cannot be estimated uniquely and simultaneously. Equation (4.21) indicates that the four parameters k_1, k_2, C_1, C_2 may be simultaneously estimated when temperatures are measured and the volumetric heat generation is prescribed, because sum of scaled sensitivity coefficients is not zero.

A simulation of the instrument was performed using the finite element code COMSOL®. The simulation was performed with assumed values of temperature-dependent thermal properties for biological materials. For simulation purposes, the assumed values of parameter were: k_1 = 0.5 W/mK, k_2 = 0.6 W/mK, C_1 = 3.5x10^6

J/m^{3}K, C_2 = 3.9 x10^6 J/m^{3}K, k_h = 3 W/mK, C_h = 720 J/m^{3}K, T_0 = 20^{o}C, T_1 = 25^{o}C and T_2 = 140°C. The heater power was 5.63 x10^7 W/m^3, which is equivalent to a total heater power of 24 W. Figure 4.1 represents the simulated profile of temperature in the instrument. For the simulation, the heater element was powered for 26 seconds. The power supply was automatically cut off once the heater temperature reached 140^{o}C. The scaled sensitivity coefficients are plotted in Figure 4.2. The scaled sensitivity coefficient of k_1 is larger for time <23 sec, and for time >23 sec k_2 is larger. This information is of great importance to design the instrument for thermal properties measurement. If we wish to estimate k_2 accurately, it is important for the experimental time for be >23 sec, for a given heater power of 24 W. Increasing the heater power will increase the scaled sensitivity coefficient of k_2; however, there is a constraint of maximum temperature rise of the product. Based on the absolute size of the scaled sensitivity coefficients (Figure 4.2) the order of accuracy (most to least) for estimation of the parameters would be k_2, k_1, C_1 and C_2. Since the scaled sensitivity of T_1-T_0 and T_2-T_0 is positive, it indicates that the temperature rise is decreased by the T_1-T_0 and T_2-T_0 sensitivity. The scaled sensitivity of C_2 is relatively small compared to the maximum temperature rise and hence might not be estimated with high accuracy. Hence, even though all the sensitivity coefficients are different shapes and uncorrelated, some of the parameters may not be estimated

well. To estimate all of the four parameters in the model, another thermocouple may be needed at a different location from the surface of the heater. Therefore, it is important to analyze the sensitivity coefficients to obtain insight into the estimation problem. The I_S is plotted in Figure 4.3. The values of I_S is on the order of 10^{-7}, which indicates that the numerical code is accurate.

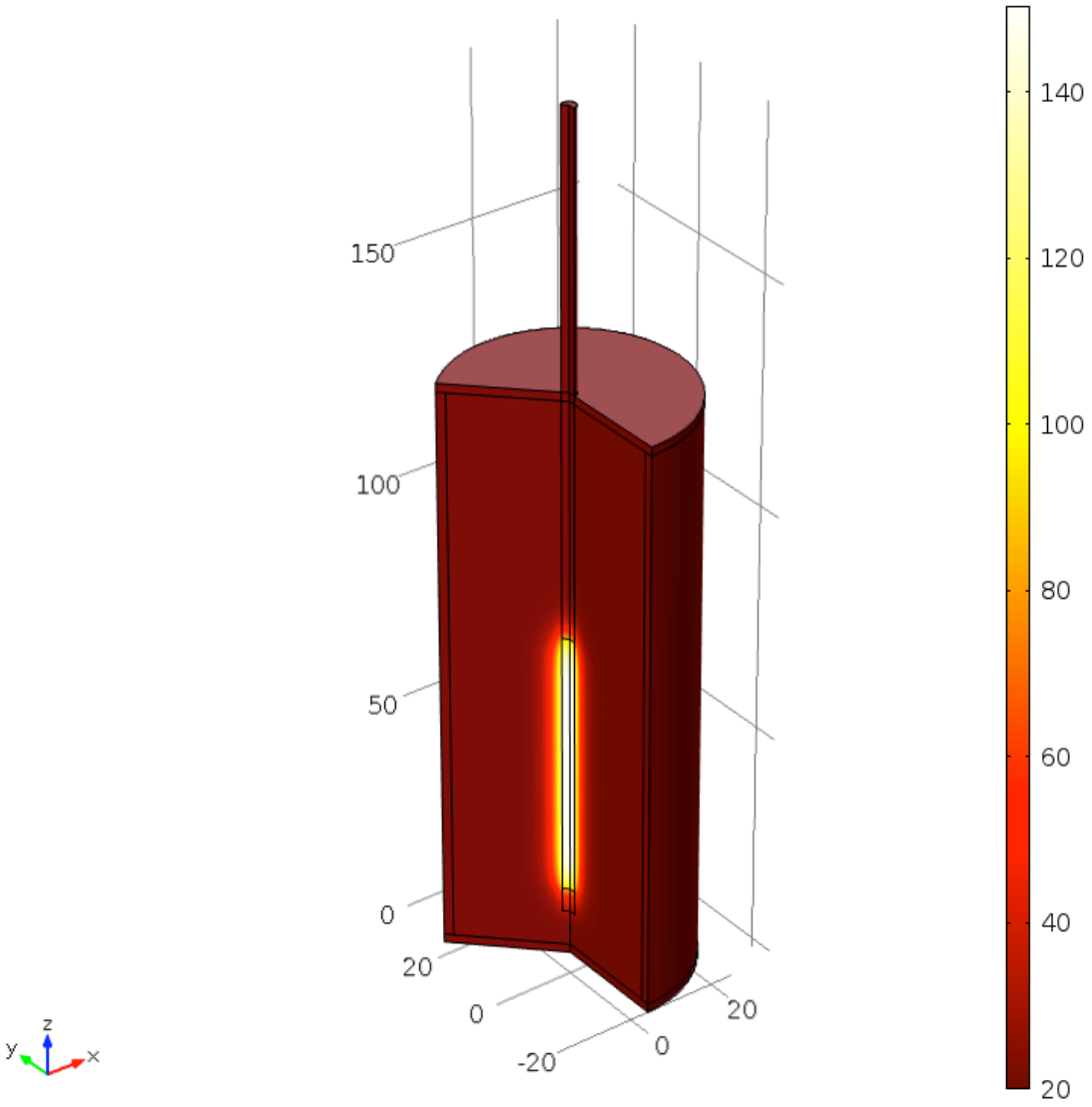

Figure 4.1 Simulated heating profile of test material

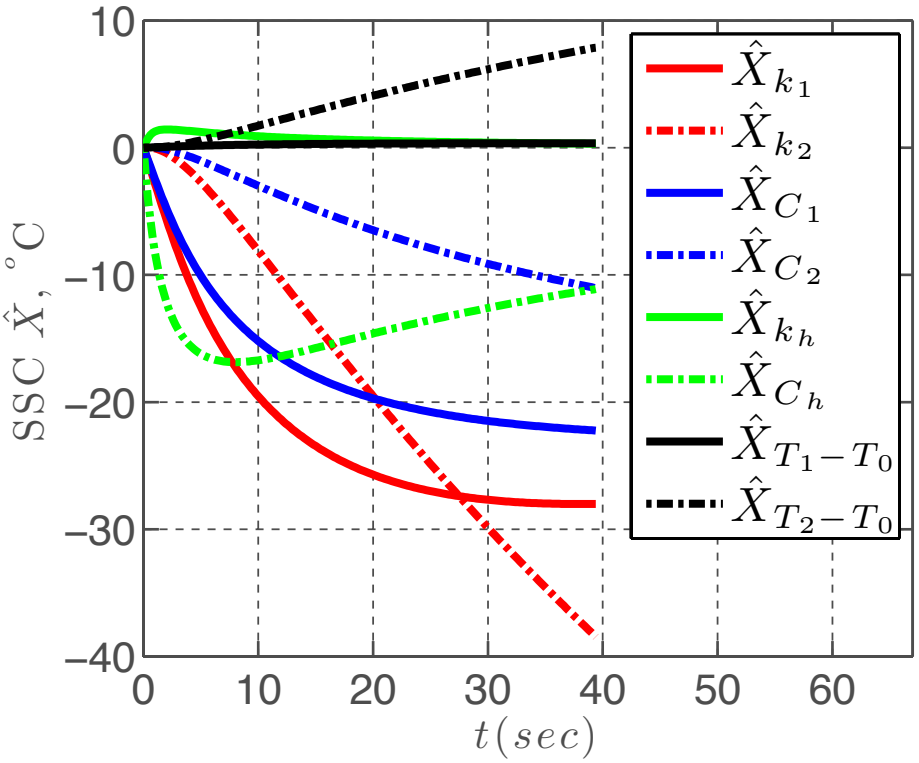

Figure 4.2 Plot of Scaled sensitivity coefficients of the parameters in the model given by Eq. (4.1), using simulated temperature data.

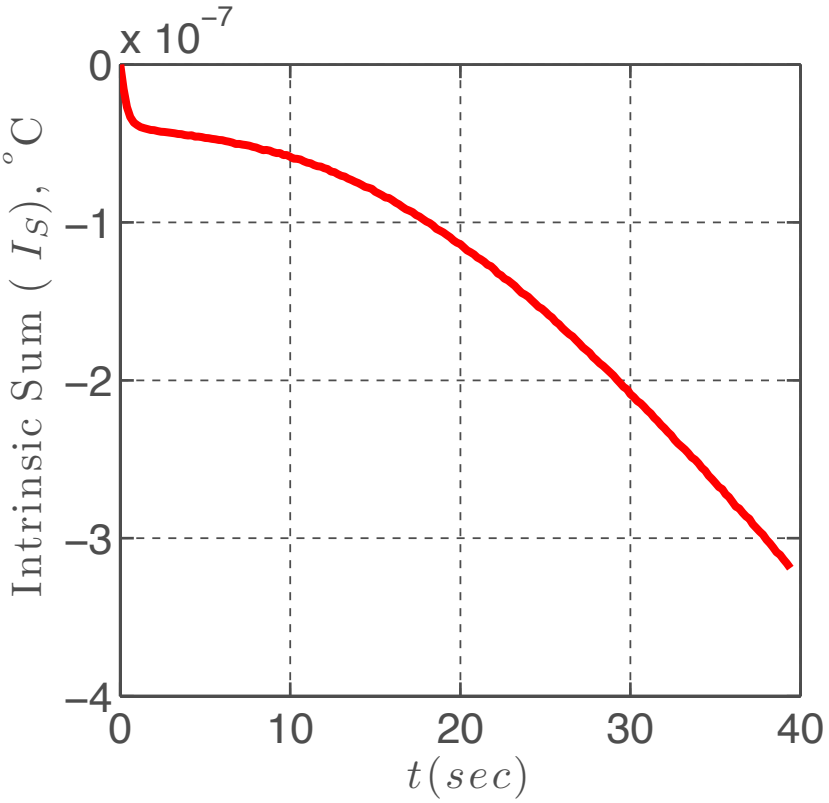

Figure 4.3 Plot of Intrinsic Sum as given by Eq. (4.21)

4.2.2 Equipment design

The design of the equipment is based on the mathematical model given by Eq. (4.1). The schematic of the probe design and the container is shown in Figure 4.1. By using the inverse problem, the thermal parameters will be estimated simultaneously within the desired temperature range, which will be representative of current processing temperatures. The transient heat conduction problem with the temperature-dependent thermal properties is given by Eq. (4.1). Thermal conductivity *k(T)* and specific heat capacity *C(T)* were modeled as functions of temperature. The spatial domain (that is, the size of the container) is sufficiently

large so that the outer boundaries do not affect the temperature distribution near the heater; hence the domain is from the center of probe to a large radius. (de Monte and others 2008). Notice that this condition includes the heat capacity of the probe, which is not always done but can be treated using the software. A sensitivity analysis is done to evaluate the accuracy of the parameters. This method of estimation of the thermal parameters is approximately 1 min or less as opposed to 5-6 hours required in the isothermal method of measurement to cover the desired temperature range.

There are several components of the instrument. The equipment consists of the following units:

1. NI 9225 3-Ch +/-300V Analog Input (National Instruments, Austin, Texas): This unit has been added to the instrument to measure the voltage going through the heater. It has a full measurement range of 300 Vrms.
2. NI 9227 4 ch current input, 5Amp, ISO, 50k, 24bit (National Instruments, Austin, Texas): This current measuring unit is used in conjunction with the voltage measuring device to measure the power and energy consumption for the heater application. This module is designed to measure 5 Amps nominal and up to 14 A peak. It can sample at 50kS/s per channel.
3. NI 9481 4-Ch 30 VDC (2 A), 60 VDC (1 A), 250 VAC (2A) EM Form A SPST Relay Module (National Instruments, Austin, Texas): The main function of

this relay device is to act as a safety switch. This is programmed to switch off the power supply to the heater when the temperature rise in the instrument is greater than 140^{o}C.

4. cDAQ-9174, CompactDAQ chassis (4 slot USB) (National Instruments, Austin, Texas): This CompactDAQ USB chassis is designed for small, portable, mixed-measurement test systems. The voltage, current, relay and voltage output modules are mounted on this CompactDAQ. It connects with the computer through a USB connection and programmed with the LabView interface.
5. NI 9263 4-Channel, 100 kS/s, 16-bit, ±10 V, Analog Output Module (National Instruments, Austin, Texas): Analog output module is used for providing specified voltage output to the heater.
6. Phase angle controller, FC11AL/2 (United Automation): Phase angle controller is used to adjust the incoming full voltage (110 V) from the main power supply. The output signal from this device is fed to the voltage output device (NI 9263).
7. Sample Cup: The testing sample holder is made from a 316 stainless steel and is rated to hold pressure up to100 psi. The tripod type legs are attached to the bottom part of the cup and provide the full stability to the whole equipment. The sample holder cylindrical cup radius is 23.5 mm, with a length of 124 mm.

8. Lid: The closing of the sample cup is accomplished from the top lid with a gasket in between. The lid is also manufactured from 316 stainless steel material. There are three NPT (National Pipe Thread) threaded holes on the lid. The first NPT is at the center of the lid and is provided to insert the heater. The second NPT is off-center and is designed to provide a pressure connection from a pressurized air tank. The third NPT is also off-center and is designed for the pressure relief valve. The pressure relief valve is rate to 50 psi.
9. Heating element: Total output power of the heater is 30 Watts. Power of heater is calculated based on the desired temperature rise in the product. The power output of the heater is programmable with a combination of the phase angle controller and the voltage output module. The heater specifications are provided below:
    a. High Watt Density: 33.4 w/in^2
    b. Diameter: 0.125", High: 3.15mm Low: 3.05mm Swage to Size
    c. Heater Length: 7", Tolerance: ±0.210"
    d. Watts: 30, ±10%
    e. Volts: 120
    f. Unheated: Leads: 4.5", Cap:0.211"
    g. Heated Length: 2.29"
    h. Lead Length: 48", ±2.4"
    i. Lead Type: Teflon 260C/500^{o}F[Swaged]

j. Tube Material: SS321

k. Potting: None (Teflon plug)

10. Pressure: a compressed air tank supplies Pressure to the instrument.
11. Software Interface: a program developed using LabVIEW (National Instruments) software controls the instrument.

A schematic of the electronics of the instrument is presented in Figure 4.4. The instrumentation has the capability to generate different heating profiles. To generate different heating profiles, a phase angle controller device (FC11AL/2) has been added to the circuit. This voltage module has different settings that can be adjusted with the program. With the settings from the voltage module, a voltage output module (NI 9263)) sends the information to the heater. This setting allows better control of the heating rate in the sample. The LabVIEW® program includes the settings for the heating profile. The voltage and ampere loggers record the power generated in the heater. A relay unit is programmed so that if the temperature rise of the heater is more than a set value, then the relay will turn off the device.

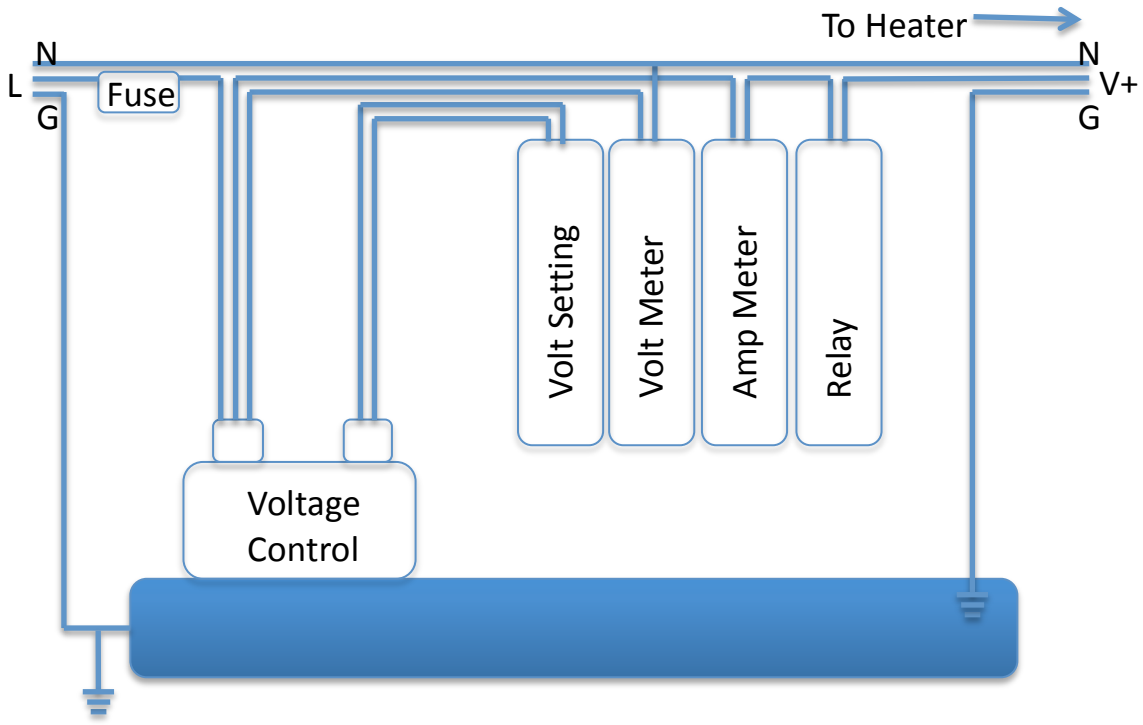

Figure 4.4 Schematic of the electronics of the temperature-dependent thermal property measurement instrument

A custom stainless steel cup was manufactured to hold the sample and the heater. This vessel is pressurized to allow a maximum temperature of 140^{o}C. The pressure fittings accommodate the heater and thermocouples. The pressurized air is connected from the pressurized tank to the vessel with a three-way valve. A safety valve is installed on the vessel to limit the maximum pressure rise. This safety valve is set to a maximum pressure rating of 50 psi. The pressure rating of the vessel itself is greater than 100 psi. The complete set-up of the instrument is represented in Figure 4.4. The output power is recorded every 0.2 sec along with the temperature. The complete set up of the instrument is represented in Figure 4.5.

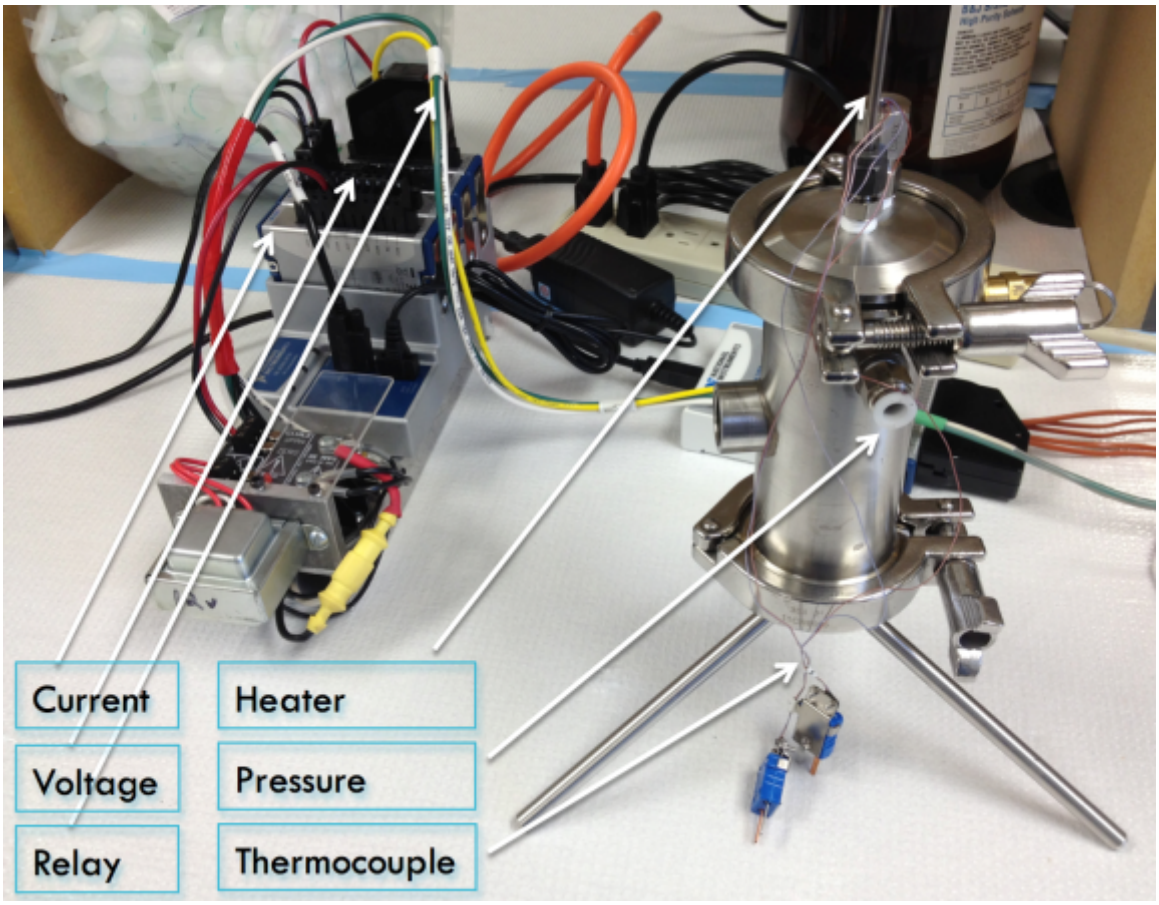

Figure 4.5 Thermal property measurement instrument with the data acquisition devices

4.2.3 Temperature calibration and sample testing

Temperature measurement using a thermocouple was found to be inaccurate, due to conduction from the heater to the thermocouple. Therefore, the heating element of the heater was used as a temperature-indicating device. The resistance of the heating element is dependent on its temperature. This information was used to calibrate the resistance of the heating element. The calibration was

performed using a silicon oil bath set at predetermined temperatures. A resistance meter (Fluke 741B) was used to measure the resistance of heater at set temperatures. Several food materials were tested to determine temperature dependent thermal conductivity, using the instrument. The foods tested were carrot puree, banana puree, banana oat puree, and sweet potato puree.

4.2.4 Sequential estimation of parameters

The sequential method of estimation updates parameters as new observations are added. Sequential estimation of parameters in a model provides good insight into building the model and determining uncertainty in parameters. For example, if parameters come to a constant value after a certain reasonable time then the experiment can be stopped, as further data will not improve the parameter estimate. Prior information of parameters can be used in sequential estimation towards estimation of parameters for a particular experiment. The advantage of sequential over OLS is that more insight is given in the estimation process, because parameters are updated with the addition of each datum. The quality of the model for a given data set is judged by how well each parameter approaches a constant before the end of the experiment.

There were only two studies found in the food literature where simultaneous sequential estimation based on Gauss minimization was used, one for estimation of both thermal conductivity and volumetric specific heat (Mohamed 2009), and one for estimation of thermal diffusivity (Mohamed 2010). The sequential procedure in this work was developed using the matrix inversion lemma (Beck and Arnold

1977b, p. 277) based on the Gauss minimization method, requiring prior information. The mathematical form of non-linear sequential estimation is derived from maximum a posteriori (MAP) estimation. The minimization function in the Gauss method can be expressed as:

$$S = \left[Y - \hat{Y}(\beta) \right]^T W \left[Y - \hat{Y}(\beta) \right] + \left[\mu - \beta \right]^T U \left[\mu - \beta \right] \qquad (4.22)$$

Where, Y is the experimental response variable and $\hat{Y}$ is predicted response, μ is prior information of parameter vector β, W is inverse of covariance matrix of errors and U is inverse of covariance matrix of parameters. The extremum of the function given by equation (4.22) can be evaluated by differentiating it with respect to β. The expression can be given as:

$$\nabla_\beta S = -2 \left[\nabla_\beta \hat{Y}(\beta) \right]^T W \left[Y - \hat{Y}(\beta) \right] - 2 \left[I \right] U \left[\mu - \beta \right] \qquad (4.23)$$

Eq. (4.23) can be set to zero, and β solved for implicitly. Standard statistical assumptions that allow the use of sequential estimation are: additive errors, zero mean, uncorrelated errors, normally distributed errors, covariance matrix of errors is completely known, no errors in independent variables and subjective prior information of parameters are known. One method to do this is an iterative scheme (Beck and Arnold 1977, p. 277):

$$A_{i+1} = P_i X^T_{i+1} \qquad (4.24)$$

$$\Delta_{i+1} = \phi_{i+1} + X_{i+1} A_{i+1} \tag{4.25}$$

$$K_{i+1} = A_{i+1} \Delta_{i+1}^{-1} \tag{4.26}$$

$$e_{i+1} = Y_{i+1} - \hat{Y}_{i+1} \tag{4.27}$$

$$b^*_{i+1} = b^*_i + K_{i+1} \left[e_{i+1} - X_{i+1} \left(b^*_i - b \right) \right] \tag{4.28}$$

$$P_{i+1} = P_i - K_{i+1} X_{i+1} P_i \tag{4.29}$$

Where b^*_{i+1} is the updated parameter (*px1*, p is the number of parameters) vector at time step i+1; b^*_i is the parameter vector at the previous time step i; *b* is the parameter vector at the previous iteration; *P* is the covariance vector matrix of parameters (*p x p*), *X* is the sensitivity coefficient matrix (*nxp*), and *e* is the error vector. The scheme is started by providing parameter estimates, computing *X* and the error vector *e*, and assuming a matrix *P*. Because we did not have accurate prior information on the covariance matrix, we set *P* as a diagonal matrix of 10^5. Matrix *P*, *X* and *e* are functions of *b* and not of *b**. The stopping criteria for *b* can be given as

$$\frac{\left| b_j^{k+1} - b_j^k \right|}{\left| b_j^k \right| + \delta_1} < \delta \tag{4.30}$$

Where, j is the index for the number of parameters. The magnitude of δ could be in the order of 10^{-4}. Another small number is δ_1 which is very small such as 10^{-8}, to avoid the problem when b_j^k tends to zero.

4.3 Results

4.3.1 Instrument calibration

The calibration curve for the heater is presented in Figure 4.6. The temperature is plotted on the y-axis and resistance on the x-axis. A linear relation was found between the resistance and temperature as given by Eq. (4.31):

$$T = 26.118R - 12609 \tag{4.31}$$

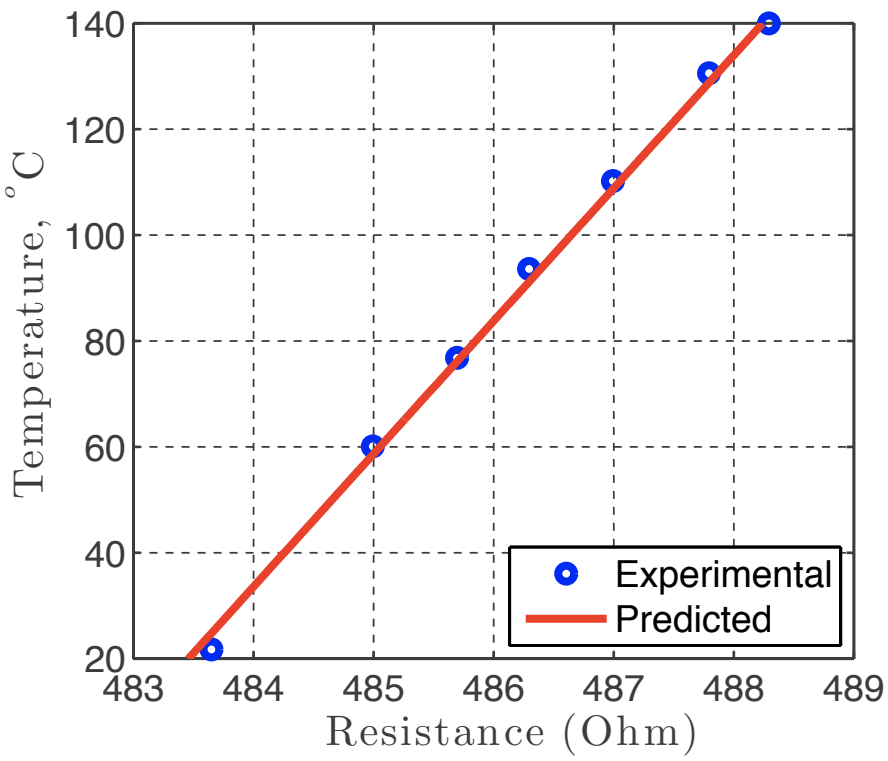

Figure 4.6 Calibration curve of resistance and temperature of the heating element

After the verification of finite element code, the resistance (converted to temperature) data collected from the instrument was analyzed using the sequential estimation procedure (Dolan and others 2012; Beck and Arnold 1977a). Sequential estimation is based on gauss minimization method and needs prior information regarding the parameters that needs to be estimated. Sequential procedure updates the parameters as each observation is added to the estimation procedure. Analysis software was developed using the principles of sequential estimation. Once the temperature data was entered in the program, the software outputs the estimated

parameters with statistical indices. There are four main output plots from the software, 1) predicted and observed temperature, 2) residuals, 3) sequential estimation, and 4) scaled sensitivity.

The instrument was calibrated with 95% glycerol. Simulated heating of glycerol at two different locations away from the surface of the heater is shown in Figure 4.7. However, for estimation of thermal conductivity, the measured temperature using the resistance of the heater was used. The power input of the heater was 24 Watts. The thermal conductivities were estimated at initial and final temperature of the heating range. The estimated value of thermal conductivity of glycerol at 19^{o}C was 0.268 W/m^{o}C and at 118.5^{o}C was 0.362 W/m^{o}C. The thermal conductivity of glycerol at 32^{o}C was 0.283 W/m^{o}C, which is in the range of reported values in literature (Zhu and others 2007).

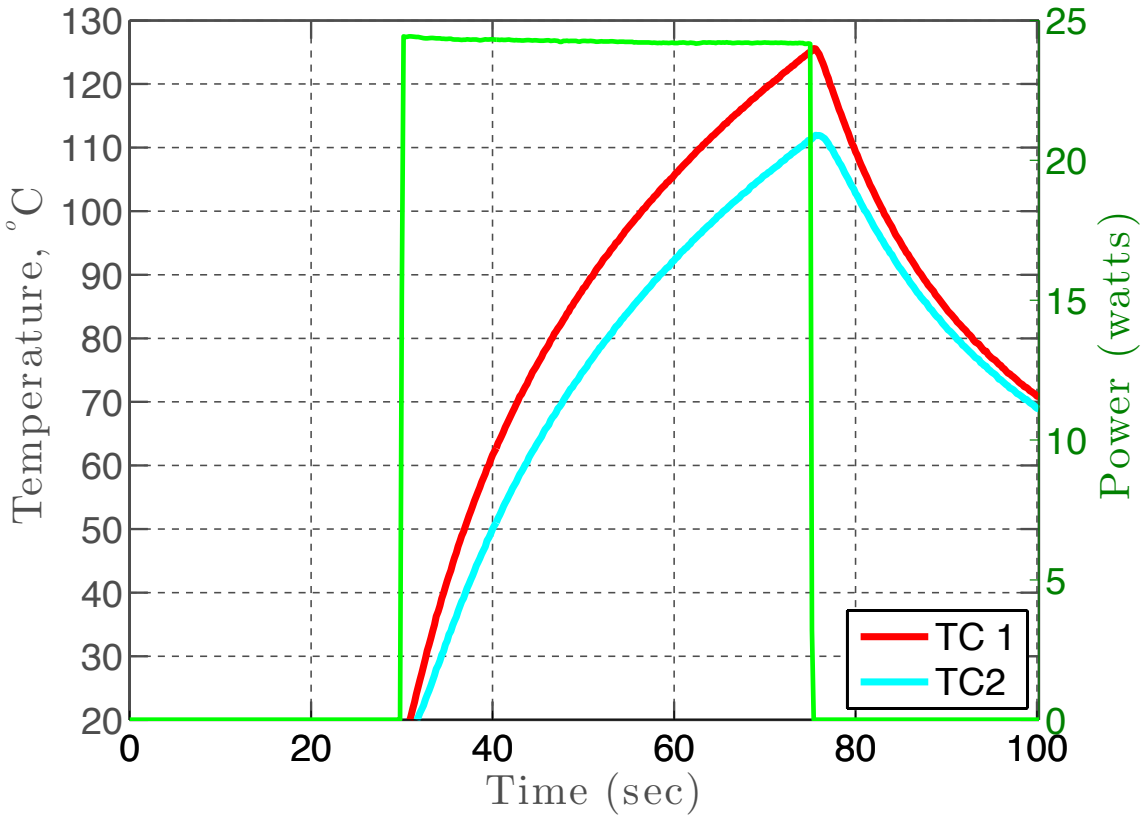

Figure 4.7 Simulated heating curves of glycerol at two different locations for a given power input

4.3.2 Instrument experimental result

Figure 4.8 shows the experimental temperature and predicted temperature versus time for the sweet potato puree. Note that the experimental duration is less than 40 seconds. For the estimation of thermal conductivities, the values of specific heat must be known. The value of glycerol volumetric heat capacity was used from literature. However, the values of temperature-dependent volumetric heat capacity of banana puree and banana oat were measured using a DSC (Differential Scanning Calorimeter, Q2000, TA Instruments, New Castle, DE).

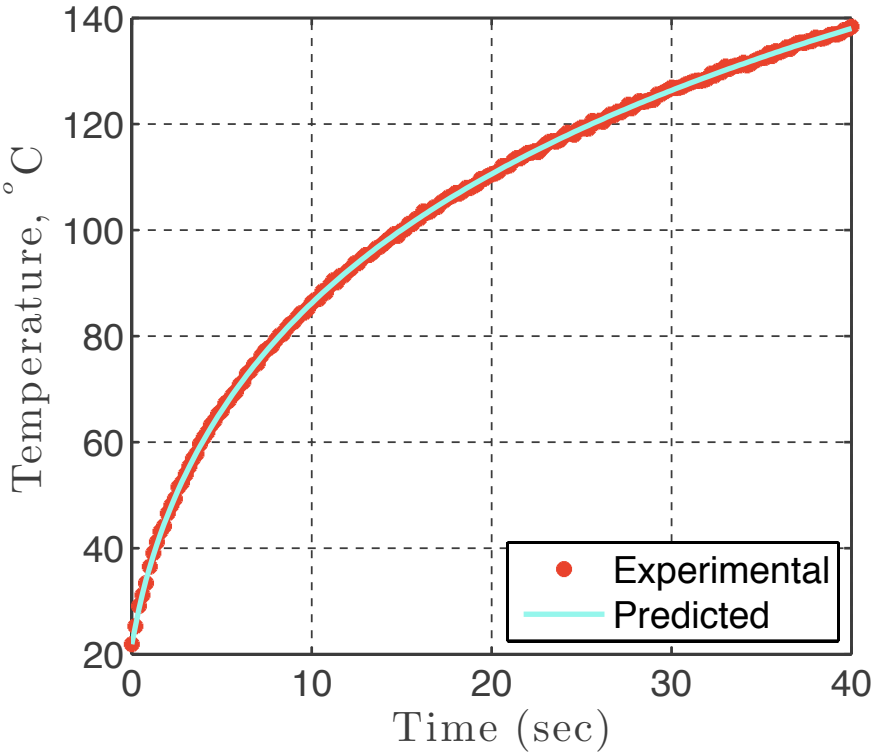

Figure 4.8 Experimental and predicted heating profile of sweet potato puree for a given power input of 24 W.

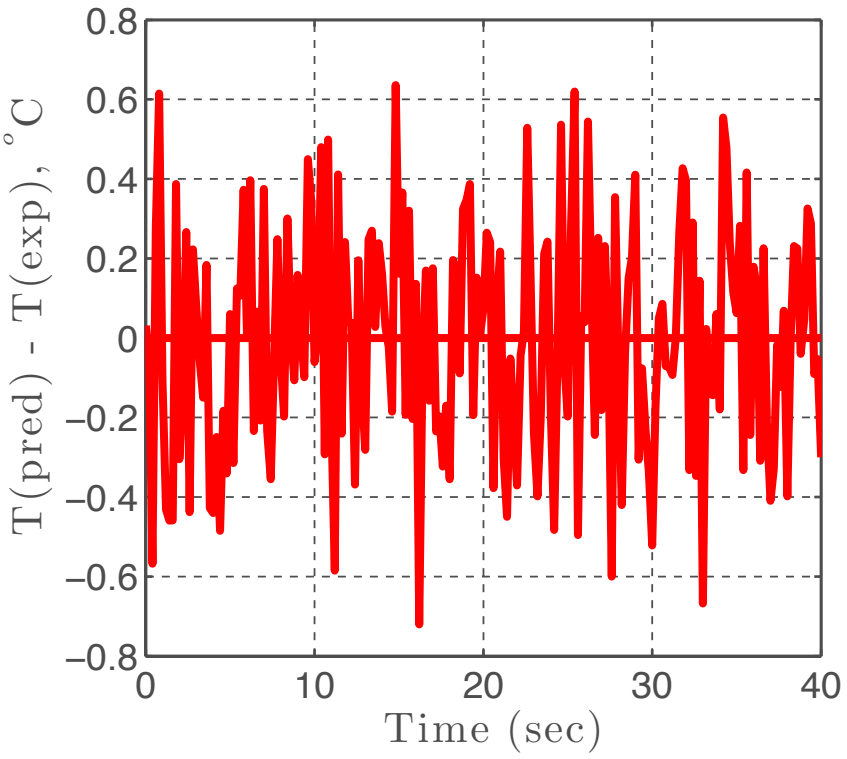

Figure 4.9 Residuals of sweet potato puree for a given power input of 24 W.

The residuals for the estimation process of sweet potato puree are presented in Figure 4.9. The residual plot does not seem to violate any standard statistical assumptions (additive, zero mean, uncorrelated, constant variance and normal distribution of residuals). It looks normally distributed and there is no apparent pattern or signature in the residuals. The estimated values of thermal conductivities and statistical indices are reported in Table 4.2. The estimated value of thermal conductivity at 25^{o}C was 0.539 W/m^{o}C. The 95% asymptotic confidence intervals are also reported in Table 4.2.

A commercially available unit (KD2 PRO, Decagon Devices) for thermal conductivity measurement was used to compare the values for sweet potato puree. The measured value of k_1 at 25^{o}C using KD2 PRO was 0.529 W/m^{o}C and 0.546 W/m^{o}C for two different tests. This is in agreement with the TPCell measurements, which was 0.539 W/m^{o}C. The composition of sweet potato puree is provided in Table 4.1 (U.S. Department of Agriculture 2013). Thermal conductivity at 25^{o}C, predicted with composition model of Choi and Okos, was 0.535 W/m^{o}C. Higher temperature experiments (140^{o}C) were not possible with KD2 PRO as it was not possible to keep the oil bath temperature in equilibrium with the sample temperature. However, the repeated use of the KD2 PRO led to the failure of the sensor without any reasonable measurement of thermal conductivity.

Table 4.1 Composition of sweet potato puree from USDA nutrient database (U.S. Department of Agriculture 2013)

Components	Percentage
Protein	1.1
Fat	0.1
Carb	13.2
Fiber	1.5
Ash	0
Water	84.8
Ice	0.00

Table 4.2 Estimated values of thermal conductivities and statistical indices for sweet potato puree

Material	Temp, ^oC	K, W/m^oC	Std error	Lower CI	Upper CI	C, $J/m^{3o}C$)
Sweet Potato 1	25	0.518	0.0019	0.515	0.521	4278660
	140	0.585	0.0024	0.581	0.589	4858670
Sweet Potato 2	25	0.532	0.0019	0.529	0.535	4278660
	140	0.575	0.0024	0.571	0.579	4858670
Sweet Potato 3	25	0.548	0.0019	0.545	0.552	4278660
	140	0.568	0.0024	0.563	0.573	4858670
Sweet Potato 4	25	0.539	0.0019	0.536	0.542	4278660
	140	0.572	0.0025	0.568	0.577	4858670
Sweet Potato 5	25	0.533	0.0018	0.530	0.537	4278660
	140	0.574	0.0024	0.569	0.578	4858670
Sweet Potato 6	25	0.522	0.0018	0.519	0.525	4278660
	140	0.585	0.0024	0.581	0.589	4858670

Table 4.3 Estimated values of thermal conductivities and statistical indices for several food materials

Material	Temp, ^oC	K, W/m^oC	Std error	Lower CI	Upper CI	C, $J/m^{3o}C$)
Banana	25	0.499	0.0027	0.494	0.505	4190510
	140	0.573	0.0048	0.563	0.583	4547100
Banana Rasp Oat	25	0.487	0.0026	0.482	0.492	4431940
	140	0.566	0.0047	0.557	0.574	5069170

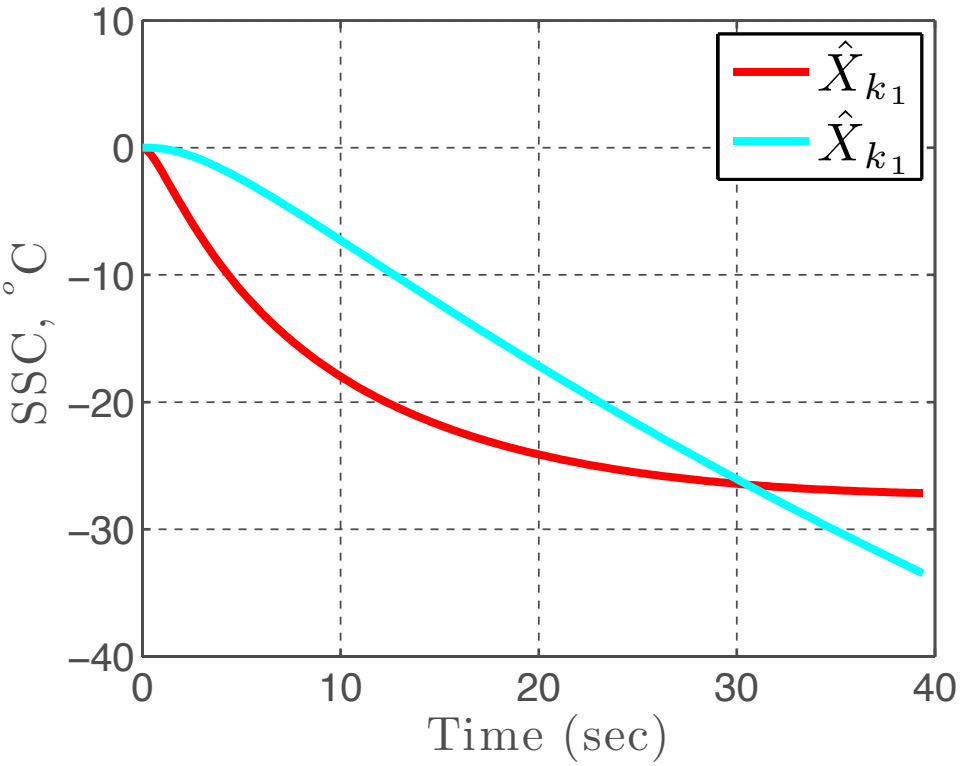

Figure 4.10 Scaled sensitivity coefficients for thermal conductivities at T_1 and T_2

The scaled sensitivity coefficients, $\hat{X}_{k_1}$ and $\hat{X}_{k_2}$ are shown in Figure 4.10 for k_1 and k_2, respectively. For initial times, the value of $\hat{X}_{k_1}$ is larger suggesting that k_1 can be estimated with good accuracy at earlier times. The value of $\hat{X}_{k_2}$ is larger towards the end of the experiment, in this case after 34 seconds. The k_2 can be estimated with good accuracy only if the experiment was performed greater than > 34 seconds. Hence, it is important to analyze the sensitivity coefficients to get insight in to the estimation problem.

Figure 4.11 shows the sequential estimation of the parameters. It is important to note that the values of k_1 and k_2 comes to a constant value after 10 seconds. This is a good sign as the parameters are not changing towards the end of the experimental time and that is what we expect from the sequential results. Sequential results provide a robust tool to check if the estimated parameters are reliable. If the value of parameter does not come to a constant toward the end of experiment, this means that there is some error in the model or in the experiment. To see the constant nature of parameters towards the end, the sequential plot was plotted for the second half of the experiment as represented in Figure 4.12. This plot reveals any trend in the parameters as each datum is added, as it removes the large values of parameters at the beginning of the experiment. Hence, sequential parameter estimation can help to diagnose problems. The parameter values reported in Table 4.2 and Table 4.3 are the values at the end of the sequential estimation procedure.

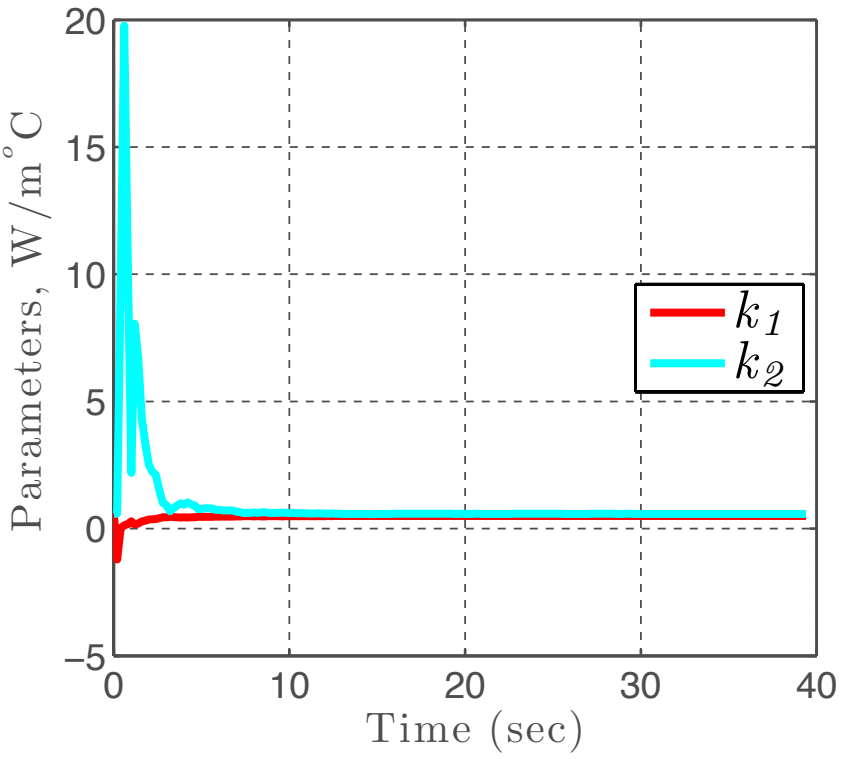

Figure 4.11 Sequential estimation of thermal conductivities at T_1 and T_2

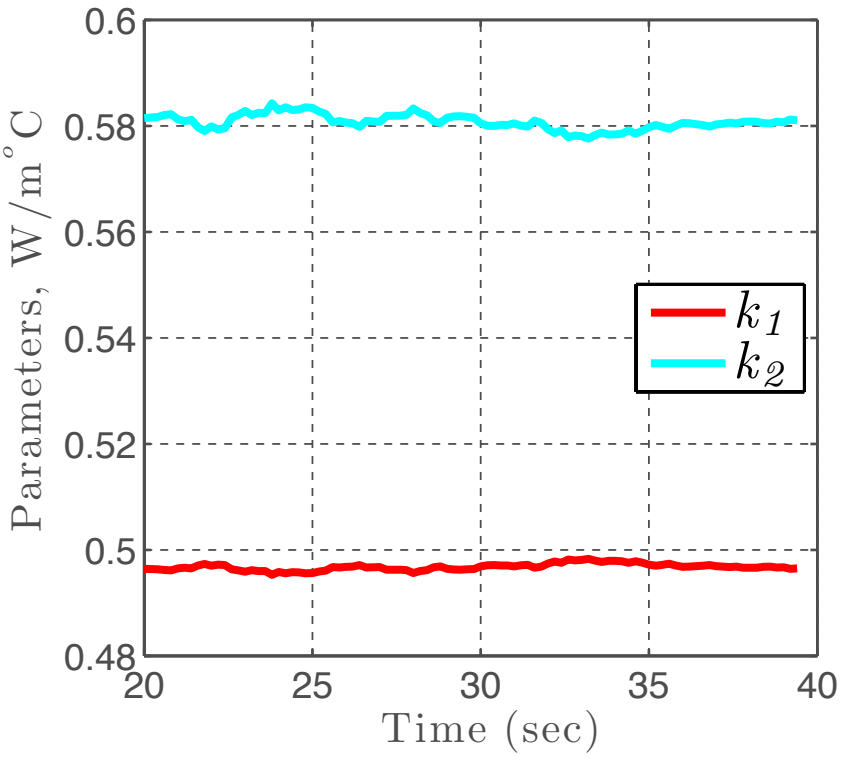

Figure 4.12 Sequential estimation of thermal conductivities at T_1 and T_2 for second half of the experimental time

4.4 Conclusions

The dimensionless derivation of scaled sensitivity coefficients was presented and implemented as an intrinsic verification method to the finite element code. The identity given by scaled sensitivity relations for heat transfer problems provides a method for checking the accuracy of a computer code at interior and boundary points and at any time. The concept is quite general and is not restricted to heat conduction or linear problems. The scaled sensitivity coefficients can also provide useful insight in to the parameter estimation problem. It can show if all the parameters in the model can be estimated and with what relative accuracy.

Based on the robust principles of intrinsic verification and insight from the scaled sensitivity coefficients, a method and instrument was presented to estimate temperature-dependent thermal properties. With the design of the instrument combined with the model capabilities, this instrument is capable of producing results in significantly less time as compared to other traditional methods. This new rapid line-source method will estimate food thermal properties in one experiment under conditions approaching an actual process (experimental run time less than 1 min). The previous labor-intensive requirement to run multiple tests at various temperatures over many hours or days can be minimized or perhaps eliminated. This new device will allow food processors to obtain rapid thermal property information to be used to design processes for maximum quality while maintaining safety.

APPENDIX

Table A.1 Data recorded from TPCell for sweet potato test 1

Time (sec)	Voltage (Volt)	Current (Amp)	Power (Watt)
0	105.7469	0.2187	23.1246
0.2	108.0289	0.2233	24.1246
0.4	108.0107	0.2232	24.1104
0.6	108.0207	0.2232	24.1094
0.8	108.0135	0.2231	24.1007
1	108.0262	0.2231	24.1009
1.2	108.0265	0.2231	24.0981
1.4	108.0019	0.2230	24.0830
1.6	107.9940	0.2229	24.0753
1.8	107.9907	0.2229	24.0704
2	107.9747	0.2228	24.0596
2.2	107.9648	0.2228	24.0523
2.4	107.9888	0.2228	24.0601
2.6	107.9921	0.2228	24.0577
2.8	107.9871	0.2227	24.0522
3	107.9955	0.2227	24.0536
3.2	108.0015	0.2227	24.0529
3.4	108.0032	0.2227	24.0521
3.6	107.9906	0.2227	24.0443
3.8	107.9892	0.2226	24.0415
4	108.0179	0.2227	24.0512
4.2	108.0121	0.2226	24.0473
4.4	107.9933	0.2226	24.0357
4.6	107.9849	0.2225	24.0301
4.8	107.9772	0.2225	24.0233
5	108.0057	0.2225	24.0349
5.2	108.0032	0.2225	24.0326
5.4	107.9927	0.2225	24.0255
5.6	107.9824	0.2224	24.0191
5.8	107.9764	0.2224	24.0135
6	107.9897	0.2224	24.0187
6.2	107.9928	0.2224	24.0176
6.4	107.9893	0.2224	24.0148
6.6	107.9774	0.2223	24.0079
6.8	107.9754	0.2223	24.0050
7	107.9914	0.2223	24.0095
7.2	108.0076	0.2224	24.0156

Table A.1 (cont'd)

Time (sec)	Voltage (Volt)	Current (Amp)	Power (Watt)
7.6	107.9779	0.2223	24.0000
7.8	107.9706	0.2222	23.9948
8	107.9988	0.2223	24.0066
8.2	108.0049	0.2223	24.0067
8.4	107.9774	0.2222	23.9943
8.6	107.9779	0.2222	23.9927
8.8	107.9723	0.2222	23.9871
9	108.0101	0.2222	24.0035
9.2	108.0094	0.2222	24.0027
9.4	107.9974	0.2222	23.9956
9.6	107.9989	0.2222	23.9954
9.8	107.9780	0.2221	23.9834
10	108.0064	0.2222	23.9954
10.2	108.0239	0.2222	24.0023
10.4	108.0011	0.2221	23.9898
10.6	107.9941	0.2221	23.9858
10.8	107.9844	0.2221	23.9810
11	107.9878	0.2221	23.9813
11.2	107.9837	0.2220	23.9771
11.4	107.9795	0.2220	23.9754
11.6	107.9847	0.2220	23.9771
11.8	107.9847	0.2220	23.9744
12	108.0142	0.2221	23.9864
12.2	108.0139	0.2221	23.9856
12.4	108.0023	0.2220	23.9802
12.6	108.0005	0.2220	23.9769
12.8	107.9850	0.2220	23.9692
13	108.0013	0.2220	23.9750
13.2	108.0105	0.2220	23.9783
13.4	108.0059	0.2220	23.9754
13.6	108.0042	0.2220	23.9742
13.8	107.9826	0.2219	23.9633
14	108.0008	0.2219	23.9701
14.2	108.0104	0.2220	23.9738
14.4	107.9832	0.2219	23.9606
14.6	107.9826	0.2219	23.9584
14.8	107.9848	0.2219	23.9594

Table A.1 (cont'd)

Time (sec)	Voltage (Volt)	Current (Amp)	Power (Watt)
15	108.0188	0.2220	23.9751
15.2	108.0305	0.2220	23.9774
15.4	108.0184	0.2219	23.9715
15.6	107.9859	0.2219	23.9574
15.8	107.9949	0.2219	23.9592
16	108.0182	0.2219	23.9698
16.2	108.0257	0.2219	23.9712
16.4	108.0046	0.2219	23.9612
16.6	108.0035	0.2218	23.9597
16.8	107.9955	0.2218	23.9553
17	108.0249	0.2219	23.9677
17.2	108.0237	0.2219	23.9658
17.4	108.0022	0.2218	23.9558
17.6	108.0086	0.2218	23.9579
17.8	108.0066	0.2218	23.9568
18	108.0308	0.2218	23.9658
18.2	108.0396	0.2218	23.9685
18.4	108.0023	0.2218	23.9520
18.6	108.0001	0.2218	23.9502
18.8	107.9723	0.2217	23.9367
19	108.0108	0.2218	23.9528
19.2	107.9987	0.2217	23.9470
19.4	107.9801	0.2217	23.9375
19.6	107.9940	0.2217	23.9438
19.8	107.9398	0.2216	23.9191
20	107.9471	0.2216	23.9206
20.2	107.9955	0.2217	23.9420
20.4	107.9950	0.2217	23.9410
20.6	108.0044	0.2217	23.9446
20.8	107.9758	0.2216	23.9312
21	108.0011	0.2217	23.9411
21.2	108.0211	0.2217	23.9494
21.4	108.0091	0.2217	23.9438
21.6	108.0071	0.2217	23.9413
21.8	107.9863	0.2216	23.9317
22	108.0192	0.2217	23.9464
22.2	108.0340	0.2217	23.9516
22.4	108.0146	0.2217	23.9427

Table A.1 (cont'd)

Time (sec)	Voltage (Volt)	Current (Amp)	Power (Watt)
22.6	108.0012	0.2216	23.9371
22.8	107.9878	0.2216	23.9298
23	108.0262	0.2217	23.9463
23.2	108.0290	0.2217	23.9459
23.4	108.0096	0.2216	23.9374
23.6	108.0151	0.2216	23.9390
23.8	107.9983	0.2216	23.9321
24	108.0232	0.2216	23.9404
24.2	108.0311	0.2216	23.9446
24.4	108.0167	0.2216	23.9369
24.6	108.0022	0.2216	23.9301
24.8	107.9906	0.2215	23.9246
25	108.0118	0.2216	23.9330
25.2	108.0227	0.2216	23.9369
25.4	108.0204	0.2216	23.9354
25.6	108.0078	0.2215	23.9283
25.8	108.0012	0.2215	23.9262
26	108.0302	0.2216	23.9380
26.2	108.0230	0.2216	23.9343
26.4	108.0201	0.2216	23.9319
26.6	108.0396	0.2216	23.9416
26.8	108.0235	0.2216	23.9328
27	108.0324	0.2216	23.9362
27.2	108.0495	0.2216	23.9443
27.4	108.1154	0.2217	23.9720
27.6	108.1240	0.2217	23.9752
27.8	108.1180	0.2217	23.9721
28	108.1349	0.2218	23.9801
28.2	108.1297	0.2217	23.9753
28.4	108.0254	0.2215	23.9288
28.6	108.0277	0.2215	23.9286
28.8	108.0013	0.2215	23.9171
29	108.0329	0.2215	23.9319
29.2	108.0447	0.2215	23.9359
29.4	108.0417	0.2215	23.9339
29.6	108.0223	0.2215	23.9246
29.8	108.0211	0.2215	23.9234
30	108.0434	0.2215	23.9318

Table A.1 (cont'd)

Time (sec)	Voltage (Volt)	Current (Amp)	Power (Watt)
30.2	108.0567	0.2215	23.9378
30.4	108.0387	0.2215	23.9297
30.6	108.0352	0.2215	23.9280
30.8	108.0284	0.2215	23.9242
31	108.0274	0.2215	23.9237
31.2	108.0407	0.2215	23.9281
31.4	108.0187	0.2214	23.9181
31.6	108.0148	0.2214	23.9176
31.8	108.0121	0.2214	23.9140
32	108.0442	0.2215	23.9266
32.2	108.0608	0.2215	23.9341
32.4	108.0327	0.2214	23.9228
32.6	108.0387	0.2214	23.9225
32.8	108.0301	0.2214	23.9203
33	108.0380	0.2214	23.9227
33.2	108.0355	0.2214	23.9207
33.4	108.0238	0.2214	23.9167
33.6	108.0088	0.2214	23.9092
33.8	107.9785	0.2213	23.8941
34	108.0031	0.2213	23.9052
34.2	108.0192	0.2214	23.9120
34.4	108.0099	0.2214	23.9082
34.6	108.0040	0.2213	23.9032
34.8	107.9874	0.2213	23.8972
35	108.0027	0.2213	23.9038
35.2	108.0366	0.2214	23.9180
35.4	108.0267	0.2214	23.9119
35.6	108.0085	0.2213	23.9033
35.8	108.0019	0.2213	23.9016
36	108.0442	0.2214	23.9198
36.2	108.0641	0.2214	23.9272
36.4	108.0571	0.2214	23.9234
36.6	108.0550	0.2214	23.9221
36.8	108.0470	0.2214	23.9179
37	108.0607	0.2214	23.9247
37.2	108.0690	0.2214	23.9274
37.4	108.0469	0.2214	23.9173
37.6	108.0331	0.2213	23.9102

Table A.1 (cont'd)

Time (sec)	Voltage (Volt)	Current (Amp)	Power (Watt)
37.8	108.0333	0.2213	23.9108
38	108.0460	0.2213	23.9155
38.2	108.0530	0.2214	23.9179
38.4	108.0371	0.2213	23.9100
38.6	108.0384	0.2213	23.9106
38.8	108.0403	0.2213	23.9118
39	108.0521	0.2213	23.9157
39.2	108.0637	0.2214	23.9218
39.4	108.0506	0.2213	23.9142
39.6	108.0307	0.2213	23.9054
39.8	108.0403	0.2213	23.9090
40	108.0570	0.2213	23.9164
40.2	108.0426	0.2213	23.9098
40.4	108.0239	0.2213	23.9013
40.6	108.0343	0.2213	23.9049
40.8	108.0228	0.2212	23.9000
41	108.0245	0.2213	23.9005
41.2	108.0353	0.2213	23.9047
41.4	108.0069	0.2212	23.8904

Table A.2 Data recorded from TPCell for sweet potato test 2

Time (sec)	Voltage (Volt)	Current (Amp)	Power (Watt)
0	103.4193	0.2139	22.1174
0.2	107.8192	0.2229	24.0322
0.4	107.8183	0.2228	24.0249
0.6	107.8332	0.2228	24.0255
0.8	107.8423	0.2228	24.0241
1	107.8203	0.2227	24.0102
1.2	107.8101	0.2226	24.0020
1.4	107.8150	0.2226	23.9989
1.6	107.7964	0.2225	23.9878
1.8	107.8233	0.2225	23.9957
2	107.8505	0.2226	24.0056
2.2	107.8238	0.2225	23.9892
2.4	107.8125	0.2224	23.9820
2.6	107.8326	0.2224	23.9869
2.8	107.8413	0.2224	23.9882
3	107.8334	0.2224	23.9823
3.2	107.8250	0.2224	23.9751
3.4	107.8134	0.2223	23.9677
3.6	107.8304	0.2223	23.9742
3.8	107.8396	0.2223	23.9751
4	107.8386	0.2223	23.9724
4.2	107.8212	0.2222	23.9625
4.4	107.8175	0.2222	23.9593
4.6	107.8419	0.2222	23.9664
4.8	107.8458	0.2222	23.9675
5	107.8493	0.2222	23.9663
5.2	107.8300	0.2222	23.9552
5.4	107.8158	0.2221	23.9468
5.6	107.8195	0.2221	23.9463
5.8	107.8248	0.2221	23.9474
6	107.8119	0.2221	23.9403
6.2	107.8027	0.2220	23.9338
6.4	107.8073	0.2220	23.9345
6.6	107.8012	0.2220	23.9303
6.8	107.8028	0.2220	23.9301
7	107.8134	0.2220	23.9328
7.2	107.8057	0.2219	23.9270
7.4	107.7882	0.2219	23.9180

Table A.2 (cont'd)

Time (sec)	Voltage (Volt)	Current (Amp)	Power (Watt)
7.6	107.7893	0.2219	23.9164
7.8	107.8042	0.2219	23.9218
8	107.8087	0.2219	23.9218
8.2	107.7971	0.2219	23.9158
8.4	107.7768	0.2218	23.9058
8.6	107.7613	0.2218	23.8965
8.8	107.7679	0.2218	23.8982
9	107.8068	0.2218	23.9146
9.2	107.8119	0.2218	23.9158
9.4	107.8113	0.2218	23.9130
9.6	107.8214	0.2218	23.9163
9.8	107.8266	0.2218	23.9176
10	107.8068	0.2218	23.9079
10.2	107.8120	0.2218	23.9094
10.4	107.7972	0.2217	23.9007
10.6	107.8204	0.2218	23.9095
10.8	107.8295	0.2218	23.9127
11	107.8259	0.2217	23.9100
11.2	107.8173	0.2217	23.9062
11.4	107.8064	0.2217	23.8980
11.6	107.8213	0.2217	23.9049
11.8	107.8231	0.2217	23.9044
12	107.8396	0.2217	23.9109
12.2	107.8217	0.2217	23.9005
12.4	107.8070	0.2216	23.8933
12.6	107.8338	0.2217	23.9045
12.8	107.8407	0.2217	23.9058
13	107.8345	0.2217	23.9029
13.2	107.8261	0.2216	23.8974
13.4	107.8133	0.2216	23.8910
13.6	107.8330	0.2216	23.8992
13.8	107.8410	0.2216	23.9023
14	107.8410	0.2216	23.9010
14.2	107.8291	0.2216	23.8941
14.4	107.8198	0.2216	23.8894
14.6	107.8443	0.2216	23.8994
14.8	107.8269	0.2216	23.8898
15	107.8386	0.2216	23.8944

Table A.2 (cont'd)

Time (sec)	Voltage (Volt)	Current (Amp)	Power (Watt)
15.2	107.8386	0.2216	23.8936
15.4	107.8302	0.2215	23.8887
15.6	107.8272	0.2215	23.8873
15.8	107.8291	0.2215	23.8869
16	107.8359	0.2215	23.8887
16.2	107.8457	0.2215	23.8922
16.4	107.8473	0.2215	23.8932
16.6	107.8873	0.2216	23.9093
16.8	107.8687	0.2216	23.8989
17	107.8754	0.2216	23.9021
17.2	107.8713	0.2216	23.9001
17.4	107.8529	0.2215	23.8905
17.6	107.8920	0.2216	23.9067
17.8	107.9898	0.2218	23.9500
18	107.9844	0.2218	23.9457
18.2	107.9694	0.2217	23.9389
18.4	107.9666	0.2217	23.9377
18.6	107.9831	0.2217	23.9427
18.8	107.9881	0.2217	23.9448
19	107.9793	0.2217	23.9394
19.2	107.9854	0.2217	23.9427
19.4	107.9673	0.2217	23.9325
19.6	107.9765	0.2217	23.9362
19.8	107.9757	0.2217	23.9356
20	107.9683	0.2217	23.9313
20.2	107.9532	0.2216	23.9231
20.4	107.9620	0.2216	23.9270
20.6	107.9585	0.2216	23.9246
20.8	107.9811	0.2216	23.9337
21	107.9582	0.2216	23.9234
21.2	107.9493	0.2216	23.9182
21.4	107.9532	0.2216	23.9198
21.6	107.9728	0.2216	23.9273
21.8	107.9874	0.2216	23.9340
22	108.0021	0.2217	23.9386
22.2	107.9963	0.2216	23.9357
22.4	107.9652	0.2216	23.9215
22.6	107.9595	0.2215	23.9178

Table A.2 (cont'd)

Time (sec)	Voltage (Volt)	Current (Amp)	Power (Watt)
22.8	107.9622	0.2216	23.9191
23	107.9619	0.2215	23.9184
23.2	107.9494	0.2215	23.9122
23.4	107.9511	0.2215	23.9118
23.6	107.9608	0.2215	23.9158
23.8	107.9635	0.2215	23.9154
24	107.9668	0.2215	23.9167
24.2	107.9614	0.2215	23.9140
24.4	107.9574	0.2215	23.9119
24.6	107.9640	0.2215	23.9138
24.8	107.9862	0.2215	23.9235
25	108.0071	0.2216	23.9304
25.2	107.9833	0.2215	23.9205
25.4	107.9743	0.2215	23.9152
25.6	107.9633	0.2215	23.9097
25.8	107.9890	0.2215	23.9217
26	107.9925	0.2215	23.9229
26.2	107.9783	0.2215	23.9152
26.4	107.9761	0.2215	23.9143
26.6	107.9916	0.2215	23.9191
26.8	107.9951	0.2215	23.9208
27	107.9962	0.2215	23.9211
27.2	107.9874	0.2215	23.9163
27.4	107.9752	0.2214	23.9099
27.6	107.9887	0.2215	23.9151
27.8	108.0027	0.2215	23.9211
28	108.0204	0.2215	23.9285
28.2	107.9956	0.2215	23.9175
28.4	107.9965	0.2215	23.9172
28.6	107.9766	0.2214	23.9075
28.8	107.9996	0.2214	23.9161
29	107.9855	0.2214	23.9105
29.2	107.9877	0.2214	23.9101
29.4	107.9828	0.2214	23.9090
29.6	107.9849	0.2214	23.9082
29.8	107.9882	0.2214	23.9106
30	107.9931	0.2214	23.9115
30.2	107.9825	0.2214	23.9054

Table A.2 (cont'd)

Time (sec)	Voltage (Volt)	Current (Amp)	Power (Watt)
30.4	107.9753	0.2214	23.9023
30.6	107.9696	0.2214	23.8992
30.8	107.9897	0.2214	23.9089
31	108.0115	0.2214	23.9172
31.2	107.9781	0.2214	23.9015
31.4	107.9660	0.2213	23.8954
31.6	107.9658	0.2213	23.8944
31.8	107.9905	0.2214	23.9056
32	108.0003	0.2214	23.9091
32.2	107.9829	0.2214	23.9023
32.4	107.9728	0.2213	23.8956
32.6	107.9746	0.2213	23.8962
32.8	107.9986	0.2214	23.9071
33	108.0079	0.2214	23.9106
33.2	107.9922	0.2213	23.9020
33.4	107.9843	0.2213	23.9001
33.6	107.9798	0.2213	23.8950
33.8	107.9868	0.2213	23.8987
34	107.9961	0.2213	23.9028
34.2	107.9804	0.2213	23.8960
34.4	107.9874	0.2213	23.8974
34.6	107.9825	0.2213	23.8953
34.8	107.9986	0.2213	23.9022
35	108.0097	0.2213	23.9064
35.2	108.0023	0.2213	23.9034
35.4	107.9948	0.2213	23.8986
35.6	108.0057	0.2213	23.9028
35.8	108.0079	0.2213	23.9049
36	107.9989	0.2213	23.8987
36.2	107.9576	0.2212	23.8800
36.4	107.9724	0.2212	23.8871
36.6	107.9612	0.2212	23.8817
36.8	107.9679	0.2212	23.8839
37	107.9516	0.2212	23.8763
37.2	107.9199	0.2211	23.8612
37.4	107.9537	0.2212	23.8764
37.6	107.9544	0.2212	23.8765
37.8	107.9616	0.2212	23.8791

Table A.2 (cont'd)

Time (sec)	Voltage (Volt)	Current (Amp)	Power (Watt)
38	107.9622	0.2212	23.8795
38.2	107.9811	0.2212	23.8868
38.4	107.9959	0.2212	23.8929
38.6	107.9917	0.2212	23.8918
38.8	107.9874	0.2212	23.8881
39	108.0006	0.2212	23.8927
39.2	107.9800	0.2212	23.8848
39.4	107.9691	0.2212	23.8799
39.6	107.9652	0.2212	23.8765
39.8	107.9937	0.2212	23.8882
40	108.0028	0.2212	23.8925
40.2	107.9851	0.2212	23.8840
40.4	107.9772	0.2212	23.8820
40.6	107.9792	0.2212	23.8804
40.8	107.9891	0.2212	23.8847
41	108.0035	0.2212	23.8909
41.2	107.9729	0.2211	23.8763
41.4	107.9851	0.2212	23.8832

Table A.3 Data recorded from TPCell for sweet potato test 3

Time (sec)	Voltage (Volt)	Current (Amp)	Power (Watt)
0	105.5313	0.2182	23.0293
0.2	108.0104	0.2233	24.1165
0.4	108.0524	0.2233	24.1283
0.6	108.0342	0.2232	24.1165
0.8	108.0353	0.2232	24.1103
1	108.0555	0.2232	24.1157
1.2	108.0059	0.2230	24.0900
1.4	108.0192	0.2230	24.0901
1.6	108.0333	0.2230	24.0946
1.8	108.0167	0.2229	24.0818
2	108.0235	0.2229	24.0817
2.2	108.0102	0.2229	24.0726
2.4	107.9830	0.2228	24.0575
2.6	107.9996	0.2228	24.0615
2.8	107.9754	0.2227	24.0475
3	107.9590	0.2227	24.0377
3.2	107.9637	0.2226	24.0379
3.4	107.9595	0.2226	24.0321
3.6	107.9964	0.2227	24.0465
3.8	108.0282	0.2227	24.0577
4	108.0229	0.2227	24.0550
4.2	108.0059	0.2226	24.0439
4.4	108.0241	0.2226	24.0490
4.6	107.9812	0.2225	24.0290
4.8	107.9581	0.2225	24.0175
5	107.9886	0.2225	24.0276
5.2	107.9837	0.2225	24.0232
5.4	108.0266	0.2225	24.0399
5.6	108.0127	0.2225	24.0322
5.8	108.0049	0.2225	24.0276
6	108.0187	0.2225	24.0323
6.2	107.9953	0.2224	24.0196
6.4	107.9986	0.2224	24.0199
6.6	107.9941	0.2224	24.0156
6.8	107.9864	0.2223	24.0104
7	108.0138	0.2224	24.0216
7.2	108.0184	0.2224	24.0217
7.4	108.0015	0.2223	24.0115

Table A.3 (cont'd)

Time (sec)	Voltage (Volt)	Current (Amp)	Power (Watt)
7.6	108.0312	0.2224	24.0229
7.8	108.0187	0.2223	24.0163
8	108.0131	0.2223	24.0127
8.2	108.0230	0.2223	24.0159
8.4	107.9970	0.2223	24.0030
8.6	108.0170	0.2223	24.0110
8.8	108.0294	0.2223	24.0155
9	108.0329	0.2223	24.0148
9.2	108.0307	0.2223	24.0130
9.4	108.0257	0.2222	24.0074
9.6	108.0187	0.2222	24.0051
9.8	108.0255	0.2222	24.0060
10	108.0208	0.2222	24.0017
10.2	107.9974	0.2221	23.9906
10.4	108.0236	0.2222	24.0014
10.6	108.0206	0.2222	23.9988
10.8	108.0124	0.2221	23.9930
11	108.0242	0.2222	23.9980
11.2	108.0072	0.2221	23.9892
11.4	107.9968	0.2221	23.9825
11.6	108.0217	0.2221	23.9933
11.8	108.0097	0.2221	23.9871
12	108.0281	0.2221	23.9927
12.2	108.0269	0.2221	23.9914
12.4	108.0026	0.2220	23.9797
12.6	108.0178	0.2221	23.9860
12.8	108.0070	0.2220	23.9800
13	108.0056	0.2220	23.9771
13.2	108.0337	0.2221	23.9902
13.4	108.0162	0.2220	23.9804
13.6	108.0539	0.2221	23.9960
13.8	108.1617	0.2223	24.0439
14	108.1430	0.2222	24.0343
14.2	108.1452	0.2222	24.0336
14.4	108.1491	0.2222	24.0350
14.6	108.1434	0.2222	24.0306
14.8	108.1476	0.2222	24.0320
15	108.1475	0.2222	24.0317

Table A.3 (cont'd)

Time (sec)	Voltage (Volt)	Current (Amp)	Power (Watt)
15.2	108.1300	0.2222	24.0215
15.4	108.1407	0.2222	24.0269
15.6	108.1129	0.2221	24.0128
15.8	108.0451	0.2220	23.9822
16	108.0599	0.2220	23.9876
16.2	108.0254	0.2219	23.9719
16.4	108.0297	0.2219	23.9721
16.6	108.0563	0.2220	23.9841
16.8	108.0456	0.2219	23.9782
17	108.0372	0.2219	23.9732
17.2	108.0290	0.2219	23.9695
17.4	108.0120	0.2218	23.9603
17.6	108.0241	0.2219	23.9655
17.8	108.0025	0.2218	23.9548
18	108.0123	0.2218	23.9575
18.2	108.0256	0.2218	23.9630
18.4	108.0232	0.2218	23.9615
18.6	108.0608	0.2219	23.9777
18.8	108.0710	0.2219	23.9807
19	108.0568	0.2219	23.9734
19.2	108.0691	0.2219	23.9782
19.4	108.0494	0.2218	23.9689
19.6	108.0620	0.2219	23.9740
19.8	108.0626	0.2219	23.9750
20	108.0561	0.2218	23.9697
20.2	108.0539	0.2218	23.9681
20.4	108.0662	0.2218	23.9723
20.6	108.0663	0.2218	23.9727
20.8	108.0684	0.2218	23.9726
21	108.0659	0.2218	23.9706
21.2	108.0640	0.2218	23.9703
21.4	108.0809	0.2218	23.9745
21.6	108.0950	0.2219	23.9814
21.8	108.0712	0.2218	23.9712
22	108.0822	0.2218	23.9732
22.2	108.0614	0.2218	23.9653
22.4	108.0469	0.2217	23.9570
22.6	108.0440	0.2217	23.9546

Table A.3 (cont'd)

Time (sec)	Voltage (Volt)	Current (Amp)	Power (Watt)
22.8	108.0391	0.2217	23.9524
23	108.0300	0.2217	23.9487
23.2	108.0408	0.2217	23.9527
23.4	108.0147	0.2216	23.9403
23.6	108.0605	0.2217	23.9599
23.8	108.0553	0.2217	23.9568
24	108.0373	0.2217	23.9466
24.2	108.0473	0.2217	23.9519
24.4	108.0503	0.2217	23.9517
24.6	108.0753	0.2217	23.9625
24.8	108.0917	0.2218	23.9697
25	108.0471	0.2217	23.9507
25.2	108.0688	0.2217	23.9589
25.4	108.0882	0.2217	23.9663
25.6	108.0817	0.2217	23.9632
25.8	108.0939	0.2217	23.9689
26	108.0842	0.2217	23.9614
26.2	108.0778	0.2217	23.9585
26.4	108.0875	0.2217	23.9633
26.6	108.0848	0.2217	23.9609
26.8	108.0667	0.2216	23.9524
27	108.0645	0.2216	23.9506
27.2	108.0533	0.2216	23.9454
27.4	108.0587	0.2216	23.9471
27.6	108.0722	0.2216	23.9541
27.8	108.0657	0.2216	23.9507
28	108.0747	0.2216	23.9523
28.2	108.0659	0.2216	23.9473
28.4	108.0448	0.2216	23.9389
28.6	108.0753	0.2216	23.9517
28.8	108.0720	0.2216	23.9491
29	108.0799	0.2216	23.9520
29.2	108.0638	0.2216	23.9449
29.4	108.0581	0.2216	23.9415
29.6	108.1031	0.2217	23.9612
29.8	108.1003	0.2217	23.9608
30	108.0667	0.2216	23.9441
30.2	108.0779	0.2216	23.9477

Table A.3 (cont'd)

Time (sec)	Voltage (Volt)	Current (Amp)	Power (Watt)
30.4	108.0714	0.2216	23.9438
30.6	108.0734	0.2216	23.9456
30.8	108.1098	0.2216	23.9605
31	108.0513	0.2215	23.9342
31.2	108.0523	0.2215	23.9355
31.4	108.0832	0.2216	23.9478
31.6	108.0743	0.2215	23.9434
31.8	108.0706	0.2215	23.9397
32	108.0902	0.2216	23.9492
32.2	108.0616	0.2215	23.9361
32.4	108.0768	0.2215	23.9415
32.6	108.0953	0.2216	23.9494
32.8	108.0721	0.2215	23.9391
33	108.0859	0.2215	23.9450
33.2	108.0934	0.2215	23.9458
33.4	108.1683	0.2217	23.9799
33.6	108.2153	0.2218	24.0013
33.8	108.2077	0.2218	23.9964
34	108.2130	0.2218	23.9986
34.2	108.2191	0.2218	24.0002
34.4	108.1997	0.2217	23.9925
34.6	108.2045	0.2217	23.9928
34.8	108.2254	0.2218	24.0021
35	108.2322	0.2218	24.0042
35.2	108.2078	0.2217	23.9933
35.4	108.1208	0.2216	23.9544
35.6	108.1300	0.2216	23.9573
35.8	108.1607	0.2216	23.9714
36	108.1247	0.2215	23.9542
36.2	108.1356	0.2216	23.9598
36.4	108.1179	0.2215	23.9509
36.6	108.0953	0.2215	23.9406
36.8	108.1092	0.2215	23.9460
37	108.1074	0.2215	23.9451
37.2	108.0927	0.2215	23.9379
37.4	108.1064	0.2215	23.9436
37.6	108.1174	0.2215	23.9484
37.8	108.0981	0.2215	23.9389

Table A.3 (cont'd)

Time (sec)	Voltage (Volt)	Current (Amp)	Power (Watt)
38	108.1094	0.2215	23.9439
38.2	108.0950	0.2214	23.9369
38.4	108.1028	0.2215	23.9401
38.6	108.1321	0.2215	23.9523
38.8	108.1375	0.2215	23.9559
39	108.1472	0.2215	23.9586
39.2	108.1290	0.2215	23.9507
39.4	108.1193	0.2215	23.9448
39.6	108.1488	0.2215	23.9578
39.8	108.1368	0.2215	23.9525
40	108.1389	0.2215	23.9532
40.2	108.1637	0.2215	23.9629
40.4	108.1241	0.2215	23.9449
40.6	108.1262	0.2215	23.9453
40.8	108.1486	0.2215	23.9551
41	108.1274	0.2215	23.9452
41.2	108.1489	0.2215	23.9541
41.4	108.1296	0.2215	23.9467
41.6	108.1345	0.2215	23.9470
41.8	108.1651	0.2215	23.9602

Table A.4 Data recorded from TPCell for sweet potato test 4

Time (sec)	Voltage (Volt)	Current (Amp)	Power (Watt)
0	105.6148	0.2184	23.0666
0.2	108.1338	0.2235	24.1725
0.4	108.1406	0.2235	24.1700
0.6	108.1549	0.2235	24.1700
0.8	108.1567	0.2234	24.1650
1	108.1367	0.2233	24.1522
1.2	108.1070	0.2232	24.1345
1.4	108.1278	0.2232	24.1393
1.6	108.1441	0.2232	24.1423
1.8	108.1425	0.2232	24.1384
2	108.1420	0.2232	24.1338
2.2	108.1823	0.2232	24.1497
2.4	108.2406	0.2233	24.1716
2.6	108.2462	0.2233	24.1728
2.8	108.2299	0.2232	24.1615
3	108.2359	0.2232	24.1615
3.2	108.2466	0.2232	24.1630
3.4	108.2239	0.2232	24.1522
3.6	108.2429	0.2232	24.1564
3.8	108.2379	0.2232	24.1534
4	108.2495	0.2231	24.1555
4.2	108.1970	0.2230	24.1301
4.4	108.1258	0.2228	24.0949
4.6	108.1269	0.2228	24.0933
4.8	108.1519	0.2229	24.1023
5	108.1350	0.2228	24.0925
5.2	108.1305	0.2228	24.0882
5.4	108.1182	0.2227	24.0822
5.6	108.1301	0.2228	24.0864
5.8	108.1241	0.2227	24.0802
6	108.1160	0.2227	24.0746
6.2	108.1276	0.2227	24.0779
6.4	108.1262	0.2227	24.0759
6.6	108.1349	0.2227	24.0776
6.8	108.1372	0.2227	24.0774
7	108.1282	0.2226	24.0700
7.2	108.1600	0.2227	24.0850
7.4	108.1444	0.2226	24.0749

Table A.4 (cont'd)

Time (sec)	Voltage (Volt)	Current (Amp)	Power (Watt)
7.6	108.1421	0.2226	24.0729
7.8	108.1283	0.2226	24.0660
8	108.1183	0.2225	24.0598
8.2	108.1416	0.2226	24.0684
8.4	108.1385	0.2225	24.0646
8.6	108.1441	0.2225	24.0664
8.8	108.1420	0.2225	24.0640
9	108.1390	0.2225	24.0615
9.2	108.1439	0.2225	24.0633
9.4	108.1324	0.2225	24.0559
9.6	108.1413	0.2225	24.0589
9.8	108.1301	0.2224	24.0529
10	108.1366	0.2224	24.0537
10.2	108.1155	0.2224	24.0437
10.4	108.1282	0.2224	24.0475
10.6	108.1428	0.2224	24.0532
10.8	108.1445	0.2224	24.0526
11	108.1271	0.2224	24.0429
11.2	108.1401	0.2224	24.0484
11.4	108.1283	0.2223	24.0401
11.6	108.1317	0.2223	24.0416
11.8	108.1353	0.2223	24.0423
12	108.1348	0.2223	24.0405
12.2	108.1542	0.2224	24.0487
12.4	108.1288	0.2223	24.0366
12.6	108.1330	0.2223	24.0370
12.8	108.1272	0.2223	24.0332
13	108.1273	0.2223	24.0330
13.2	108.1403	0.2223	24.0368
13.4	108.1205	0.2222	24.0267
13.6	108.1391	0.2223	24.0352
13.8	108.1332	0.2222	24.0307
14	108.1290	0.2222	24.0292
14.2	108.1365	0.2222	24.0304
14.4	108.1187	0.2222	24.0217
14.6	108.1302	0.2222	24.0253
14.8	108.1297	0.2222	24.0243
15	108.1168	0.2221	24.0177

Table A.4 (cont'd)

Time (sec)	Voltage (Volt)	Current (Amp)	Power (Watt)
15.2	108.1107	0.2221	24.0129
15.4	108.1223	0.2221	24.0183
15.6	108.1376	0.2222	24.0239
15.8	108.1528	0.2222	24.0301
16	108.1195	0.2221	24.0135
16.2	108.1433	0.2221	24.0234
16.4	108.1113	0.2221	24.0086
16.6	108.1069	0.2221	24.0069
16.8	108.1141	0.2221	24.0076
17	108.0658	0.2220	23.9853
17.2	108.0975	0.2220	23.9992
17.4	108.0936	0.2220	23.9971
17.6	108.1022	0.2220	23.9997
17.8	108.0985	0.2220	23.9974
18	108.0962	0.2220	23.9969
18.2	108.1688	0.2221	24.0268
18.4	108.1705	0.2221	24.0273
18.6	108.1627	0.2221	24.0227
18.8	108.1512	0.2221	24.0163
19	108.1722	0.2221	24.0251
19.2	108.1940	0.2221	24.0345
19.4	108.1857	0.2221	24.0296
19.6	108.2005	0.2221	24.0359
19.8	108.2006	0.2221	24.0348
20	108.1878	0.2221	24.0273
20.2	108.1996	0.2221	24.0332
20.4	108.1892	0.2221	24.0281
20.6	108.2069	0.2221	24.0350
20.8	108.2035	0.2221	24.0324
21	108.1865	0.2221	24.0236
21.2	108.1314	0.2219	23.9989
21.4	108.1384	0.2219	24.0004
21.6	108.1816	0.2220	24.0212
21.8	108.2236	0.2221	24.0378
22	108.3029	0.2223	24.0728
22.2	108.2952	0.2222	24.0684
22.4	108.2836	0.2222	24.0630
22.6	108.2709	0.2222	24.0565

Table A.4 (cont'd)

Time (sec)	Voltage (Volt)	Current (Amp)	Power (Watt)
22.8	108.2789	0.2222	24.0580
23	108.2546	0.2221	24.0481
23.2	108.2776	0.2222	24.0579
23.4	108.2621	0.2221	24.0491
23.6	108.2554	0.2221	24.0460
23.8	108.1949	0.2220	24.0186
24	108.1307	0.2219	23.9891
24.2	108.1403	0.2219	23.9926
24.4	108.1283	0.2218	23.9871
24.6	108.1292	0.2218	23.9875
24.8	108.1312	0.2218	23.9870
25	108.1071	0.2218	23.9756
25.2	108.1335	0.2218	23.9875
25.4	108.1263	0.2218	23.9820
25.6	108.1310	0.2218	23.9849
25.8	108.1454	0.2218	23.9911
26	108.1251	0.2218	23.9809
26.2	108.1278	0.2218	23.9800
26.4	108.1214	0.2218	23.9780
26.6	108.1148	0.2218	23.9759
26.8	108.1234	0.2218	23.9784
27	108.1186	0.2218	23.9758
27.2	108.1320	0.2218	23.9794
27.4	108.1334	0.2218	23.9798
27.6	108.1262	0.2217	23.9768
27.8	108.1264	0.2217	23.9766
28	108.1157	0.2217	23.9718
28.2	108.1271	0.2217	23.9751
28.4	108.1238	0.2217	23.9736
28.6	108.1106	0.2217	23.9665
28.8	108.1198	0.2217	23.9696
29	108.1141	0.2217	23.9671
29.2	108.1324	0.2217	23.9746
29.4	108.1335	0.2217	23.9738
29.6	108.1294	0.2217	23.9727
29.8	108.1212	0.2217	23.9688
30	108.1055	0.2216	23.9610
30.2	108.1116	0.2217	23.9638

Table A.4 (cont'd)

Time (sec)	Voltage (Volt)	Current (Amp)	Power (Watt)
30.4	108.1091	0.2216	23.9605
30.6	108.1102	0.2216	23.9614
30.8	108.1221	0.2217	23.9665
31	108.1104	0.2216	23.9617
31.2	108.1190	0.2217	23.9648
31.4	108.1173	0.2216	23.9619
31.6	108.1183	0.2216	23.9624
31.8	108.1115	0.2216	23.9585
32	108.0975	0.2216	23.9516
32.2	108.1176	0.2216	23.9610
32.4	108.1163	0.2216	23.9595
32.6	108.1178	0.2216	23.9600
32.8	108.1291	0.2216	23.9644
33	108.1036	0.2216	23.9523
33.2	108.1260	0.2216	23.9624
33.4	108.1386	0.2216	23.9675
33.6	108.1310	0.2216	23.9619
33.8	108.0843	0.2215	23.9424
34	108.0687	0.2215	23.9347
34.2	108.1067	0.2215	23.9508
34.4	108.1489	0.2216	23.9694
34.6	108.1598	0.2216	23.9723
34.8	108.1490	0.2216	23.9674
35	108.1331	0.2216	23.9614
35.2	108.1375	0.2216	23.9627
35.4	108.1510	0.2216	23.9678
35.6	108.1372	0.2216	23.9621
35.8	108.1491	0.2216	23.9665
36	108.1542	0.2216	23.9677
36.2	108.1426	0.2216	23.9613
36.4	108.1569	0.2216	23.9676
36.6	108.1481	0.2216	23.9634
36.8	108.1445	0.2216	23.9615
37	108.1373	0.2216	23.9588
37.2	108.1207	0.2215	23.9504
37.4	108.1304	0.2215	23.9530
37.6	108.1808	0.2216	23.9759
37.8	108.1970	0.2217	23.9838

Table A.4 (cont'd)

Time (sec)	Voltage (Volt)	Current (Amp)	Power (Watt)
38	108.1862	0.2216	23.9782
38.2	108.1923	0.2217	23.9813
38.4	108.1852	0.2216	23.9763
38.6	108.1946	0.2216	23.9800
38.8	108.1860	0.2216	23.9764
39	108.2081	0.2217	23.9852
39.2	108.2222	0.2217	23.9923
39.4	108.2257	0.2217	23.9915
39.6	108.2574	0.2217	24.0048
39.8	108.2588	0.2218	24.0066
40	108.2348	0.2217	23.9947
40.2	108.2363	0.2217	23.9951
40.4	108.2508	0.2217	24.0019
40.6	108.2416	0.2217	23.9963
40.8	108.2480	0.2217	23.9994
41	108.2397	0.2217	23.9943

Table A.5 Data recorded from TPCell for sweet potato test 5

Time (sec)	Voltage (Volt)	Current (Amp)	Power (Watt)
0	105.4658	0.2181	23.0017
0.2	108.0402	0.2233	24.1301
0.4	108.0369	0.2233	24.1214
0.6	108.0612	0.2233	24.1278
0.8	108.0469	0.2232	24.1149
1	108.0563	0.2232	24.1151
1.2	108.0517	0.2231	24.1088
1.4	108.0411	0.2231	24.0994
1.6	108.0460	0.2231	24.1000
1.8	108.0512	0.2230	24.0972
2	108.0558	0.2230	24.0956
2.2	108.0398	0.2229	24.0856
2.4	108.0299	0.2229	24.0793
2.6	107.9888	0.2228	24.0571
2.8	107.9874	0.2227	24.0532
3	108.0118	0.2228	24.0613
3.2	108.0289	0.2228	24.0664
3.4	108.0171	0.2227	24.0587
3.6	108.0163	0.2227	24.0556
3.8	108.0123	0.2227	24.0511
4	108.0367	0.2227	24.0611
4.2	108.0571	0.2227	24.0666
4.4	108.0701	0.2227	24.0697
4.6	108.0626	0.2227	24.0657
4.8	108.0638	0.2227	24.0635
5	108.0578	0.2227	24.0599
5.2	108.0456	0.2226	24.0518
5.4	108.0422	0.2226	24.0490
5.6	108.0491	0.2226	24.0483
5.8	108.0606	0.2226	24.0513
6	108.0588	0.2226	24.0492
6.2	108.0569	0.2225	24.0469
6.4	108.0442	0.2225	24.0398
6.6	108.0711	0.2225	24.0504
6.8	108.2056	0.2228	24.1074
7	108.2155	0.2228	24.1101
7.2	108.2210	0.2228	24.1109
7.4	108.2112	0.2228	24.1057

Table A.5 (cont'd)

Time (sec)	Voltage (Volt)	Current (Amp)	Power (Watt)
7.6	108.2000	0.2227	24.0990
7.8	108.2028	0.2227	24.0979
8	108.2140	0.2227	24.1023
8.2	108.2000	0.2227	24.0923
8.4	108.1947	0.2227	24.0905
8.6	108.2005	0.2227	24.0924
8.8	108.2037	0.2227	24.0919
9	108.2061	0.2226	24.0913
9.2	108.2120	0.2226	24.0929
9.4	108.2183	0.2226	24.0943
9.6	108.2183	0.2226	24.0917
9.8	108.2156	0.2226	24.0911
10	108.2236	0.2226	24.0919
10.2	108.2209	0.2226	24.0907
10.4	108.2134	0.2226	24.0860
10.6	108.2225	0.2226	24.0888
10.8	108.2331	0.2226	24.0909
11	108.2318	0.2226	24.0874
11.2	108.1991	0.2225	24.0741
11.4	108.1880	0.2225	24.0681
11.6	108.1911	0.2225	24.0680
11.8	108.1868	0.2224	24.0647
12	108.2350	0.2225	24.0857
12.2	108.2435	0.2225	24.0878
12.4	108.2485	0.2225	24.0895
12.6	108.2492	0.2225	24.0885
12.8	108.2588	0.2225	24.0917
13	108.2677	0.2226	24.0953
13.2	108.2464	0.2225	24.0836
13.4	108.2518	0.2225	24.0856
13.6	108.2475	0.2225	24.0831
13.8	108.2608	0.2225	24.0872
14	108.2643	0.2225	24.0880
14.2	108.2576	0.2225	24.0846
14.4	108.2517	0.2224	24.0797
14.6	108.2234	0.2224	24.0667
14.8	108.2332	0.2224	24.0700
15	108.2528	0.2224	24.0762

Table A.5 (cont'd)

Time (sec)	Voltage (Volt)	Current (Amp)	Power (Watt)
15.2	108.2742	0.2225	24.0864
15.4	108.2932	0.2225	24.0926
15.6	108.2718	0.2224	24.0850
15.8	108.2814	0.2224	24.0870
16	108.2587	0.2224	24.0758
16.2	108.2633	0.2224	24.0770
16.4	108.2700	0.2224	24.0803
16.6	108.2792	0.2224	24.0816
16.8	108.2901	0.2224	24.0864
17	108.2993	0.2224	24.0899
17.2	108.3009	0.2224	24.0892
17.4	108.2721	0.2224	24.0745
17.6	108.2535	0.2223	24.0666
17.8	108.2625	0.2223	24.0704
18	108.2685	0.2223	24.0717
18.2	108.2589	0.2223	24.0659
18.4	108.2623	0.2223	24.0668
18.6	108.2494	0.2223	24.0596
18.8	108.2377	0.2222	24.0551
19	108.2507	0.2223	24.0600
19.2	108.2264	0.2222	24.0488
19.4	108.2124	0.2222	24.0411
19.6	108.1967	0.2221	24.0329
19.8	108.2022	0.2221	24.0338
20	108.2242	0.2222	24.0431
20.2	108.2222	0.2222	24.0421
20.4	108.2001	0.2221	24.0317
20.6	108.2053	0.2221	24.0332
20.8	108.2179	0.2221	24.0388
21	108.2178	0.2221	24.0392
21.2	108.2263	0.2221	24.0409
21.4	108.2347	0.2221	24.0430
21.6	108.2407	0.2222	24.0461
21.8	108.2211	0.2221	24.0372
22	108.2255	0.2221	24.0375
22.2	108.2245	0.2221	24.0365
22.4	108.2324	0.2221	24.0392
22.6	108.2281	0.2221	24.0366

Table A.5 (cont'd)

Time (sec)	Voltage (Volt)	Current (Amp)	Power (Watt)
22.8	108.1973	0.2220	24.0218
23	108.1936	0.2220	24.0208
23.2	108.2121	0.2220	24.0274
23.4	108.2981	0.2222	24.0649
23.6	108.2929	0.2222	24.0620
23.8	108.2975	0.2222	24.0639
24	108.2818	0.2222	24.0555
24.2	108.2540	0.2221	24.0422
24.4	108.1784	0.2219	24.0083
24.6	108.1736	0.2219	24.0063
24.8	108.1618	0.2219	24.0007
25	108.1760	0.2219	24.0056
25.2	108.1794	0.2219	24.0061
25.4	108.1702	0.2219	24.0024
25.6	108.1683	0.2219	23.9998
25.8	108.1444	0.2218	23.9894
26	108.1616	0.2219	23.9972
26.2	108.1701	0.2219	23.9994
26.4	108.1824	0.2219	24.0042
26.6	108.1689	0.2219	23.9979
26.8	108.1576	0.2218	23.9919
27	108.1712	0.2218	23.9973
27.2	108.1684	0.2218	23.9948
27.4	108.1768	0.2218	23.9990
27.6	108.1717	0.2218	23.9958
27.8	108.1589	0.2218	23.9893
28	108.1412	0.2218	23.9822
28.2	108.1485	0.2218	23.9850
28.4	108.1507	0.2218	23.9838
28.6	108.1571	0.2218	23.9870
28.8	108.1738	0.2218	23.9953
29	108.1595	0.2218	23.9875
29.2	108.1688	0.2218	23.9908
29.4	108.1717	0.2218	23.9914
29.6	108.1619	0.2218	23.9872
29.8	108.1615	0.2218	23.9862
30	108.1555	0.2217	23.9829
30.2	108.1584	0.2217	23.9831

Table A.5 (cont'd)

Time (sec)	Voltage (Volt)	Current (Amp)	Power (Watt)
30.4	108.1507	0.2217	23.9799
30.6	108.1472	0.2217	23.9771
30.8	108.1575	0.2217	23.9814
31	108.1587	0.2217	23.9817
31.2	108.1606	0.2217	23.9821
31.4	108.1628	0.2217	23.9836
31.6	108.1611	0.2217	23.9806
31.8	108.1624	0.2217	23.9803
32	108.1465	0.2217	23.9750
32.2	108.1491	0.2217	23.9736
32.4	108.1488	0.2217	23.9744
32.6	108.1604	0.2217	23.9783
32.8	108.1649	0.2217	23.9795
33	108.1468	0.2217	23.9712
33.2	108.1488	0.2216	23.9710
33.4	108.1087	0.2216	23.9530
33.6	108.0912	0.2215	23.9456
33.8	108.1581	0.2216	23.9731
34	108.1659	0.2217	23.9777
34.2	108.1496	0.2216	23.9689
34.4	108.1316	0.2216	23.9599
34.6	108.1396	0.2216	23.9654
34.8	108.1788	0.2217	23.9813
35	108.1867	0.2217	23.9848
35.2	108.2189	0.2217	23.9967
35.4	108.2233	0.2218	23.9985
35.6	108.2237	0.2218	23.9991
35.8	108.2342	0.2218	24.0031
36	108.2376	0.2218	24.0056
36.2	108.2198	0.2217	23.9968
36.4	108.2302	0.2218	24.0007
36.6	108.2449	0.2218	24.0065
36.8	108.1957	0.2217	23.9834
37	108.1636	0.2216	23.9691
37.2	108.2127	0.2217	23.9920
37.4	108.2308	0.2217	23.9982
37.6	108.2115	0.2217	23.9894
37.8	108.2001	0.2217	23.9835

Table A.5 (cont'd)

Time (sec)	Voltage (Volt)	Current (Amp)	Power (Watt)
38	108.1966	0.2216	23.9810
38.2	108.1928	0.2216	23.9795
38.4	108.1958	0.2216	23.9805
38.6	108.2251	0.2217	23.9933
38.8	108.2145	0.2217	23.9874
39	108.2089	0.2217	23.9852
39.2	108.2346	0.2217	23.9962
39.4	108.2227	0.2217	23.9897
39.6	108.2299	0.2217	23.9921
39.8	108.2196	0.2217	23.9879
40	108.2182	0.2217	23.9866
40.2	108.2152	0.2216	23.9857
40.4	108.2217	0.2217	23.9881
40.6	108.1966	0.2216	23.9777
40.8	108.2022	0.2216	23.9788
41	108.1996	0.2216	23.9761
41.2	108.2135	0.2216	23.9823
41.4	108.1955	0.2216	23.9741
41.6	108.2073	0.2216	23.9777

Table A.6 Data recorded from TPCell for sweet potato test 6

Time (sec)	Voltage (Volt)	Current (Amp)	Power (Watt)
0	92.7069	0.1917	17.7745
0.2	107.8255	0.2229	24.0377
0.4	107.8238	0.2229	24.0295
0.6	107.8218	0.2228	24.0245
0.8	107.8279	0.2228	24.0228
1	107.8352	0.2227	24.0199
1.2	107.8424	0.2227	24.0180
1.4	107.8799	0.2228	24.0306
1.6	107.8697	0.2227	24.0221
1.8	107.8796	0.2227	24.0246
2	107.8877	0.2227	24.0233
2.2	107.8831	0.2226	24.0183
2.4	107.8716	0.2226	24.0108
2.6	107.8788	0.2226	24.0097
2.8	107.8919	0.2226	24.0138
3	107.8908	0.2225	24.0102
3.2	107.8916	0.2225	24.0076
3.4	107.8614	0.2224	23.9914
3.6	107.8737	0.2224	23.9950
3.8	107.8780	0.2224	23.9932
4	107.8810	0.2224	23.9922
4.2	107.8887	0.2224	23.9937
4.4	107.8868	0.2224	23.9902
4.6	107.8915	0.2224	23.9907
4.8	107.8956	0.2223	23.9901
5	107.8839	0.2223	23.9836
5.2	107.8904	0.2223	23.9838
5.4	107.8770	0.2223	23.9766
5.6	107.8785	0.2222	23.9753
5.8	107.8846	0.2222	23.9767
6	107.8853	0.2222	23.9745
6.2	107.8895	0.2222	23.9753
6.4	107.8817	0.2222	23.9688
6.6	107.8731	0.2221	23.9639
6.8	107.8856	0.2222	23.9672
7	107.8777	0.2221	23.9632
7.2	107.8724	0.2221	23.9580
7.4	107.8622	0.2221	23.9517

Table A.6 (cont'd)

Time (sec)	Voltage (Volt)	Current (Amp)	Power (Watt)
7.6	107.8612	0.2220	23.9502
7.8	107.8737	0.2221	23.9548
8	107.8715	0.2220	23.9518
8.2	107.8687	0.2220	23.9488
8.4	107.8427	0.2220	23.9367
8.6	107.8425	0.2219	23.9346
8.8	107.8513	0.2219	23.9370
9	107.8591	0.2220	23.9396
9.2	107.8622	0.2219	23.9392
9.4	107.8653	0.2219	23.9391
9.6	107.8708	0.2219	23.9413
9.8	107.8698	0.2219	23.9393
10	107.8705	0.2219	23.9376
10.2	107.8837	0.2219	23.9423
10.4	107.8697	0.2219	23.9358
10.6	107.8627	0.2219	23.9299
10.8	107.8752	0.2219	23.9358
11	107.8723	0.2219	23.9319
11.2	107.8765	0.2218	23.9319
11.4	107.8744	0.2218	23.9317
11.6	107.8752	0.2218	23.9296
11.8	107.8312	0.2217	23.9100
12	107.8414	0.2217	23.9130
12.2	107.8737	0.2218	23.9261
12.4	107.8788	0.2218	23.9266
12.6	107.8860	0.2218	23.9297
12.8	107.8869	0.2218	23.9285
13	107.8832	0.2218	23.9255
13.2	107.8793	0.2218	23.9238
13.4	107.8604	0.2217	23.9143
13.6	107.8656	0.2217	23.9152
13.8	107.8415	0.2217	23.9040
14	107.8481	0.2217	23.9057
14.2	107.8522	0.2217	23.9063
14.4	107.8556	0.2217	23.9067
14.6	107.8413	0.2216	23.8992
14.8	107.8549	0.2216	23.9058
15	107.8604	0.2216	23.9064

Table A.6 (cont'd)

Time (sec)	Voltage (Volt)	Current (Amp)	Power (Watt)
15.2	107.8433	0.2216	23.8983
15.4	107.8246	0.2215	23.8880
15.6	107.8242	0.2215	23.8879
15.8	107.8435	0.2216	23.8946
16	107.8314	0.2215	23.8889
16.2	107.8507	0.2216	23.8949
16.4	107.8405	0.2215	23.8909
16.6	107.8546	0.2216	23.8967
16.8	107.8594	0.2216	23.8974
17	107.8563	0.2216	23.8958
17.2	107.8603	0.2215	23.8959
17.4	107.8355	0.2215	23.8842
17.6	107.8462	0.2215	23.8878
17.8	107.8349	0.2215	23.8822
18	107.8255	0.2214	23.8770
18.2	107.8447	0.2215	23.8858
18.4	107.8324	0.2215	23.8795
18.6	107.8460	0.2215	23.8842
18.8	107.8698	0.2215	23.8948
19	107.8497	0.2215	23.8851
19.2	107.8431	0.2214	23.8815
19.4	107.8428	0.2214	23.8795
19.6	107.8544	0.2215	23.8846
19.8	107.8493	0.2214	23.8813
20	107.8355	0.2214	23.8746
20.2	107.8522	0.2214	23.8816
20.4	107.8435	0.2214	23.8770
20.6	107.8342	0.2214	23.8709
20.8	107.8426	0.2214	23.8748
21	107.8548	0.2214	23.8798
21.2	107.8617	0.2214	23.8811
21.4	107.8169	0.2213	23.8603
21.6	107.8394	0.2214	23.8704
21.8	107.8453	0.2214	23.8720
22	107.8435	0.2213	23.8702
22.2	107.8510	0.2214	23.8735
22.4	107.8369	0.2213	23.8667
22.6	107.8564	0.2214	23.8756

Table A.6 (cont'd)

Time (sec)	Voltage (Volt)	Current (Amp)	Power (Watt)
22.8	107.8719	0.2214	23.8811
23	107.8613	0.2213	23.8750
23.2	107.8759	0.2214	23.8805
23.4	107.8507	0.2213	23.8691
23.6	107.8569	0.2213	23.8720
23.8	107.8707	0.2214	23.8775
24	107.8486	0.2213	23.8662
24.2	107.8764	0.2213	23.8773
24.4	107.8616	0.2213	23.8711
24.6	107.8736	0.2213	23.8768
24.8	107.8836	0.2213	23.8795
25	107.8598	0.2213	23.8680
25.2	107.8783	0.2213	23.8766
25.4	107.8649	0.2213	23.8708
25.6	107.8589	0.2213	23.8653
25.8	107.8845	0.2213	23.8771
26	107.8673	0.2213	23.8689
26.2	107.8743	0.2213	23.8723
26.4	107.8686	0.2213	23.8684
26.6	107.8626	0.2212	23.8645
26.8	107.8716	0.2213	23.8688
27	107.8609	0.2212	23.8627
27.2	107.8750	0.2213	23.8692
27.4	107.8506	0.2212	23.8573
27.6	107.8577	0.2212	23.8588
27.8	107.8591	0.2212	23.8607
28	107.8476	0.2212	23.8543
28.2	107.8348	0.2211	23.8473
28.4	107.8358	0.2212	23.8480
28.6	107.8439	0.2212	23.8514
28.8	107.8630	0.2212	23.8594
29	107.8470	0.2212	23.8522
29.2	107.8396	0.2211	23.8470
29.4	107.8478	0.2212	23.8505
29.6	107.8696	0.2212	23.8593
29.8	107.8768	0.2212	23.8618
30	107.8744	0.2212	23.8599
30.2	107.8932	0.2212	23.8684

Table A.6 (cont'd)

Time (sec)	Voltage (Volt)	Current (Amp)	Power (Watt)
30.4	107.8575	0.2211	23.8525
30.6	107.8395	0.2211	23.8441
30.8	107.8739	0.2212	23.8585
31	107.8611	0.2211	23.8523
31.2	107.8840	0.2212	23.8619
31.4	107.8655	0.2211	23.8533
31.6	107.8742	0.2212	23.8572
31.8	107.8755	0.2212	23.8576
32	107.8517	0.2211	23.8466
32.2	107.8783	0.2211	23.8564
32.4	107.8448	0.2211	23.8424
32.6	107.8380	0.2211	23.8376
32.8	107.8470	0.2211	23.8421
33	107.8607	0.2211	23.8461
33.2	107.8729	0.2211	23.8523
33.4	107.8443	0.2210	23.8389
33.6	107.8372	0.2210	23.8353
33.8	107.8609	0.2211	23.8457
34	107.8739	0.2211	23.8505
34.2	107.8739	0.2211	23.8514
34.4	107.8547	0.2211	23.8424
34.6	107.8609	0.2211	23.8442
34.8	107.8743	0.2211	23.8493
35	107.8548	0.2210	23.8403
35.2	107.8710	0.2211	23.8474
35.4	107.9024	0.2211	23.8596
35.6	107.8774	0.2211	23.8495
35.8	107.8886	0.2211	23.8527
36	107.8713	0.2211	23.8455
36.2	107.8742	0.2211	23.8463
36.4	107.8815	0.2211	23.8481
36.6	107.8763	0.2211	23.8465
36.8	107.8851	0.2211	23.8491
37	107.8829	0.2210	23.8473
37.2	107.8793	0.2210	23.8454
37.4	107.8682	0.2210	23.8407
37.6	107.8730	0.2210	23.8422
37.8	107.8869	0.2210	23.8483

Table A.6 (cont'd)

Time (sec)	Voltage (Volt)	Current (Amp)	Power (Watt)
38	107.8681	0.2210	23.8386
38.2	107.8684	0.2210	23.8391
38.4	107.8512	0.2210	23.8316
38.6	107.8829	0.2210	23.8451
38.8	107.8949	0.2210	23.8495
39	107.8902	0.2210	23.8471
39.2	107.8725	0.2210	23.8394
39.4	107.8878	0.2210	23.8458
39.6	107.8867	0.2210	23.8441
39.8	107.8906	0.2210	23.8456
40	107.8814	0.2210	23.8407
40.2	107.8830	0.2210	23.8425
40.4	107.8137	0.2209	23.8108
40.6	107.6953	0.2206	23.7582
40.8	107.7478	0.2207	23.7816
41	107.7984	0.2208	23.8030
41.2	107.8438	0.2209	23.8219
41.4	107.8550	0.2209	23.8269
41.6	107.8462	0.2209	23.8227
41.8	107.8688	0.2209	23.8307

REFERENCES

REFERENCES

Beck JV. 1970. Nonlinear estimation applied to the nonlinear inverse heat conduction problem. International Journal of Heat and Mass Transfer 13(4):703-16.

Beck JV, Arnold KJ. 1977a. Parameter Estimation. New York: Wiley.

Beck JV, Arnold KJ. 1977b. Parameter estimation in engineering and science. New York: Wiley.

Betta G, Rinaldi M, Barbanti D, Massini R. 2009. A quick method for thermal diffusivity estimation: Application to several foods. Journal of Food Engineering 91(1):34-41.

Bristow KL, Kluitenberg GJ, Horton R. 1994a. Measurement of Soil Thermal Properties with a Dual-Probe Heat-Pulse Technique. Soil Sci. Soc. Am. J. 58(5):1288-94.

Bristow KL, Kluitenberg GJ, Horton R. 1994b. Measurement of soil thermal properties with a dual-probe heat-pulse technique. Soil science society of America Journal 58(5):1288-94.

COMSOL. 2012. COMSOL Multiphysics. 42a ed: COMSOL Inc., Burlington, Massachusetts, United States.

de Monte F, Beck JV, Amos DE. 2008. Diffusion of thermal disturbances in two-dimensional Cartesian transient heat conduction. International Journal of Heat and Mass Transfer 51(25-26):5931-41.

Denys S, Hendrickx ME. 1999. Measurement of the thermal conductivity of foods at high pressure. J Food Sci 64(4):709-13.

Dolan K, Valdramidis V, Mishra D. 2012. Parameter estimation for dynamic microbial inactivation; which model, which precision? Food Control.

Gratzek JP, Toledo RT. 1993. Solid Food Thermal-Conductivity Determination at High-Temperatures. J Food Sci 58(4):908-13.

Halliday PJ, Parker R, Smith AC, Steer DC. 1995. The thermal conductivity of maize grits and potato granules. J Food Eng 26(3):273-88.

Mariani VC, Do Amarante ÁCC, Dos Santos Coelho L. 2009. Estimation of apparent thermal conductivity of carrot purée during freezing using inverse problem. International Journal of Food Science & Technology 44(7):1292-303.

Mishra DK, Dolan KD, Yang L. 2008. Confidence intervals for modeling anthocyanin retention in grape pomace during nonisothermal heating. J Food Sci 73(1):E9-E15.

Mishra DK, Dolan KD, Yang L. 2011. Bootstrap confidence intervals for the kinetic parameters of degradation of anthocyanins in grape pomace. Journal of Food Process Engineering 34(4):1220-33.

Mohamed IO. 2009. Simultaneous estimation of thermal conductivity and volumetric heat capacity for solid foods using sequential parameter estimation technique. Food Res Int 42(2):231-6.

Mohamed IO. 2010. Development of a simple and robust inverse method for determination of thermal diffusivity of solid foods. J Food Eng 101(1):1-7.

Monteau J-Y. 2008. Estimation of thermal conductivity of sandwich bread using an inverse method. J Food Eng 85(1):132-40.

Murakami EG, Sweat VE, Sastry SK, Kolbe E, Hayakawa K, Datta A. 1996. Recommended design parameters for thermal conductivity probes for nonfrozen food materials. J Food Eng 27(2):109-23.

Nahor HB, Scheerlinck N, Verniest R, De Baerdemaeker J, Nicolai BM. 2001. Optimal experimental design for the parameter estimation of conduction heated foods. J Food Eng 48(2):109-19.

Roy CJ. 2005. Review of code and solution verification procedures for computational simulation. Journal of Computational Physics 205(1):131-56.

Salari K, Knupp P. 2000. Code Verification by the Method of Manufactured Solutions. Other Information: PBD: 1 Jun 2000. p. Medium: P; Size: 124 pages.

Scheerlinck N, Berhane NH, Moles CG, Banga JR, Nicolai BM. 2008. Optimal dynamic heat generation profiles for simultaneous estimation of thermal food

properties using a hotwire probe: Computation, implementation and validation. Journal of Food Engineering 84(2):297-306.

Shariaty-Niassar M, Hozawa M, Tsukada T. 2000. Development of probe for thermal conductivity measurement of food materials under heated and pressurized conditions. J Food Eng 43(3):133-9.

USDA National Nutrient Database for Standard Reference, Release 26. Nutrient Data Laboratory Home Page, http://www.ars.usda.gov/ba/bhnrc/ndl. 2013.

Yang C-y. 1999. Estimation of the temperature-dependent thermal conductivity in inverse heat conduction problems. Applied Mathematical Modelling 23(6):469-78.

Yang C-y. 2000a. Determination of the temperature dependent thermophysical properties from temperature responses measured at medium's boundaries. International Journal of Heat and Mass Transfer 43(7):1261-70.

Zhu S, Ramaswamy HS, Marcotte M, Chen C, Shao Y, Le Bail A. 2007. Evaluation of thermal properties of food materials at high pressures using a dual-needle line-heat-source method. J Food Sci 72(2):E49-E56.

Zueco J, Alhama F, González Fernández CF. 2004. Inverse determination of the specific heat of foods. J Food Eng 64(3):347-53.

Chapter 5

Nutritional Values Of The Food Material And Comparison Of Degradation In Aseptic And Conventional Thermal Processing

Abstract

Thermal degradation of ascorbic acid and thiamin was studied in different processing conditions. A sample food matrix, sweet potato puree, was chosen for the study and was fortified with ascorbic acid and thiamin. The objective of this study was to develop a methodology to determine the product quality using mathematical modeling technique coupled with optimal experimental design based on a chemical agent's kinetic behavior. Experiments for retort processing were performed using a water immersion still retort. Several time-temperature combinations, for a particular lethality value were considered for retort and aseptic processing. The time and temperature combination in the aseptic system was obtained by varying the flow rate of the product and temperature setting of the coiled heater. Temperature-dependent thermal properties were used to predict temperature inside the product. The time-temperature history of the product was then used in the kinetic model to estimate the kinetic parameters by minimizing the sum of squares of measured and predicted nutrient degradation. A robust model may help to optimize the food processing by simulating the experimental conditions on computer rather than doing numerous experiments in lab or pilot plant. For retort processing, different processing times at 121.1^{o}C were used. Quantification of vitamin C and thiamin was performed with high performance liquid

chromatography system. Degradation kinetics of the nutrients were analyzed using temperature-dependent thermal properties of the sweet potato puree. Kinetic parameters for the nutrient retention were estimated to compute the nutrient retention in retort and aseptic processing conditions. The reaction rate for ascorbic acid in aseptic processing and retort processing was 0.0073 min^{-1} and 0.0114 min^{-1} at a reference temperature of 127^{o}C, respectively. The activation energy for ascorbic acid in aseptic processing and retort processing was 26.62 KJ/g-mol and 3.43 KJ/g-mol, respectively. The kinetic parameter of thiamin could not be estimated due to insufficient degradation in aseptic as well as in retort processing.

5.1 Introduction

The most important and widely used food preservation method is thermal processing. Quality of processed food is considered a key factor from a nutritional point of view. However, due to microbiological safety reasons quality is often compromised. Over-heating and under-heating are two major concerns for the food industry. Due to food safety concerns and limitations of the proper control systems, the food industry has a tendency to over-processing the products. To ensure a safe product, the most heat-resistant pathogenic or spoilage organism that will grow at expected storage temperatures must be taken into account. This organism might be *Clostridium botulinum* in the low-acid food. The thermal process is designed in such a way that probability of survival of *C. botulinum* in low-acid food is no higher than one in 10^{12} cans. Validation of the thermal process is normally done with

thermocouples inserted into the coldest spot of the package containing the food. The time-temperature history of the product can be used to calculate the lethality received by the product using standard calculation methods. If the thermal process is more conservative in nature, then it tends to over-process the product. Over-processing of the food product leads to the loss of vital nutrients and lower overall quality of the product, whereas under-heating the product leads to product spoilage due to microbial growth and poses health concern for the consumers. Hence, it is important to optimize the processing conditions to achieve the highest nutritional retention and keep the product safe from microorganism growth at the same time.

The effect of thermal processing on nutrient degradation can be defined by the kinetic parameters in the mathematical model. The time-temperature history of the product can be used to model the process and estimate the kinetic parameters in the model. Thermal parameters, such as thermal conductivity and heat capacity, are important for simulating the time-temperature history of the product. Even though the thermal processes are dynamic and cover a large temperature range ($20^{o}C$ – $140^{o}C$), the thermal properties are often considered constant in modeling the kinetic parameters. Thermal properties of food vary considerably with temperature (Dolan and Mishra 2013). The rate of quality change varies exponentially with temperature. Hence, a thermal process designed to be run at $140^{o}C$, may have significant impact on quality if the thermal properties used in the model are measured at room temperature ($20^{o}C$)(Gratzek and Toledo 1993).

Food processing systems are dynamic in nature, meaning the processing temperature will be varying with time. Hence, performing experiments at isothermal temperature is usually a simplified way of generating data in lab settings. However, isothermal experiments do not truly replicate the dynamic behavior, and the kinetic parameters obtained from isothermal experiments may be misleading (Levieux and others 2007; Banga and others 2003). The nonisothermal method of estimating the kinetic parameters has advantages over the isothermal method (Banga and others 2003). The nonisothermal method simulates the actual thermal process rather than doing experiments that are different than the actual process and isothermal in nature (Margarida C. Vieira 2001; Dolan and others 2007; Banga and others 2003; Cohen and others 1994; Cohen and Saguy 1985). Estimation of kinetic parameters has been studied in literature using the nonisothermal method by performing experiments in a retort (Mishra and others 2008; Dolan and others 2007; Nasri and others 1993). However, there is little research done on evaluation of kinetic parameters in aseptic system experiments. Cohen and Saguy (1985) and Cohen and others (1994) proposed a method to estimate the kinetic parameters for continuous thermal processing of grapefruit juice. Paired Equivalent Isothermal Exposures (PEIE) method was used to evaluate the kinetic parameters in continuous flow system (Margarida C. Vieira 2001). A review on nutritional comparison was carried out for Vitamin B, C and phenolic compounds for fresh, frozen and canned fruits and vegetables (Rickman and others 2007). In another study, optimal experimental design was used for estimating the kinetic parameters

in the Arrhenius model with a linearly increasing temperature profile (Cunha and Oliveira 2000).

Retention of thiamin was measured for various retort temperatures. The losses were 7.4 - 55.2% for a temperature range of 104 – 121.1^{o}C, respectively (Ariahu and Ogunsua 1999). However, kinetic parameter estimation was not done in the paper. Kinetics of degradation of vitamin C in peas sealed and retorted in large cans was studied (M. A. Rao 1981). Degradation kinetics of vitamin C in orange juice was studied under conventional, ohmic and microwave heating processes. Isothermal experiments were performed and it was found that ohmic heating retained maximum amount of vitamin C (Vikram and others 2005). There are very few studies in literature that have been done on the optimal experimental design for kinetic evaluation of food in aseptic processing. Modeling of the kinetics based on temperature-dependent thermal properties also was not found in the literature surveyed. Application of the optimal design to obtain the best times for experiment for accurate estimation of parameters is very limited in food engineering area. *D*-optimal design was used for the kinetic parameter estimation of thermal degradation kinetics of ascorbic acid at low water contents (Frías and others 1998).

Very few studies are available comparing the nutritional degradation/retention of retorted and aseptically processed foods. A comprehensive study of optimum nutrient retention comparison in aseptic and conventional processing is limited in the literature. The objective of this study is to compare the heat stability of heat liable compounds in aseptic and conventional

processing and to compare the degradation kinetics in those processes. The nutrients selected for this study were ascorbic acid and thiamin mixed in a food matrix of sweet potato puree.

5.2 Materials and Methods

5.2.1 Sample preparation

Sweet potato puree (Yamco LLC, NC) was used for aseptic and retort experiments. Nutritional fortification of vitamin C and thiamin was done with premixed fortified samples (fortitech®, NY). Premix was mixed adequately with the sweet potato puree in a food mixer. A 4 oz glass jar was used for retort processing. Also, for the aseptic processing, 4 oz jars were filled with the product. The samples were stored at refrigerated temperature before analysis.

5.2.2 Aseptic and retort trials

Several time-temperature combinations, for a particular F_o value, were used for retort and aseptic processing. Experiments for the retort processing were performed using a vertical water immersion still retort, as shown in a schematic in Figure 5.1. The retort temperature profile was selected to represent commercial processing food processing for a minimum F_0 value of 6 min. Other time-temperature combinations were designed to be lower than F_0 =6 min. Jars filled with a mixed sample of sweet potato and vitamin premix were put on the rack and lowered in the retort. The test was started as soon as the retort was filled with cold water and door was locked. After the pre-selected test condition was achieved, the

retort was cooled down below 25^{o}C and samples were collected and stored at refrigerated condition (2^{o}C) until further analysis.

The experimental runs for the aseptic process were performed on Microthermics® equipment as shown in Figure 5.2. The equipment consists of a positive displacement pump, two heaters, a hold tube and two coolers. A steam controller controls the heater's hot water set point of the aseptic system. Flow rate can be adjusted with the positive displacement pump. Test conditions were achieved with the flow rate setting and the heater temperature set points. A data recorder (NI 9213, National Instruments) was attached to the equipment to record experimental temperature at the end of each unit. Temperature profiles were selected to represent commercial aseptic processing. The cooled product after the coolers was filled in 4-oz glass jars and stored at refrigerated condition (2^{o}C) until further analysis.

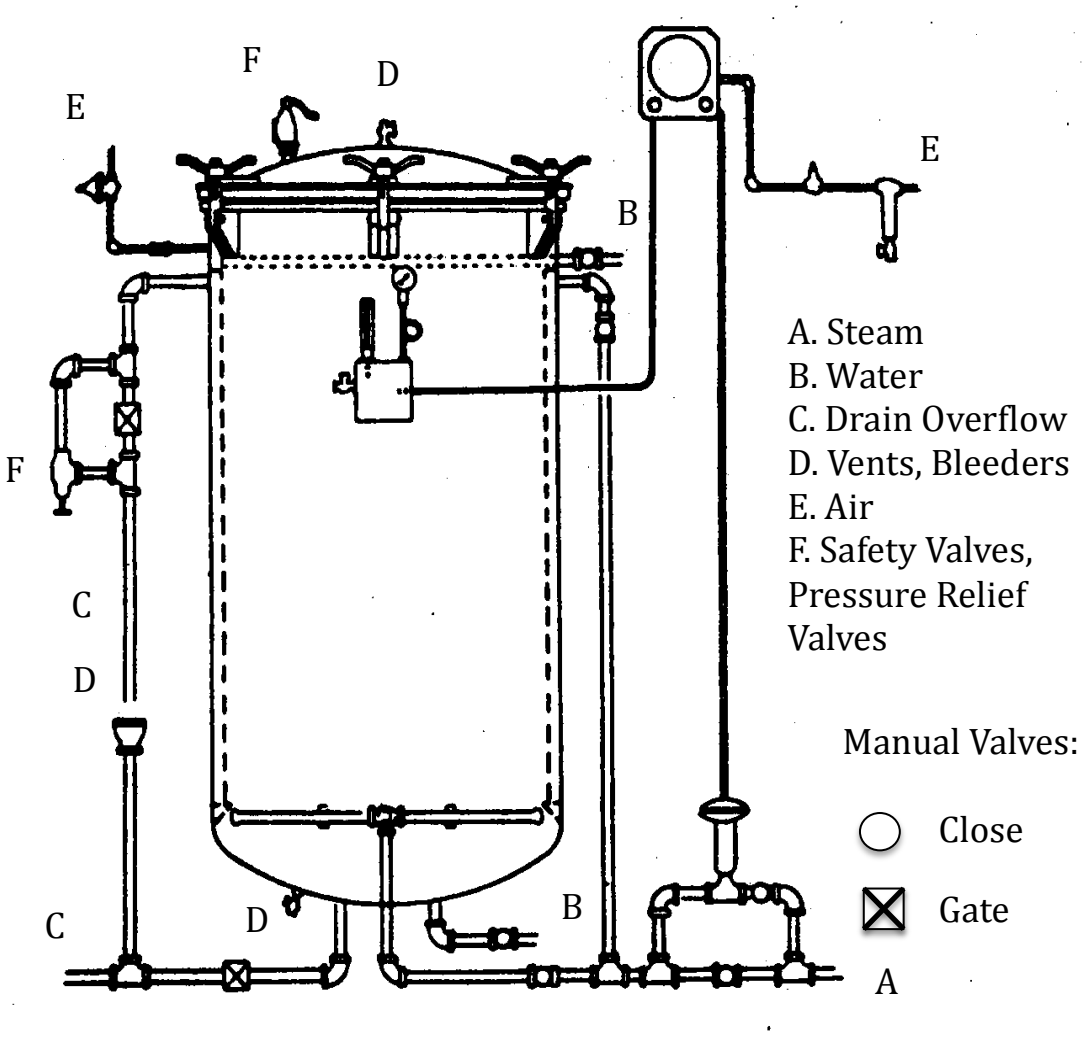

Figure 5.1 Vertical still water immersion retort

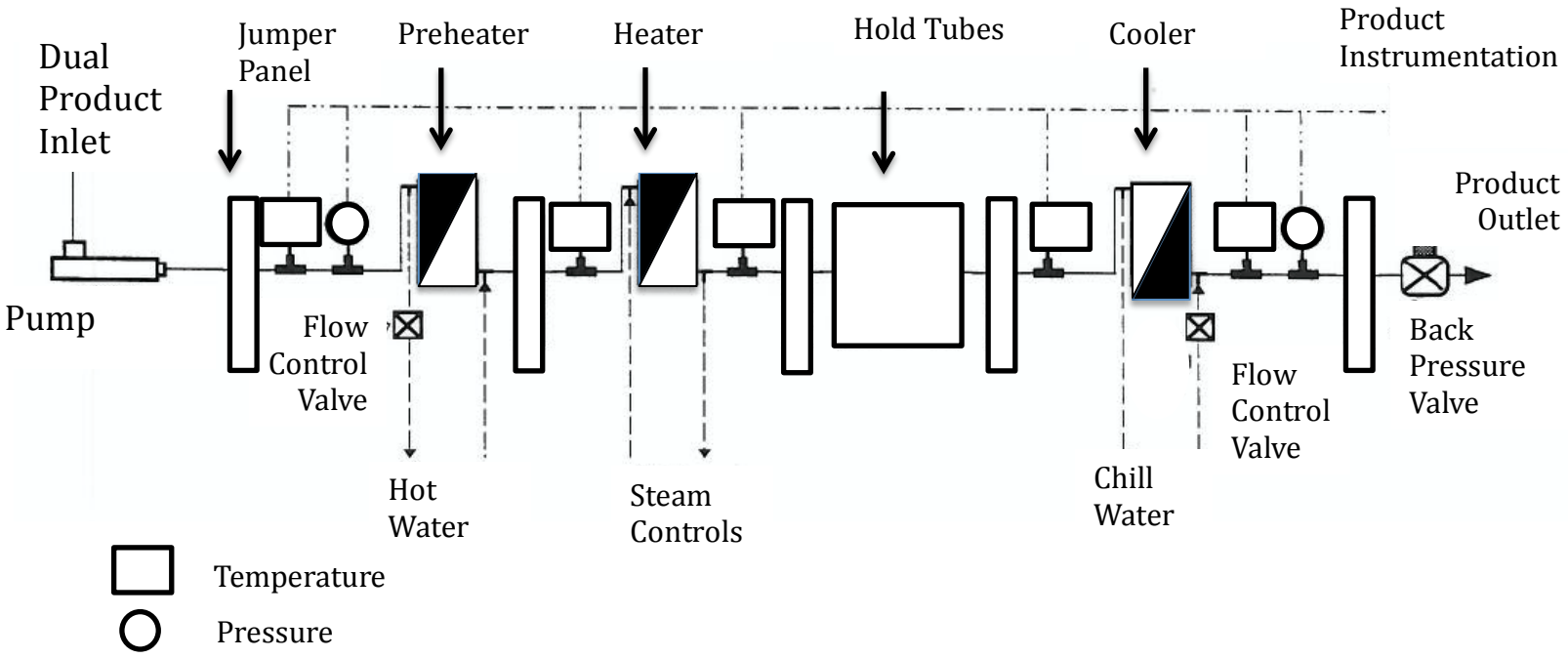

Figure 5.2 Microthermics equipment for aseptic processing

5.2.3 Analytical methods

Quantification of vitamin C and thiamin was performed with a high performance liquid chromatography system, using a rapid detection method for vitamin C (Furusawa 2001). The method uses 10 g of sample and 70 ml of meta-phosphoric acid. The sample was then left for 5 min. The HPLC was fitted with a column (waters carbohydrate, 125 Å, 10 µm, 3.9 * 300 mm) and a guard column (Bondpak AZ/Corasil, 37-50 µm) at ambient temperature. The injection volume was 20 µl. The mobil phase was 80:20 ACN:phosphate buffer, flow rate of 2.5 ml/min with a UV@ 254 nm detector. The run time was approximately 10 minutes.

Thiamin was also quantified with HPLC method (Pinto and others 2002). The injection volume was 50 µl through a column (Spherisorb ODS 5 µm, 4.6 X 250 nm with a flow rate of 1.5 ml/minute. The run time was approximately 10 minutes.

5.3 Mathematical model

5.3.1 Sterilization value

The general method for the lethal rate (Bigelow and others 1920) forms the basis for modern thermal process calculations. In order to calculate the process time for a product, thermal death time (F) should be known at all temperatures to which the product has been exposed. The equation for the thermal death time as a function of temperature can be written in the form of F notation as,

$$F_r / F = 10^{\left(1/z\right)\left(T-T_r\right)} \tag{5.1}$$

Thermal death time F_r is calculated at a reference temperature T_r. The ratio F_r/F is called lethal rate and is expressed as L (Ball 1923).

$$L = 10^{\left(1/z\right)\left(T-T_r\right)} \tag{5.2}$$

L is calculated at each temperature T and lethal rate can be plotted against. The total area under the lethal rate curve can be obtained by integrating the curve over the time-temperature history and is referred as lethality (F) (Patashnik 1953). F can be expressed as:

$$F = \int_0^t 10^{\left(1/z\right)\left(T-T_r\right)} dt \tag{5.3}$$

The process lethality calculated based on equation (5.3) must match the anticipated lethality for the specific product in order to determine the process time.

5.3.2 Thermal degradation kinetics

Thermal destruction kinetics is important to characterize the thermal process for a specific product. Kinetics can be defined as the study of rate of reaction, which varies with several factors, such as moisture, pH, temperature, concentration and other processing factors. The reaction rate equation is given as:

$$-\frac{dC}{dt} = kC^n \tag{5.4}$$

The relationship between k and temperature is generally modeled by the Arrhenius Equation:

$$k = k_r e^{\frac{-E_a}{R}\left(\frac{1}{T}-\frac{1}{T_r}\right)} \tag{5.5}$$

The use of a reference temperature T_r ensures that the correlation between k_r and E_a is not 1.0 or -1.0. T_r can arbitrarily be set to an average value of temperature range used in experiments (Van Boekel 1996). Alternatively, the value of T_r can be optimized by using an inverse problem to get a best estimate of T_r (Schwaab and Pinto 2007).

Most reactions in food, such as nutrient retention, quality factors and microorganism destruction follow first-order reaction kinetics. Hence, for a first order (n = 1) reaction, Eq. (5.4) can be written as:

$$C/C_o = e^{-k_r \Psi} \tag{5.6}$$

Where Ψ is the time temperature history and is the integrated value of temperature $T(t)$ over the entire time domain.

$$\psi = \int_0^t e^{\frac{-E_a}{R_g}\left(\frac{1}{T(t)}-\frac{1}{T_r}\right)} dt \tag{5.7}$$

Retention can be calculated for any product by using Eq. (5.6) provided that the kinetic parameters for particular compound (k_r and E_a), and time-temperature history are known. Time-temperature history was calculated with COMSOL® (COMSOL 2012) and MATLAB® (MATLAB 2012) using temperature-dependent thermal properties. TPCell measured temperature-dependent thermal conductivity, while heat capacity was measure by a Differential Scanning Calorimeter. Microthermics experiments data were analyzed using Eq. (5.6) and(5.7).

For kinetic analysis of retort data, the Arrhenius model was considered. Rate constant and activation energy were estimated using the mathematical model (Mishra and others 2008) for degradation in a can. The mass average retention of nutrients can be described by Eq. (5.8).

$$\left(\frac{\bar{C}}{C_o}\right)_{pred} = 2\int\int e^{-k_r \int_0^t e^{\frac{-E_a}{R_g}\left(\frac{1}{T(r,z',t)}-\frac{1}{T_r}\right)} dt} \, r\, dr dz \tag{5.8}$$

Sensitivity coefficients were calculated for all the parameters in the model (Beck 1977). The scaled sensitivity coefficient is defined as:

$$\hat{\beta}_i = \beta_i \frac{\partial C}{\partial \beta_i} \tag{5.9}$$

These scaled sensitivity coefficients will provide better insight in deciding which parameters are more sensitive to variation in processing conditions. Statistical indices were calculated to ascertain the accuracy of the estimated parameters. Sensitivity coefficients are good indicators of the identifiability of the several parameters occurring in the model (Beck and Arnold 1977c).

Alternatively, the scaled sensitivity coefficient can be approximated by the finite difference method as:

$$\beta_i \frac{\partial C}{\partial \beta_i} \approx \frac{C((1+\delta)\beta_i) - C(\beta_i)}{\delta} \tag{5.10}$$

Where, *d* is a very small number such as 0.001.

5.4 Results

The chromatogram of the vitamin C analysis is presented in Figure 5.3. The ascorbic acid peak occurs at 4.8 minutes. The peak for thiamin occurs around 20 seconds, as shown in Figure 5.4.

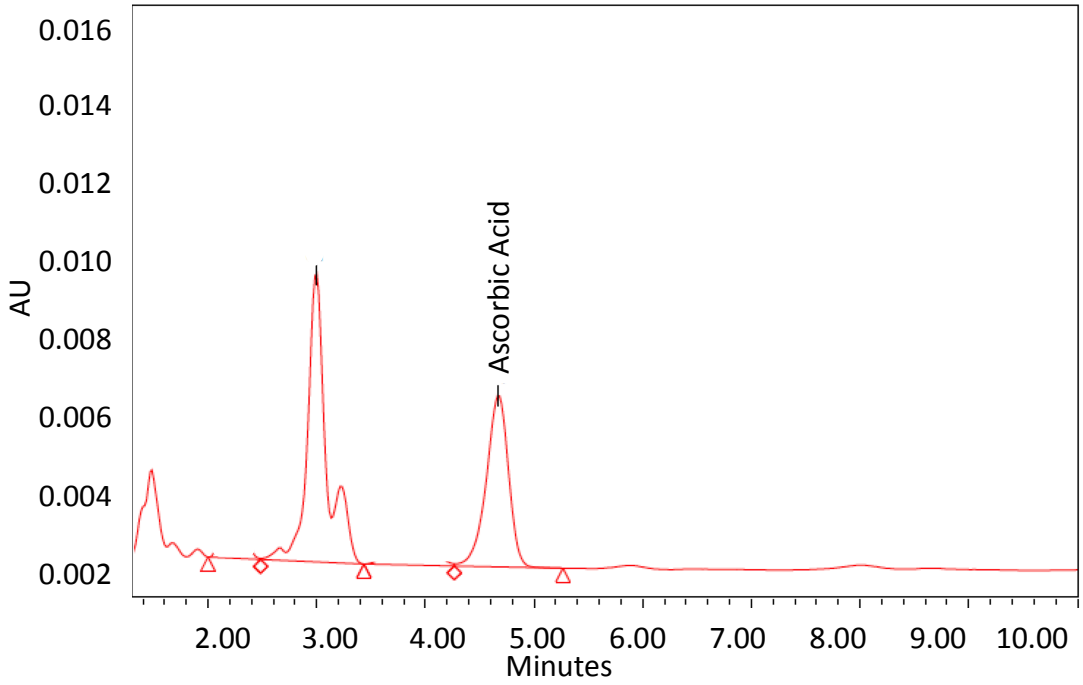

Figure 5.3 Chromatogram for HPLC analysis of vitamin C as ascorbic acid

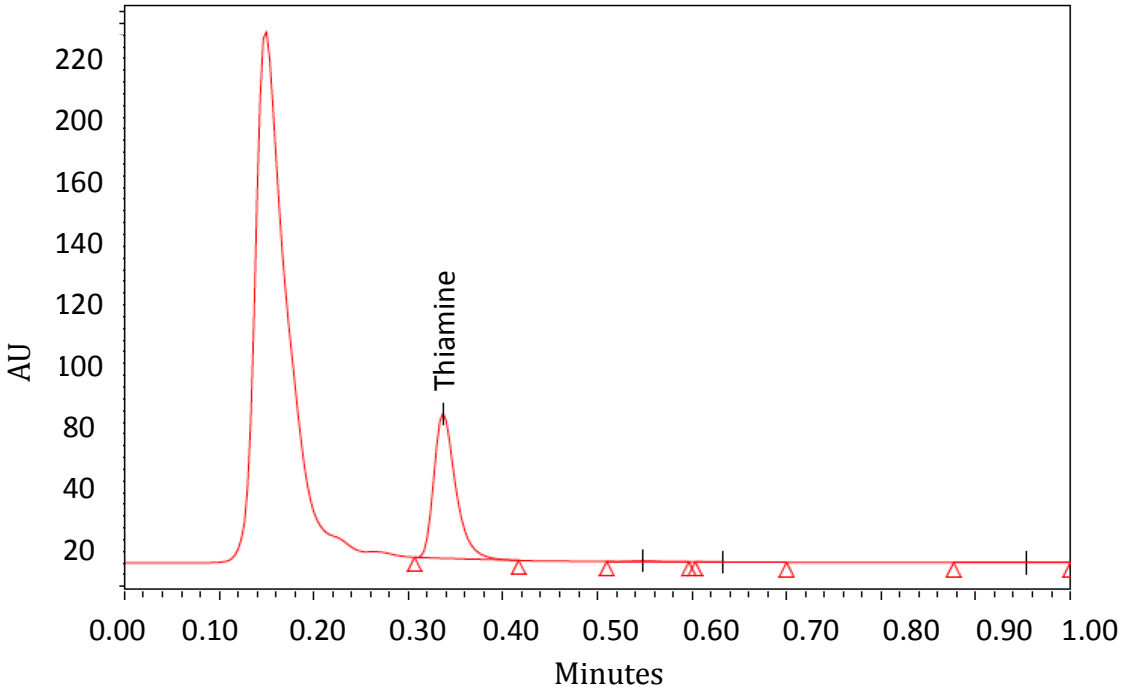

Figure 5.4 Chromatogram for HPLC analysis of thiamin

5.4.1 Aseptic Experiment

Viscosity of the sweet potato puree at several temperatures was determined using rheometer (RS600, Haake, Thermo Scientific). Reynolds number is calculated using Eq. (5.11).

$$N_{\mathrm{Re},PL} = \left(\frac{D^n \left(\overline{u}\right)^{2-n} \rho}{8^{n-1} K} \right) \left(\frac{4n}{3n+1} \right)^n \tag{5.11}$$

Where volumetric average velocity is given by,

$$\overline{u} = \frac{V}{A} = \frac{4Q}{\pi D^2} \tag{5.12}$$

Laminar flow of a power law fluid exists in the tube if $N_{\mathrm{Re},PL} < \left(N_{\mathrm{Re},PL}\right)_{critical}$

$$\left(N_{\mathrm{Re},PL}\right)_{critical} = 2100 + 875(1-n) \tag{5.13}$$

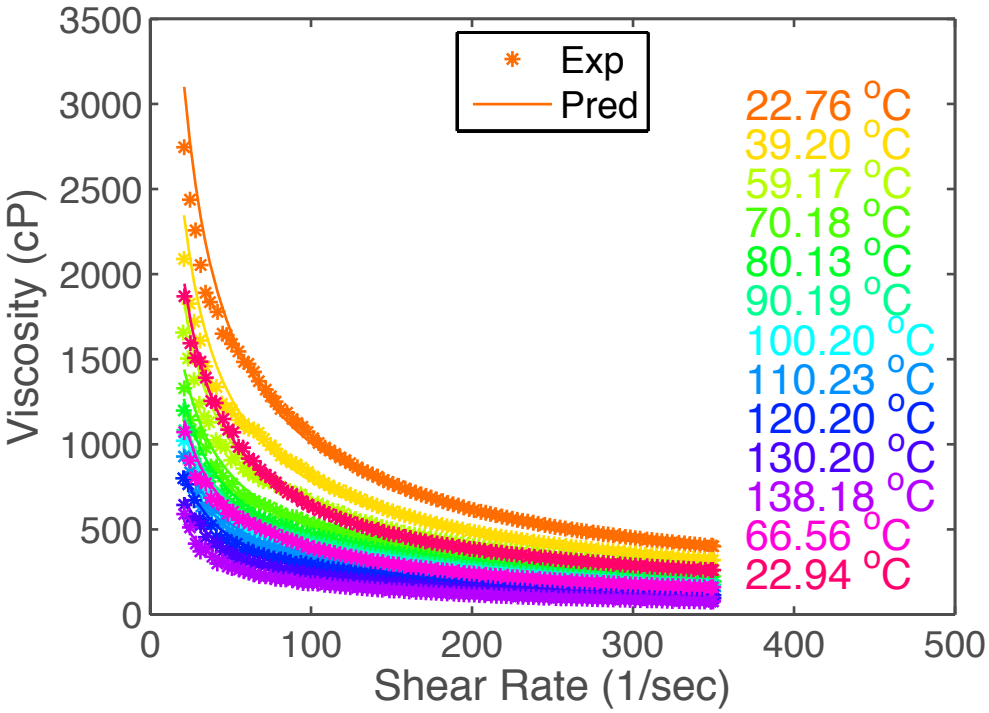

Figure 5.5 Viscosity of sweet potato puree measured at different temperatures, Q = 2 lpm and D = 0.43 in.

Table 5.1 Viscosity of sweet potato puree and Reynolds number

Temp (^{o}C)	K (Pa.s^{n})	n	Viscosity, cP @ 100/s	Reynolds Number	Critical Reynolds Number
22.76	28.37	0.28	1009.74	9.70	2848.74
39.20	19.87	0.30	785.41	12.53	2795.78
59.17	14.65	0.32	634.28	15.60	2752.96
70.18	10.59	0.35	523.31	19.06	2695.77
80.13	9.20	0.35	456.91	21.83	2693.65
90.19	8.74	0.34	413.66	24.04	2713.97
100.20	8.22	0.33	383.05	25.94	2720.63
110.23	7.62	0.32	332.20	29.79	2749.83
120.20	6.88	0.31	281.78	35.00	2778.79
130.20	5.75	0.30	232.68	42.36	2784.09
138.18	4.37	0.31	183.00	53.96	2768.40
66.56	9.63	0.30	385.91	25.53	2789.11
22.94	17.70	0.28	637.21	15.37	2842.72

Reynolds number of sweet potato puree is lower than that of the critical Reynolds number (Table 5.1) and hence the flow profile in aseptic system is laminar. For aseptic experiments, the time-temperature data for experimental design is provided in Table 5.2, along with the vitamin C and thiamin data. The diameter of tubes in aseptic system is 0.43' and a hold tube of 70 feet length was used for all experiments. The velocity through the system for 1 lpm flow rate was 0.58 ft/sec and for 2 lpm was 1.17 ft/sec. The simulated and experimental time temperature profile is shown in Figure 5.6. The average value of the unprocessed sample of sweet potato vitamin C was 809 mg/100g. The simulated profile was used for kinetic parameter estimation. Sequential estimation results are shown in Table 5.3. The estimated value of rate constant was 0.0114 min^{-1} and the activation energy was 12 KJ/mol. The standard errors for rate constant and activation energy were 0.0011 min^{-1} and 2.560 KJ/mol, respectively. The reference temperature used in the analysis was 127^{o}C. The kinetics of thiamin could not be performed, as there was not enough degradation (table 5.2) of thiamin even at higher temperatures.

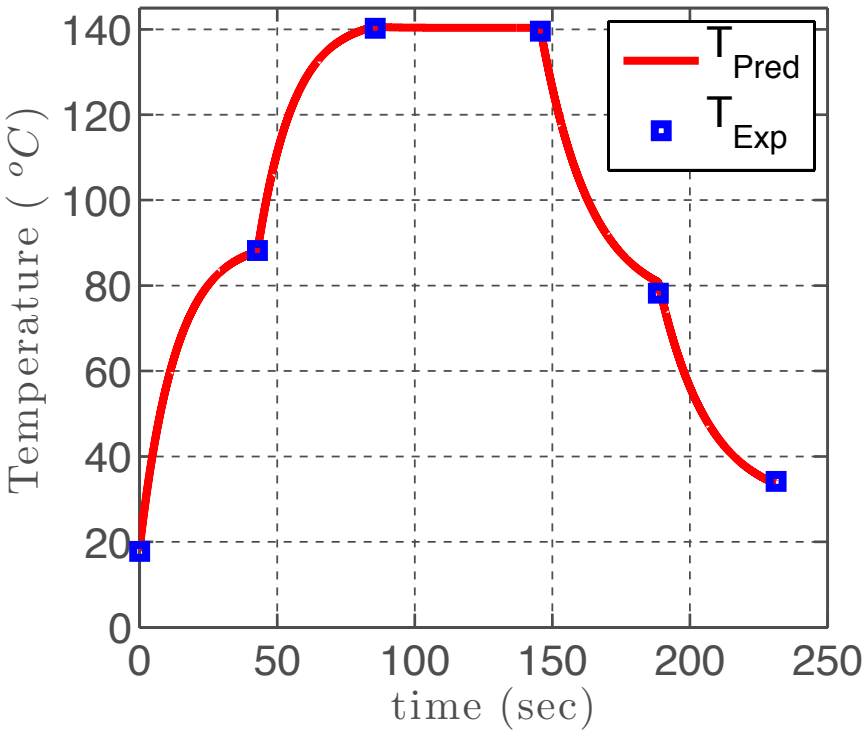

Figure 5.6 Experimental and predicted temperature profile of sweet potato puree (Test 2) as it goes through various sections of aseptic system.

Table 5.2 Time-temperature data for aseptic experiment

Test	Flow Rate (lpm)	IT (°C)	Pre-Heater (°C)	Heater (°C)	Hold Tube (°C)	Vit C, mg/100g	Thiamin, mg/100g
Raw	0	-	-	-	-	809	0.356
	0	-	-	-	-	802	0.342
	0	-	-	-	-	816	0.374
1	1	16.67	91.94	122.56	121.94	790	0.220
	1	16.67	91.94	122.56	121.94	782	0.204
	1	16.67	91.94	122.56	121.94	784	0.283
2	1	16.67	90.94	124.39	123.72	762	0.274
	1	16.67	90.94	124.39	123.72	770	0.165
	1	16.67	90.94	124.39	123.72	765	0.211
3	1	16.67	90.56	127.78	127.22	745	0.270
	1	16.67	90.56	127.78	127.22	756	0.294
	1	16.67	90.56	127.78	127.22	755	0.218
4	1	16.67	91.11	128.89	128.28	732	0.267
	1	16.67	91.11	128.89	128.28	736	0.281
	1	16.67	91.11	128.89	128.28	748	0.222
5	1	16.67	93.44	134.67	134.06	712	0.276
	1	16.67	93.44	134.67	134.06	721	0.284
	1	16.67	93.44	134.67	134.06	720	0.208
6	2	17.78	90.56	107.78	107.22	773	0.315
	2	17.78	90.56	107.78	107.22	769	0.239
	2	17.78	90.56	107.78	107.22	767	0.204
7	2	17.78	90.94	111.11	110.56	768	0.198
	2	17.78	90.94	111.11	110.56	778	0.293
	2	17.78	90.94	111.11	110.56	783	0.256
8	2	17.78	90.11	117.78	116.94	785	0.316
	2	17.78	90.11	117.78	116.94	781	0.249
	2	17.78	90.11	117.78	116.94	779	0.281
9	2	17.78	89.44	122.39	121.94	768	0.204
	2	17.78	89.44	122.39	121.94	771	0.224
	2	17.78	89.44	122.39	121.94	770	0.234
10	2	17.78	88.06	129.72	129.11	767	0.243
	2	17.78	88.06	129.72	129.11	771	0.235
	2	17.78	88.06	129.72	129.11	761	0.239
11	2	17.78	87.11	134.56	133.44	732	0.232
	2	17.78	87.11	134.56	133.44	726	0.212
	2	17.78	87.11	134.56	133.44	714	0.222

Table 5.2 (cont'd)

Test	Flow Rate (lpm)	IT (°C)	Pre-Heater (°C)	Heater (°C)	Hold Tube (°C)	Vit C, mg/100g	Thiamin, mg/100g
12	2	17.78	88.22	140.22	139.56	686	0.210
	2	17.78	88.22	140.22	139.56	700	0.183
	2	17.78	88.22	140.22	139.56	702	0.226

Table 5.3 Parameter estimates and statistical indices for kinetic parameters of vitamin C degradation in aseptic system

Parameters	Final Estimates	Standard error	Relative error, %	Lower confidence level	Upper confidence level	T_r, °C
k_r, min^{-1}	0.01140	0.00110	9.61855	0.00935	0.01344	127
E_a, J/mol	26621.93	2560.21	9.62	21848.24	31392.02	127

Experimental and predicted degradation of vitamin C, (C/C_0) in sweet potato puree is shown in Figure 5.7. Since there were two flow rates and several time-temperature combinations, the selection of x-axis was based on Eq. (5.7). The maximum degradation was about 12% at the hold tube temperature of 139.56 °C. This processing temperature was selected to provide a F_0 value of >6 min, to simulate a commercial aseptic process.

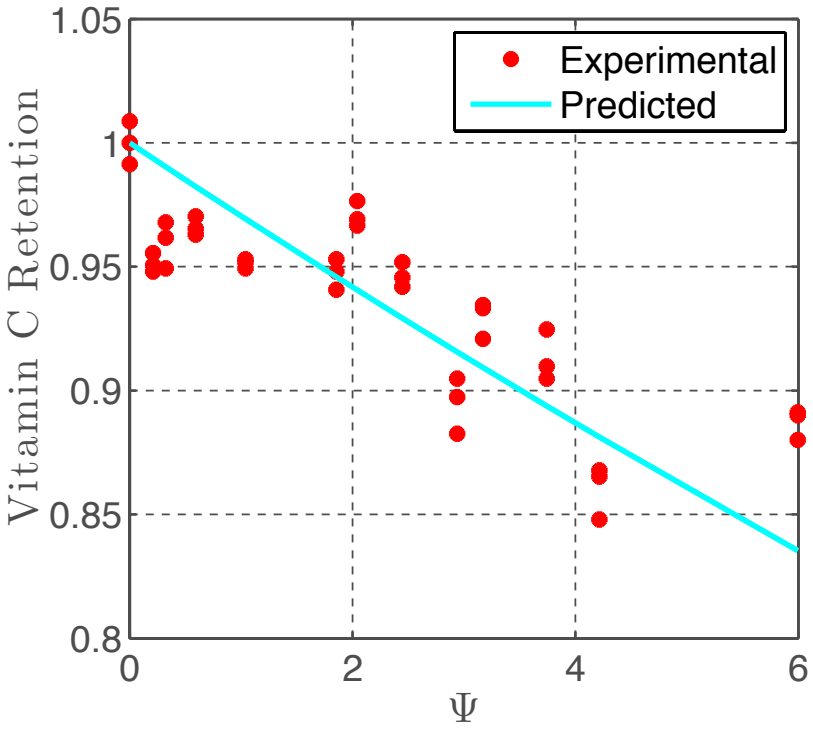

Figure 5.7 Experimental and predicted degradation of vitamin C in aseptically processed sweet potato puree

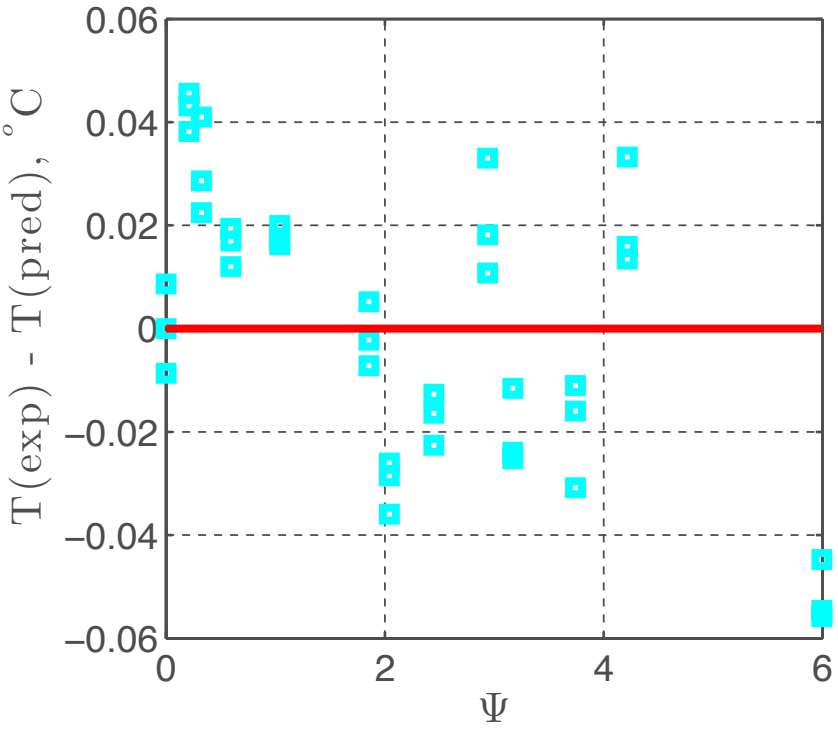

Figure 5.8 Residuals of vitamin C in aseptic processing

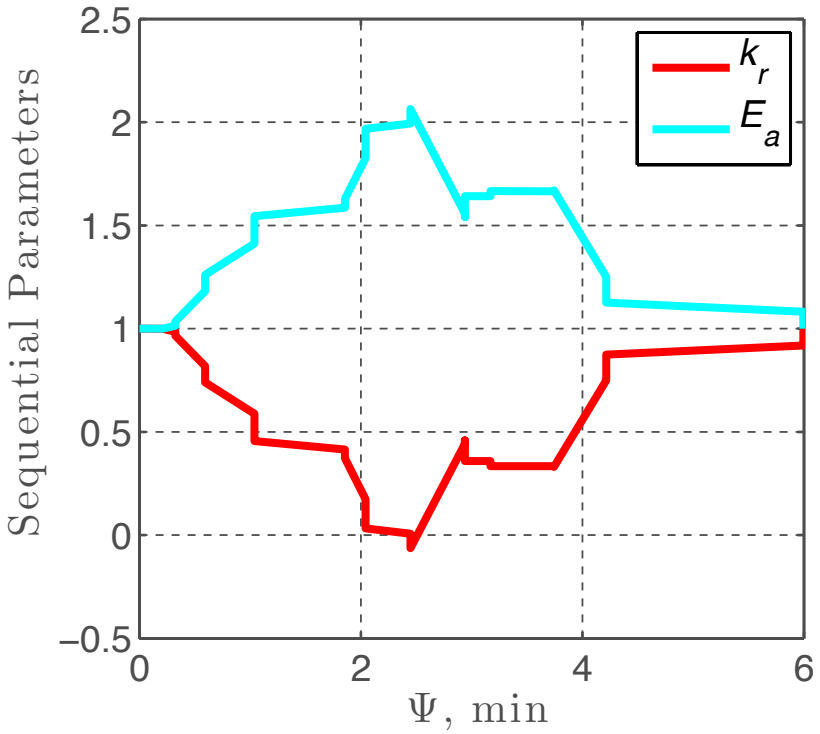

Figure 5.9 Sequential parameter estimates of vitamin C in aseptic processing

The residuals are plotted in Figure 5.8 and the sequential parameters estimates are plotted in Figure 5.9. The sequential parameters are normalized with the final estimate of the parameter. This is because of the different scales of k_r as compared to E_a. The sequentially estimated parameters come to a constant towards the end of experiment.

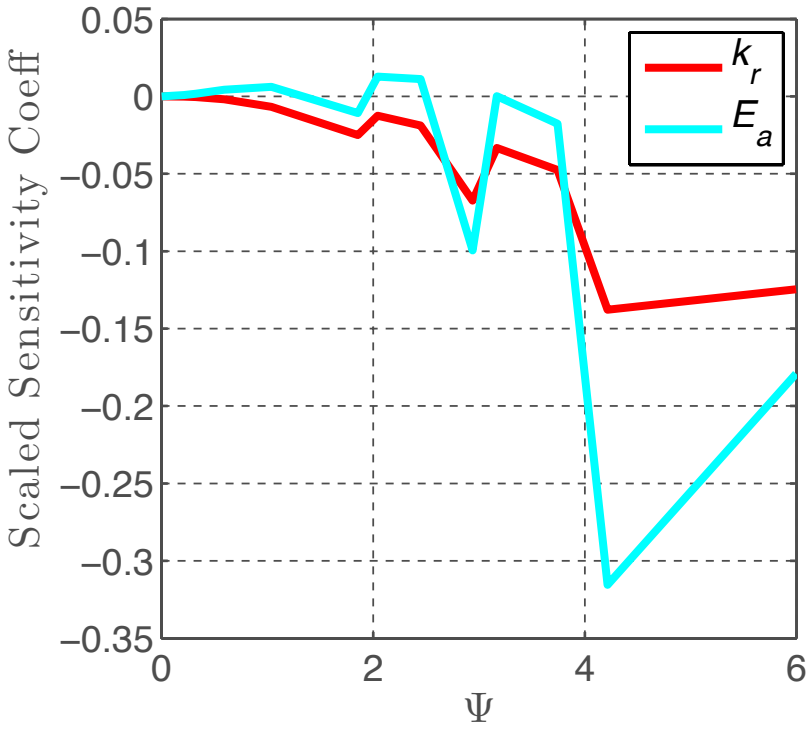

Figure 5.10 Scaled sensitivity coefficient of k_r and E_a in the kinetic degradation model of vitamin C in sweet potato puree processed in retort

Scaled sensitivity coefficients are shown in Figure 5.10. It can be inferred that the magnitude of scaled sensitivity of rate constant is low as compared to the total scale, which is 1 unit, in this case. This suggests that there would be difficulty in estimating this parameter. However, the magnitude of scaled sensitivity of activation energy is comparatively larger.

5.4.2 Retort Experiments

Retention of vitamin C and thiamin for the retort trials is presented in Table 5.4. For all the conditions, the retort temperature was 121.67 ^{o}C. The time presented in Table 5.4 includes the come-up time of the retort. Simulation of the

glass jar heated in the retort was done using COMSOL®. Figure 5.11 provides a simulated temperature profile of sweet potato in a glass jar. Since Gauss points were chosen for integration over space in the glass jar, a simulated time-temperature profile at nine difference Gauss points (T_1 - T_9) is shown in Figure 5.11.

Table 5.4 Time-temperature and vitamin C data for retort experiments

Test	Time (min)	Retort Temperature (^{O}C)	Vit C (mg/100g)	Thiamin (mg/100g)
Unprocessed	0	-	886	0.275
	0	-	908	0.261
	0	-	812	0.26
1	14	121.67	857	0.249
	14	121.67	879	0.239
	14	121.67	884	0.285
2	18	121.67	800	0.342
	18	121.67	796	0.293
	18	121.67	805	0.31
3	22	121.67	780	0.369
	22	121.67	768	0.35
	22	121.67	764	0.3
4	26	121.67	747	0.284
	26	121.67	742	0.297
	26	121.67	730	0.274
5	30	121.67	742	0.311
	30	121.67	751	0.265
	30	121.67	724	0.246
6	34	121.67	707	0.24
	34	121.67	727	0.18
	34	121.67	711	0.283
7	38	121.67	704	0.25
	38	121.67	664	0.294
	38	121.67	676	0.204
8	46	121.67	664	0.142
	46	121.67	652	0.22
	46	121.67	671	0.264
9	52	121.67	642	0.13
	52	121.67	651	0.151
	52	121.67	648	0.166
10	52	121.67	646	0.264
	52	121.67	649	0.342
	52	121.67	620	0.374

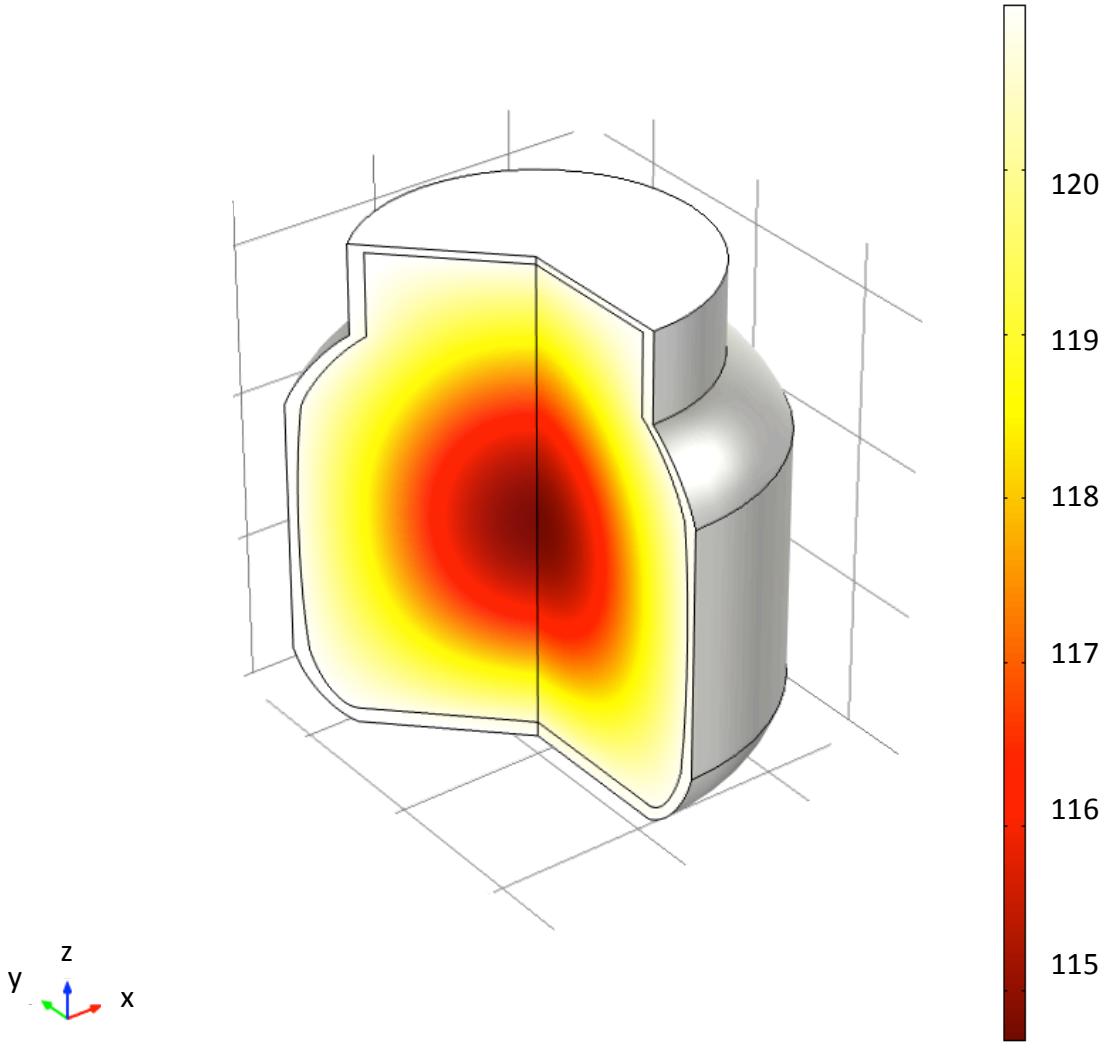

Figure 5.11 Simulated temperature profile of sweet potato puree in a glass jar processed in retort

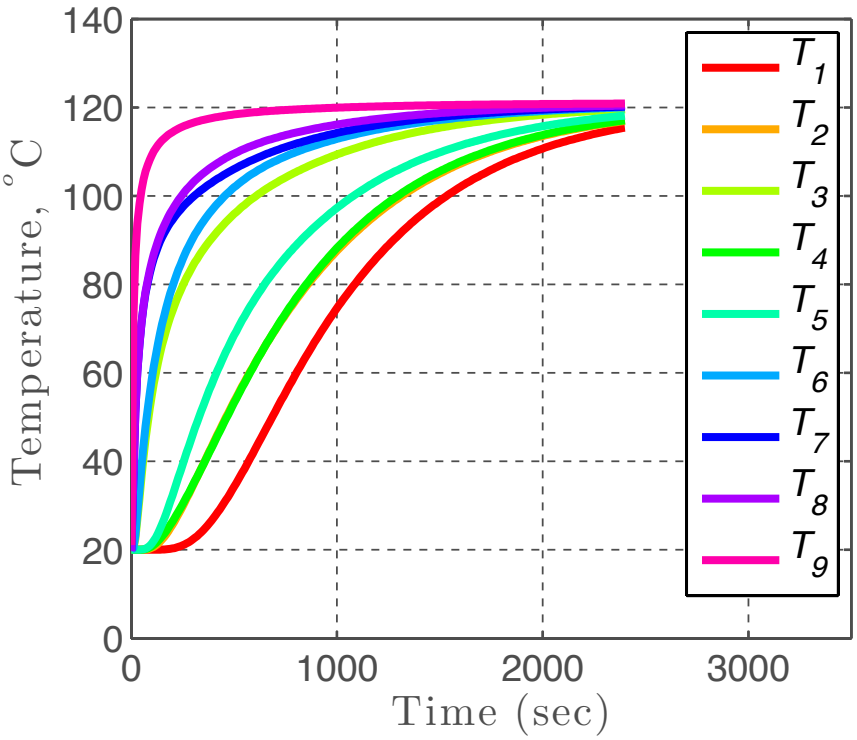

Figure 5.12 Simulated temperature profile of sweet potato puree at gauss points in a glass jar processed in retort

Table 5.5 Parameter estimates and statistical indices for kinetic parameters of vitamin C degradation in retort

Parameters	Final Estimates	Standard error	Relative error, %	Lower confidence level	Upper confidence level	Tr, ^{o}C
k_r, min^{-1}	0.00660	0.00029	4.32443	0.00615	0.00706	88
E_a, J/ g-mol	3430.14	148.51	4.33	3188.71	3664.94	88

The kinetic parameter estimates for the degradation of vitamin C in sweet potato during processing in retort are presented in Table 5.5. The estimated value of

rate constant was 0.0066 min^{-1} and the activation energy was 3.43 KJ/g-mol. The standard errors for rate constant and activation energy were 0.00029 min^{-1} and 0.148 KJ/g-mol, respectively. The reference temperature used in the analysis was 88 ^{o}C. The confidence interval of parameters is also presented in Table 5.5. The experimental and predicted degradation are presented in Figure 5.13. The maximum degradation was about 30% and that was at the longest processing time of 40 min. This was also the commercial thermal process with a delivered lethality of 6 min at the center of the can. Residuals are plotted in Figure 5.14 and there is no apparent sign of correlation. Sequentially estimated parameters are shown in Figure 5.15, the parameters come to a constant towards the end of experiment. Scaled sensitivity coefficient, as shown in Figure 5.16, is large for k_r as compared to E_a.

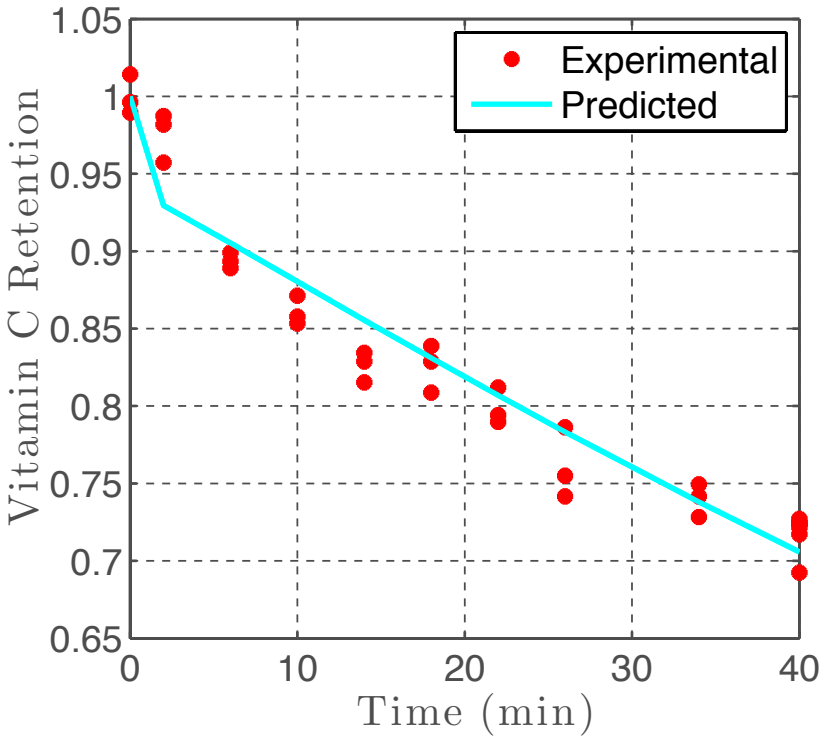

Figure 5.13 Experimental and predicted degradation of vitamin C in retort processing

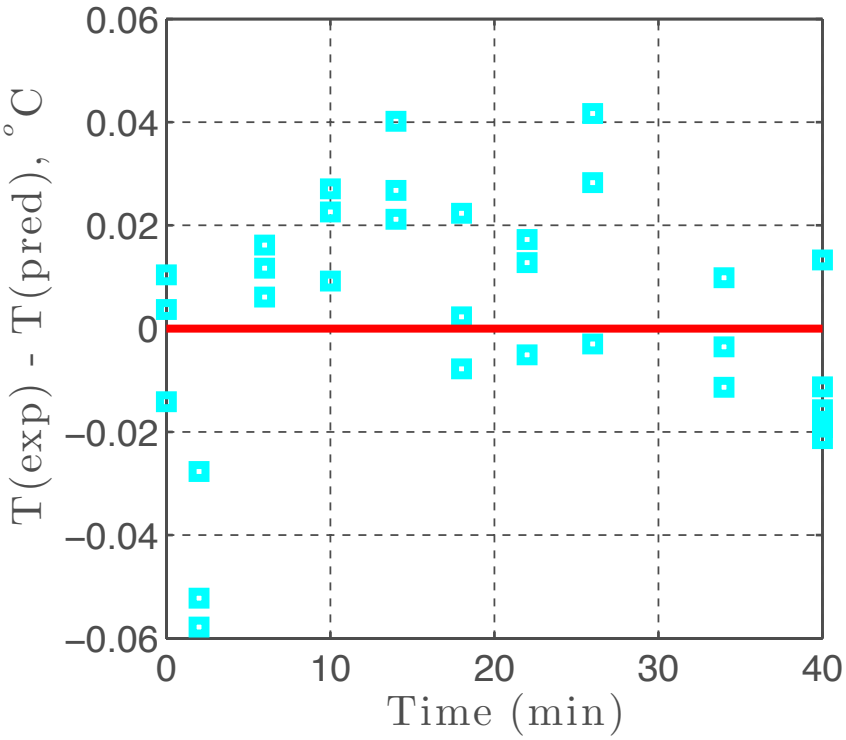

Figure 5.14 Residuals of vitamin C degradation in retort experiment

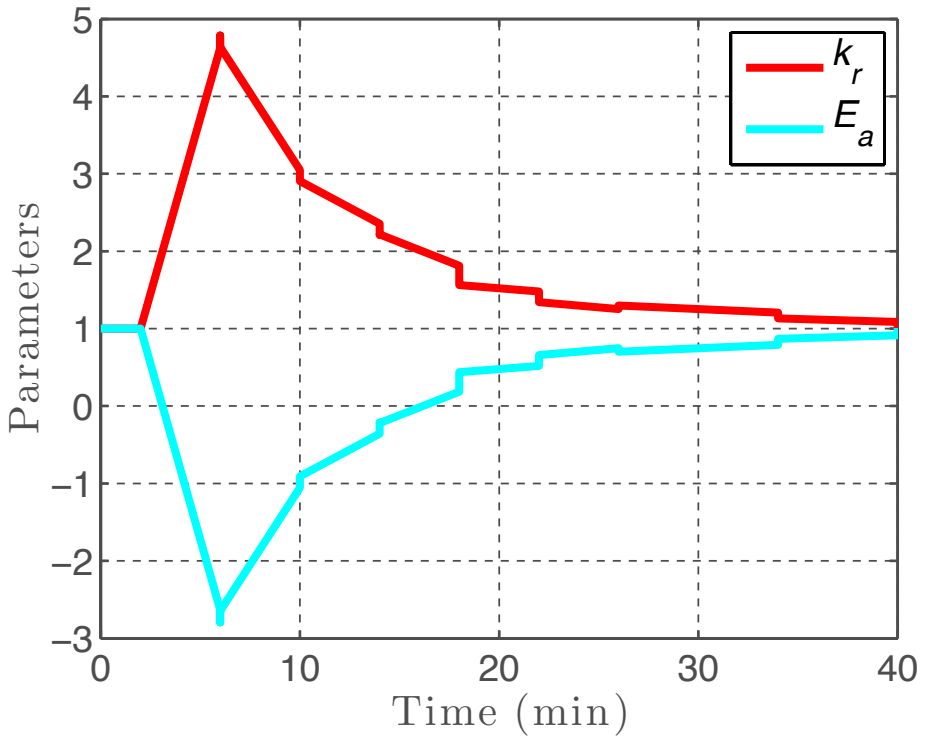

Figure 5.15 Normalized sequential parameter estimates of vitamin C in retort

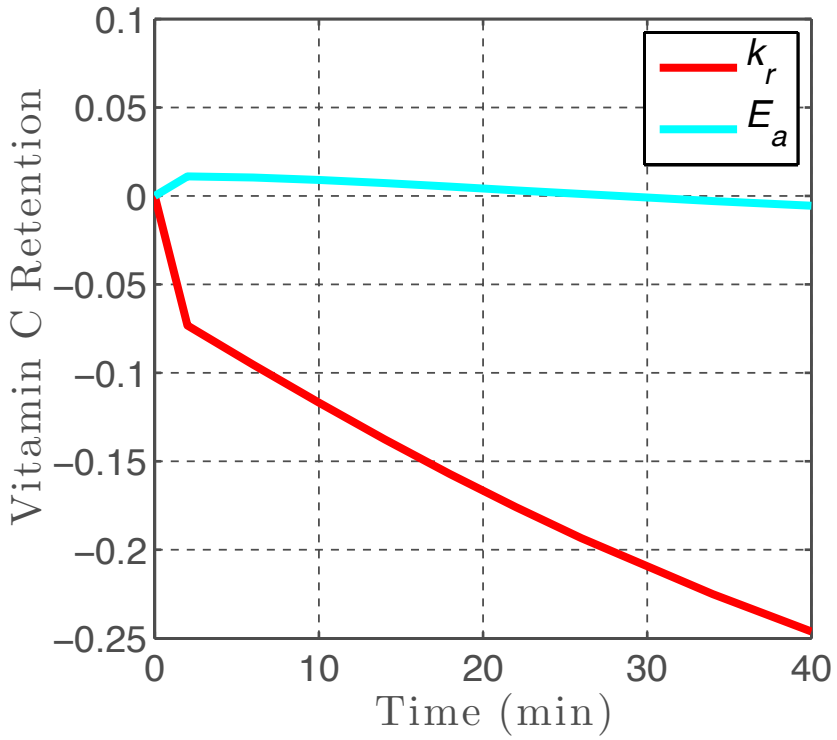

Figure 5.16 Scaled sensitivity coefficient of k_r and E_a in the kinetic degradation model

Thiamin was not sufficiently degraded to perform kinetic analysis. The optimization we discussed so far is related to the parameter estimation problem in the model. Parameters in the kinetic model of nutrient kinetics and enzyme inactivation can be estimated with optimal experiments. This type of optimization leads to the global optimization. The global optimization is based on different processing conditions of a processing system. The maximum retention of a nutrient can be achieved by processing the product in such a condition that will allow the proper sterilization of the product and well as proper inactivation of the enzyme. Optimum conditions for the thermal processing of soy milk were determined in the study of (Kwok and others 2002). Optimality was achieved by using the degradation

of thiamin, riboflavin, color and flavor and the inactivation of trypsin inhibitor activity (TIA). The optimal condition in this study was found to be a single step UHT process, for example, 143^{o}C/60 s, with satisfactory inactivation of TIA, color and flavor in acceptable limit and retention of thiamin between 90 and 93%. In another study (Manoj M. Nadkarni 1985), optimal nutrient retention was determined by the use of optimal control theory for the conduction-heated canned food. They found that the rapid heating and rapid cooling rates as permitted by the process constraints was the optimal control, and provided the maximum nutrient retention for a given reduction in microbial load. Also, it was recommended that only one heating and cooling cycle should be used during the sterilization process instead of several steps of heating and cooling. Similar results were obtained for the conduction heated food in retortable pouches (Yoshimi Terajima 1996). Response surface methodology (RSM) is helpful as an initial study to observe trends. However RSM has drawbacks because of the local and stationary nature of the algebraic models. Model-based optimization approach has been developed in recent years that accounts for the time-dependent robustness in the model and hence has great power to improve food processing techniques.

The dynamic temperature profile obtained from the retort and the aseptic system will be helpful in determining the maximum nutrient retention in the product. It will also help in determining the type of temperature profile that best suits the maximum retention.

5.5 Conclusions

Nutritional studies were performed to compare retention of vitamins in the aseptic system with conventional retort processing. Vitamin C and thiamin were selected as model vitamins. The retention in the aseptic system was higher as compared to the retort processing. The retention of vitamin C for the commercial process (F_0 = 6 min) of aseptic system was 85% and for retort it was 70%. So, the aseptic process was higher in retention. Temperature-dependent thermal properties were used in the modeling of kinetic of degradation of nutrients. Modeling of the kinetic parameters of degradation for both vitamins showed differences in the kinetic parameters. For the retort processing, the rate constant at a reference temperature of 127 ^{o}C was 0.0073 min^{-1} and for aseptic processing it was 0.0114 min^{-1}. This difference might be because of the difference in temperature history for both the processing systems. The maximum temperature in aseptic processing was 140 ^{o}C and for retort processing was 121.67 ^{o}C. The degradation of thiamin was not enough to estimate the kinetic parameters in both systems. The aseptic process is better for the retention of nutrients such as vitamin C.

REFERENCES

REFERENCES

Ariahu CC, Ogunsua OA. 1999. Effect of thermal processing on thiamine retention, in-vitro protein digestibility, essential amino acid composition, and sensory attributes of periwinkle-based low acid foods. p. 121-34.

Ball CO. 1923. Thermal process time for canned foods. bull. Natl. Res. Counsil 7, Part 1 (37), 76.

Banga JR, Balsa-Canto E, Moles CG, Alonso AA. 2003. Improving food processing using modern optimization methods. Trends in Food Science & Technology 14(4):131-44.

Beck JV, and Arnold, K.J. . 1977. Parameter estimation in engineering and science: John Wiley and Sons, NY.

Beck JV, Arnold KJ. 1977c. Parameter Estimation in Engineering and Science. New York: Wiley.

Bigelow WC, Bohart GS, Richardson AC, Ball CO. 1920. Heat penetration in processing canned foods. National Canners Association. Bull. No. 16L.

Cohen E, Birk Y, Mannheim CH, Saguy IS. 1994. Kinetic Parameter Estimation for Quality Change during Continuous Thermal Processing of Grapefruit Juice. p. 155-8.

Cohen E, Saguy I. 1985. Statistical evaluation of Arrhenius model and its applications in predicting of food quality losses. p. 273.

COMSOL. 2012. COMSOL Multiphysics. 42a ed: COMSOL Inc., Burlington, Massachusetts, United States.

Cunha LM, Oliveira FAR. 2000. Optimal experimental design for estimating the kinetic parameters of processes described by the first-order Arrhenius model under linearly increasing temperature profiles. Journal of Food Engineering 46(1):53-60.

Dolan KD, Mishra DK. 2013. Parameter Estimation in Food Science. Annual review of food science and technology 4:401-22.

Dolan KD, Yang L, Trampel CP. 2007. Nonlinear regression technique to estimate kinetic parameters and confidence intervals in unsteady-state conduction-heated foods. Journal of Food Engineering 80(2):581-93.

Frías JM, Oliveira JC, Cunha LM, Oliveira FA. 1998. Application of D-optimal design for determination of the influence of water content on the thermal degradation kinetics of ascorbic acid at low water contents. Journal of Food Engineering 38(1):69-85.

Furusawa N. 2001. Rapid high-performance liquid chromatographic identification/quantification of total vitamin C in fruit drinks. Food Control 12(1):27-9.

Gratzek JP, Toledo RT. 1993. Solid Food Thermal-Conductivity Determination at High-Temperatures. J Food Sci 58(4):908-13.

Kwok K-C, Liang H-H, Niranjan K. 2002. Optimizing Conditions for Thermal Processes of Soy Milk. p. 4834-8.

Levieux D, Geneix N, Levieux A. 2007. Inactivation-denaturation kinetics of bovine milk alkaline phosphatase during mild heating as determined by using a monoclonal antibody-based immunoassay. Journal of Dairy Research 74(03):296-301.

M. A. Rao CYLJKHJC. 1981. A Kinetic Study of the Loss of Vitamin C, Color, and Firmness During Thermal Processing of Canned Peas. p. 636-7.

Manoj M. Nadkarni TAH. 1985. Optimal Nutrient Retention during the Thermal Processing of Conduction-Heated Canned Foods: Application of the Distributed Minimum Principle. p. 1312-21.

Margarida C. Vieira AATCLMS. 2001. Kinetic Parameters Estimation for Ascorbic Acid Degradation in Fruit Nectar Using the Partial Equivalent Isothermal Exposures (PEIE) Method under Non-Isothermal Continuous Heating Conditions. p. 175-81.

MATLAB. 2012. MATLAB and Statistics Toolbox Release. 2012b ed: The MathWorks Inc., Natick, Massachusetts, United States.

Mishra DK, Dolan KD, Yang L. 2008. Confidence intervals for modeling anthocyanin retention in grape pomace during nonisothermal heating. J Food Sci 73(1):E9-E15.

Nasri H, Simpson R, Bouzas J, Torres JA. 1993. Unsteady-state method to determine kinetic parameters for heat inactivation of quality factors: Conduction-heated foods. Journal of Food Engineering 19(3):291-301.

Patashnik M. 1953. A simplified procedure for thermal process evaluation. Fd Technol., Champaign 7, 1.

Pinto E, Pedersén M, Snoeijs P, Van Nieuwerburgh L, Colepicolo P. 2002. Simultaneous Detection of Thiamine and Its Phosphate Esters from Microalgae by HPLC. Biochemical and Biophysical Research Communications 291(2):344-8.

Rickman JC, Barrett DM, Bruhn CM. 2007. Nutritional comparison of fresh, frozen, and canned fruits and vegetables II. Vitamin A and carotenoids, vitamin E, minerals and fiber. Journal of the Science of Food and Agriculture 87(7).

Schwaab M, Pinto JC. 2007. Optimum reference temperature for reparameterization of the Arrhenius equation. Part 1: Problems involving one kinetic constant. Chemical Engineering Science 62(10):2750-64.

Van Boekel M. 1996. Statistical Aspects of Kinetic Modeling for Food Science Problems. Journal of Food Science 61(3):477-86.

Vikram VB, Ramesh MN, Prapulla SG. 2005. Thermal degradation kinetics of nutrients in orange juice heated by electromagnetic and conventional methods. Journal of Food Engineering 69(1):31-40.

Yoshimi Terajima YN. 1996. Retort Temperature Profile for Optimum Quality during Conduction-Heating of Foods in Retortable Pouches. p. 673-8.

Chapter 6

Overall Conclusions

6.1 Conclusions

Based on the dimensionless derivation of the scaled sensitivity coefficients, an identity, intrinsic sum, was developed. Intrinsic sum was used to verify the numerical code for its accuracy to provide temperature predictions. It was also used to get insight into the parameter estimation problem. It was also shown that if the sum of all scaled sensitivity coefficients is equal to zero, then not all the parameters can be estimated uniquely and simultaneously. However, if the sum of scaled sensitivity coefficients is not equal to zero, then it might be possible to estimate all parameters uniquely and simultaneously. In the case of heat transfer problems where heat flux is a boundary condition, it was shown that thermal conductivity and specific heat can be estimated simultaneously. This was because the sum of all scaled sensitivity coefficients was equal to the temperature rise of the product. This was the fundamental principal behind design of TPCell instrument for measuring temperature-dependent thermal properties. TPCell was designed to measure thermal properties up to 140^{o}C with a testing time of less than a minute. TPCell is fully programmable to provide different heating rates for different types of materials. Several food products were tested and the thermal conductivity was reported. The thermal conductivity at room temperature had good agreement with other values reported in literature. The temperature-dependent thermal

conductivity obtained from TPCell was used to model the kinetic parameters of degradation for vitamin C and thiamin.

Nutrient studies were performed to compare the degradation of vitamin C and thiamin in aseptic and retort processing conditions. The aseptic processing system had a better retention than retort processing for vitamin C. For the retort processing, the rate constant at a reference temperature of 127^{o}C was 0.0073 min^{-1} and for aseptic processing it was 0.0114 min^{-1}. This difference might be because of the difference in temperature for both the systems. The maximum temperature in aseptic processing was 140^{o}C and for retort processing was 121.67^{o}C. The degradation of thiamin was not enough to estimate the kinetic parameters in both systems. The aseptic process is better for the retention of nutrients such as vitamin C.

The food industry will benefit from this research with regard to the thermal properties at elevated temperatures. With the new and novel processes relying on faster heating and faster cooling, the majority of the time spent by food products is at higher temperatures. So, the temperature-dependent thermal properties would provide a means to optimize the quality of the food product while keeping the food safe. Without the knowledge of accurate thermal properties at elevated temperatures, food processors tend to be conservative with the thermal process and end up with poor quality of the processed food.

6.2 Recommendations for future work

Here are recommendations for future work related to current research and to make advancements with TPCell.

1. Investigate the effect of reactions such as, endothermic reactions, glass transition, protein denaturation and lipid melting on thermal conductivity of food materials.
2. Perform more experimental runs with TPCell for several different temperature ranges, such as $20^{o}C$ - $80^{o}C$, and compare the results with the complete range of $20^{o}C$ - $140^{o}C$.
3. Perform experiments with TPCell on solid materials.
4. Investigate the effect of temperature profile of TPCell heater on estimated thermal conductivity. Does the temperature history effect thermal conductivity?
5. Investigate the effect of oxygen, carbon dioxide and headspace in the jar on degradation of nutrients.